



SAAD DAHLEB BLIDA'S UNIVERSITY



Faculty of Technology

Department of Civil Engineering

MASTER THESIS IN CIVIL ENGINEERING

Specialty: Steel and Composite Constructions

**Seismic Fragility Curves and Resilience of HealthCare
Facilities in Algeria (Case Study of the
Great Blida)**

Submitted by:

RAFIK LEMOUCHI

MOURAD KERRAUCHE

Proposed and supervised by:

Dr. Rafik TALEB

Blida, September 2020



Acknowledgements

To our dear parents and brothers.

To our dear family.

To our dear friends

I cannot find the right and sincere words to express my affection and my thoughts to you, to me you are brothers, sisters and friends on whom I can count.

As a testament to the friendship, that unites us and to the memories of all the times we have spent together, I dedicate this work to you and I wish you a life full of health and happiness.

Thanks

As a preamble to this brief we thank ALLAH who helped us and gave us patience and courage during these long years of study.

We would like to thank Dr. Rafik Taleb who supervised this dissertation, he always listened and was available throughout the production of this dissertation, as well as for the inspiration, the help and the time he was kind enough to devote to us, and without whom this dissertation would never have seen the light of day.

We would like to extend our sincere thanks to the people who have provided us with their assistance and who have contributed to the development of this dissertation as well as to the success of this difficult academic year.

These thanks go first to the faculty and administrative staff of the Faculty of Civil Engineering, for the richness and quality of their teaching, and who go to great lengths to provide their students with up-to-date training.

We would like to thank Dr B.Menadi and Professor S.kenai, for having accepted to chair our jury.

We would also like to thank the committee members at the university of Blida 1, for having accepted to examine this dissertation.

We do not forget our parents for their contribution, their support and their patience.

Finally, we address our most sincere thanks to our college Khalil chelha, Mr. Shurui Kuro, and Ikhlef abd el wadoud for their assistance and all our relatives and friends, who have always encouraged us during the preparation of this dissertation.

Thanks to all of you

Abstract:

Healthcare facilities are vital for the society, and when faced to earthquakes it becomes apparent that their services can make the difference between a vulnerable society and a resilient one. This work aims to contribute to the seismic risk mitigation of healthcare facilities in Algeria through the nonlinear dynamic analysis and seismic performance evaluation as well as the estimation of the seismic fragility function using incremental dynamic analysis which is an important tool in multiple seismic assessment procedures. After the estimation of seismic fragility curves a set of solutions and recommendations are given to improve the structural behaviour of healthcare facilities in the state of Blida, and thus decrease the effects of earthquakes such as the unfortunate event of the 2003 Boumerdes earthquake.

Keywords: healthcare facilities, earthquakes, nonlinear analysis, incremental dynamic analysis, pushover analysis, fragility, performance assessment.

Résumé :

Les établissements hospitaliers sont des éléments vitaux pour la société, et face à des événements sismiques, il devient évident que leurs services peuvent faire une grande différence entre une société vulnérable et une société résiliente. Ce travail vise à contribuer à l'atténuation du risque sismique des établissements hospitaliers en Algérie à travers des analyses dynamique non-linéaires et l'évaluation de la performance sismique ainsi que l'estimation des courbes de fragilité sismique en utilisant une analyse dynamique incrémentale, qui est un outil important dans de multiples procédures d'évaluation sismique. Après l'estimation de cette fragilité, un ensemble de solutions et de recommandations est donné pour améliorer le comportement structurel des établissements de santé dans l'état de Blida, et ainsi diminuer les effets des tremblements de terre comme le malheureux séisme de Boumerdes en 2003.

Mots clés : établissements de santé, tremblements de terre, analyse non linéaire, analyse dynamique incrémentale, analyse pushover, fragilité, évaluation des performances.

الملخص:

تعتبر مرافق الرعاية الصحية ضرورية للمجتمع، وعندما تواجه خطر الزلازل يصبح من الواضح أن خدماتها يمكن أن تحدث فرقاً بين مجتمع ضعيف وآخر مرن، ويهدف هذا العمل إلى التخفيف من المخاطر الزلزالية في الجزائر من خلال تقدير وظيفة الهشاشة باستخدام الديناميكية المتزايدة التحليل، وهي أداة مهمة في إجراءات التقييم الزلزالي المتعددة. بعد تقدير الهشاشة المذكورة تم تقديم مجموعة من الحلول والتوصيات لتحسين السلوك الهيكلي لمنشآت الرعاية الصحية في ولاية البلدة، وبالتالي تقليل آثار الزلازل لتفادي أحدث مشابهة لزلزال بومرداس 2003

الكلمات المفتاحية: مرافق الرعاية الصحية، الزلازل، التحليل غير الخطي، التحليل الديناميكي المتزايد، التحليل التمهيدي، الهشاشة، تقييم الأداء.

TABLE OF CONTENTS

Table of Contents

Acknowledgements	I
Thanks.....	II
TABLE OF CONTENTS	VI
List of illustrations	X
List of tables.....	XII
Acronyms	XIII
General Introduction	XV
Research motivation	XVI
Research objectives	XVI
Research methodology	XVI
Obstacles	XVII
Chapter 01	1
1.1 Literature review	2
1.1.1 Physical factors	2
1.1.2 Organizational and societal factors	3
1.1.3 Hospitals, bridges & roads network	4
1.1.4. Framework models	4
1.2. Hospitals and disasters	5
1.2.1. Damage to healthcare facilities	6
1.3. Healthcare typologies in Algeria.....	9
1.3.1. The advantages of categorization	9
1.4. Fragility functions	10
1.4.1 Definition	10
1.4.2. Development	10
1.4.3. Objectives	11
1.4.4Results	11
1.5 Introduction to Seismic Hazard Analysis.....	12
1.5.1 Introduction	12
1.5.2. PROBABILISTIC SEISMIC HAZARD ANALYSIS	12
1.5.2.1 PSHA uncertainties	12
1.5.2.2 PSHA steps	18

1.5.2.3 PSHA implementation	19
1.5.2.4 DISAGREGATION	20
1.5.3 UNIFORM HAZARD ANALYSIS	20
1.5.3.1 the advantages and the limitations of using UHS	21
1.5.4 CONDITIONAL MEAN SPECTRUM	22
1.5.4.1 Creating a Conditional mean spectrum	22
1.5.4.2 compute Conditional Mean Spectrum	25
1.5.4.3. The advantages and disadvantages of CMS	26
1.6. Conclusion	27
Chapter 02.....	28
2. Introduction.....	29
2.1 Materials.....	29
2.1.1 Steel	29
2.1.1.1 Stress-strain model	29
2.1.2 Concrete	30
2.1.2.2 Stress-strain model	30
2.2. Inelastic infill panels	31
2.2.1. Infill panels parameters	32
2.3.Modelling	33
2.3.1 SeismoStruct	33
2.4. Nonlinear analysis.....	35
2.4.1. Typical uses of nonlinear analysis	36
2.4.2. Nonlinear Static analysis	36
2.4.2.1. Disadvantages of static nonlinear analysis	37
2.4.3. Nonlinear Dynamic analysis	37
2.4.3.1. The advantages of nonlinear dynamic analysis	37
2.4.3.2 The disadvantages of nonlinear dynamic analysis	37
2.5. Limit states.....	38
2.6. Hinges	39
2.7. Selected nonlinear analyses.....	39
2.7.1. Introduction	39
2.7.2 The pushover analysis	39
2.7.2.2 The objectives	40
2.7.2.3. The methodology	40
2.7.2.5. The pushover curves	42

2.7.3.1 The objectives of the IDA	44
2.7.3.2 IDA procedure	44
2.8. Conclusion	45
Chapter 03.....	46
3.1 Introduction.....	47
3.2 The considered models.....	47
3.2.1 The collected data	47
3.2.2 Geographical locations of the healthcare facilities	48
3.2.3 The geometric configuration	48
3.2.4 The selection processes	49
3.3 The chosen typology	50
3.3.1 Structural characteristics	51
3.3.2 Geometric configuration	53
3.4 Conclusion	55
Chapter 04.....	56
4.1 Introduction.....	57
4.2. Ground motion selection	57
4.2.1. Target spectrum selection	58
4.2.2 Ground motion scaling	59
4.2.3 Application of ground motions to structural model	59
4.3-ANALYSIS RESULTS AND ACCEPTANCE CRITERIA	60
4.3.1. Displacement	60
4.3.1.1. Inter-story drift (IDR)	60
4.3.2 Second order effect (P-Δ effect)	65
4.3.3. Chord rotation	66
4.3.4 The axial load ratio	70
4.4. Conclusion	71
Chapter 05.....	72
5.1 Introduction.....	73
5.2 Collapse fragility development	73
5.2.1 Collapse fragility development using IDA	73
5.2.2 Collapse fragility development using truncated IDA	73
5.3 Pushover based derivation of fragility curves	74
5.3.1 SPO2IDA	74
5.3.2 SPO2FRAG	74

5.3.2.1 Definition	74
5.4 Fragility curves development.....	77
5.4.1 Fragility functions for the CAC building with infills	77
5.4.2 Fragility functions for the CAC building without infills	79
5.4.3 Fragility functions for the TOT building	82
5.5 Results discussion	86
5.6 Solutions and recommendations	87
Concluding remarks	88
References.....	89

List of illustrations

Figure 1. 1: graphical illustration of the research methodology. -----	XVII
Figure 1. 2: Collapse of the fifth floor of the Municipal Hospital, Kobe, 1995. (Paho, 2000). -----	6
Figure 1. 3: Damage to the emergency wing of Thenia hospital (Achour, 2007). -----	8
Figure 1. 4: collapse roof of another wing of Thenia hospital (achour,2007). -----	9
Figure 1. 5: collapse fragility function for a hypothetical building. (FEMA P 58-1). -----	11
Figure 1. 6: Source zone geometries: (a) point source; (b) two-dimensional areal sources; (c): three dimensional volumetric sources (kramer, 1996) -----	13
Figure 1. 7: Typical distribution of observed earthquake magnitudes, along with Gutenberg-Richter And bounded Gutenberg-Richter recurrence laws fit to the observations. [Baker 2008] -----	15
Figure 1. 8: The-Characteristic-Earthquake-Model-from-Youngs-and-Coppersmith-1985-On-the-a-is-theAnother recurrence law is the slip dependent recurrence law, this concerns the faults which have an important amount of annual slip, and it was noted that this slip had -----	16
Figure 1. 9: Illustration of the conditional probability of exceeding a ground motion parameter (Kramer, 1996) [FEMA P58-1] -----	17
Figure 1. 10: Steps in probabilistic seismic hazard assessment (Kramer, 1996) [FEMA p58-1]. -----	18
Figure 1. 11: Example disaggregation for SA(1.0s) at a site in Palo Alto, California (USGS, 2008) . [Baker 2015] -----	20
Figure 1. 12: Combining hazard curves from individual periods to generate a uniform hazard spectrum with a $4 \cdot 10^{-4}$ rate of exceedance for a site in Los Angeles. (a) Hazard curve for SA(0.3s), -----	21
Figure 1. 13: uniform hazard spectrum with 2%probability of exceedance in 50 years, Conditional mean spectrum, And scaled conditional mean spectrum for a rock site in San Francisco.(FEMA p58-1). -----	22
Figure 1. 14: scatter plots of values from a large suite of ground motions. The points associated with the ground motion in figure 5 are highlighted. (a) (1s) versus (2s): (b) (1s) versus (0.2s) (baker, 2008). -----	25
Figure 1. 15: conditional mean values of spectral acceleration at all periods, given sa (1s), and the example castaie old ridge route ground motion.(Baker 2008) -----	25
Figure 2. 1: Menegeto-pinto steel model with Monti-Nuti post elastic buckling -----	29
Figure 2. 2: steel parameters extracted from SeismoStruct 2020. -----	30
Figure 2. 3: the Chang and Mander nonlinear concrete stress strain model. -----	31
Figure 2. 4: the characteristics of concrete extracted from SeismoStruct 2020. -----	31
Figure 2. 5: Cristafully 1997 inelastic-infill panel model (SeismoStruct manual) -----	32
Figure 2. 6: inelastic infill panels characteristics extracted from SeismoStruct 2020. -----	33
Figure 2. 7: 3D numerical model example of an RC building by SeismoStruct -----	35
Figure 2. 8: Component or element deformation acceptance criteria (FEMA 356, 2000) -----	38
Figure 2. 9: a SDOF system equivalent to a MDOF model (Eurocode 8-1) -----	40
Figure 2. 10: a typical pushover curve. -----	42
Figure 2. 11: Idealized Force-Displacement Curves FEMA 356 -----	43
Figure 3. 1: the geographical location of the targeted healthcare facilities. -----	48
Figure 3. 2: architectural plan of the ORL building -----	49
Figure 3. 3: plan view of the first floor of the C3 bloc. -----	53
Figure 3. 4: photo of the TOT building. -----	53
Figure 3. 5: plan view of the first floor of the A1 bloc. -----	54
Figure 3. 6: photo of the Anti-Cancer Centre (CAC) building. -----	54

Figure 3. 7: a close up on the geographical location of the CAC and the TOT healthcare facilities. -----55

Figure 4. 1: Boumerdes earthquake ground motions recorded from the station of Azazga, a) the E-W component, b) the N-S component. -----58

Figure 4. 2: RPA-based target acceleration response spectrum. -----58

Figure 4. 3: Blida Uniform hazard spectra, damped at 5%, for a return period of 475 years (Hamadache and al,2012) -----59

Figure 4. 4: Numerical model of the TOT bloc C3. -----60

Figure 4. 5: inter-story drift checks in the X direction.-----63

Figure 4. 6: inter-story drift checks in the X direction.-----64

Figure 4. 7: inter-story drift checks in the X direction.-----64

Figure 4. 8: inter-story drift checks in the X direction.-----65

Figure 4. 9: Chord rotation for structural wall coupling beams (ASCE 7-16,2016). -----67

Figure 4. 10: chord rotation capacity surpassed in TOTC3 block column 32-1. -----69

Figure 4. 11: chord rotation capacity surpassed in TOTC3 block beam 148-1. -----69

Figure 5. 1: .a) Example incremental dynamic analyse results, used to identify IM values associated with collapse for each ground motion. b) Observed fractions of collapse as a function of IM, and o fragility function. (Baker, 2015).-----73

Figure 5. 2: a) Example truncated IDA analysis results. b) Observed fractions of collapse as a function of IM (Baker, 2015). -----74

Figure 5. 3: Dynamic characteristics of a structure.-----75

Figure 5. 4: IDA fractile curves. -----75

Figure 5. 5: Graphical representation of performance limit states. -----76

Figure 5. 6: the CAC BLOC with masonry infills pushover curve.-----77

Figure 5. 7: the CAC bloc with infills pushover curve fitted using a quadrilinear-fitting scheme. -----78

Figure 5. 8: the IDA fractile curves of the CAC bloc with infills. -----78

Figure 5. 9: the CAC bloc with infills fragility curve-----79

Figure 5. 10: the CAC BLOC without masonry infills pushover curve.-----80

Figure 5. 11: the CAC bloc without infills pushover curve fitted using a quadrilinear-fitting scheme.-----80

Figure 5. 12: the IDA fractile curves of the CAC bloc without infills. -----81

Figure 5. 13: the CAC bloc without infills fragility curve. -----81

Figure 5. 14: the TOT bloc pushover curve.-----82

Figure 5. 15: TOT bloc pushover curve fitted using a quadrilinear fitting scheme. -----83

Figure 5. 16: the IDA fractile curves of the TOT bloc. -----83

Figure 5. 17: the TOT fragility curve.-----84

Figure 5. 18: a comparaison between the CAC Block with and without infills. -----85

List of tables

Table 1 1: general effects of earthquakes on selected hospitals (Paho, 2000) -----	7
Table 2 1: performance limit states (FEMA 356, 2000) -----	42
Table 3 1: the available data for the targeted healthcare facilities. -----	47
Table 3 2: the targeted healthcare facilities for this study -----	50
Table 3 3: healthcare typologies in the great Blida -----	50
Table 3 4: basic characteristics of TOT blocks A1, D1 and D2. -----	51
Table 3 5: basic characteristics of TOT blocks C1, C2 and C3. -----	52
Table 3 6: basic characteristics of CAC blocks A, B and C. -----	52
Table 4 1: the resulting displacement in the X direction using time history analysis -----	61
Table 4 2: the resulting displacement in the Y direction using time history analysis -----	62
Table 4 3: the resulting displacement in the X direction using time history analysis -----	62
Table 4 4: the resulting displacement in the Y direction using time history analysis -----	63
Table 4 5: P- Δ effect verification for the TOT bloc. -----	66
Table 4 6: P- Δ effect verification for the CAC bloc. -----	66
Table 4 7: chord rotation checks in both ends of the vertical and horizontal elements. -----	68
Table 4 8: chord rotation checks in both ends of the vertical and horizontal elements. -----	70
Table 4 9: The axial load ratio verifications for the TOT blocs. -----	70
Table 4 10: The axial load ratio verifications for the CAC blocs. -----	71
Table 5 1: the probability of exceeding performance levels for the three blocks at $S_a=1g$. -----	85

Acronyms

β^i : is the logarithmic standard deviation.

Θ_i : is the median value of the probability distribution.

Φ : is the standard normal (Gaussian) cumulative distribution function.

$F_Y(y)$: is the value of the cumulative distribution function of Y at m and r.

θ : is the median value of Y.

β : is the dispersion.

λ : is the average rate of recurrence of the event.

T : is the time period.

n_s : the number of sources considered.

n_R : the number of distances considered.

n_M : the number of magnitudes considered.

$\mu_{\epsilon(T_i)|\epsilon(T^*)}$: the mean of $\epsilon(T_i)$ given $\epsilon(T^*)$.

$\rho(T_i, T^*)$: is the correlation factor.

$\mu_{lns_a}(M, R, T_i)$: the predicted mean deviation.

$\delta_{lns_a}(T_i)$: the predicted standard deviation.

$\rho(T_i, T^*)$: the correlation factor.

m_i : is the mass in the i-th storey.

S_A : the response spectrum acceleration at the effective fundamental period of vibration.

g : the acceleration of gravity.

C_0 : Modification factor to relate spectral displacement of an equivalent single-degree-of-freedom (SDOF) system to the roof displacement of the building multiple degree of Freedom (MDOF).

C_1 : Modification factor to relate expected maximum inelastic displacements to displacements calculated for linear elastic response calculated.

C_2 : Modification factor to represent the effect of pinched hysteresis shape, cyclic stiffness degradation, and strength deterioration.

T_e : the fundamental period.

R : coefficient de comportement.

δ_{ek} : the resulting displacement of seismic forces.

P_k : the total load of the levels starting the level "k" upwards.

V_k : the shear load on the level "k".

Δ_k : the relative displacement of the two consecutive levels "k" and "k-1".

h_k : the height of the level "k".

Nd: is the vertical load acting on the element.

Bc :is the raw section of the element.

Fcj: is the characteristic strength of the concrete.

General Introduction

Healthcare facilities are one of the most important components of a society, and since they constitute the final point in the rescue chain (Miniate & lasio, 2012), they represent a pivotal role in the resilience of communities in facing natural disasters, because when an extreme event affects an entire region, resilient hospitals will bounce back to functionality rapidly which could improve the response of the entire community (Cimellaro et al. 2009).

And Since health care facilities are critical for the overall public health services, this study aims to highlight the structural behaviour of the healthcare infrastructure in Algeria, with the district of great Blida as a case study. This dissertation covers topics related to potential structural collapse generated by earthquake events as well as the mitigation measures necessary to ensure that a facility remains intact, and its functionality remains undisturbed. It aims to give the reader a closer look on the complexity of healthcare facilities and provides certain tools to assess said facilities. Risk mitigation solutions that will protect the population are presented as well as how to decrease the chances of having large financial losses in the event of an earthquake. The dissertation is not intended to cover in detail technical aspects that have been the subject of academic publications, although the necessary references are included for the benefit of the reader who wishes to study these topics more in depth.

Chapter 01: presents the study's motivation, the problem description and the research methodology used in this work. The cases of healthcare facilities affected by earthquakes on both a national and an international level are reviewed including descriptions of the types of damage most commonly observed in those facilities. An introduction to dynamic time history analysis is made in later sections.

Chapter 02: focuses on nonlinear analysis, presenting both of the analyses used in this study (the static pushover analysis and incremental dynamic analysis), and capitalizing on the principles used in chapter 1, after which the nonlinear material models used during the study are presented and the process of their selection is explained.

Chapter 03: provides the essential data of the healthcare facilities targeted for this study, and the process of their selection is explained, in the end the final models that would be the test subjects of this study are defined.

Chapter 04: the performance of the numerical models is assessed using dynamic time history analysis, and based on that assessment the final models are selected, to create a more reliable procedure for earthquake loss estimation.

Chapter 05: presents the final step of this work, where the fragility curves are developed for multiple structural models, and based on those results, conclusions are Drawn on the construction practices in Algeria. later on, recommendations and solutions are provided to improve those practices, in order to decrease the vulnerability of healthcare facilities.

Research motivation

Natural hazards have always presented an obstacle in the face of engineers, and in many cases stood in the face of the affected country's development. Algeria has seen its own share of earthquake events, which destroyed its healthcare facilities such as the 1980 Chlef earthquake and the 2003 Boumerdes earthquake. The latter affected more than 200 facilities in the states of Algiers, Boumerdes and others. This proved that the healthcare system was fragile and vulnerable to seismic damage, which is unacceptable, especially when it comes to such facilities, where the disruption of their functions would lead to further losses. Now seventeen years later, the question remains whether this system is capable of withstanding such pressure, and if not, what are the stakes this time, especially since the population has risen considerably since then. This work requires the skills and the abilities to use a variety of technological tools.

Research objectives

This study aims to highlight the fragility/vulnerability of health care facilities in the district of great Blida, and is an attempt and a contribution to enrich the scientific research in this particular field of study. Later on, the tools prepared in this study can then be used as a stepping stone, for other works with the same objectives, or they can be used for other works to estimate the fragility of other facilities and systems, or simply to estimate the fragility of healthcare facilities on a national level. The goal of this study is also to gain a grasp on the nonlinear behaviour of complex structures, and how to use their results in the most efficient manner.

Research methodology

This study was conducted following multiple steps, starting with data collection which consumed a huge amount of time. The information concerning 8 different healthcare facilities in the state of Blida was collected. However, only a limited number of facilities were selected for the final step of fragility curve development, this due to two different reasons the first being that the typologies of these constructions are fairly similar in a lot of cases, and the second reason is the incomplete data, and the

difficulties encountered to obtain new data in the time of Covid 19 where most facilities were in complete lockdown. The next step is to analyse this data and then proceed with following protocols.

The steps followed in this work are summarized in figure1.1:

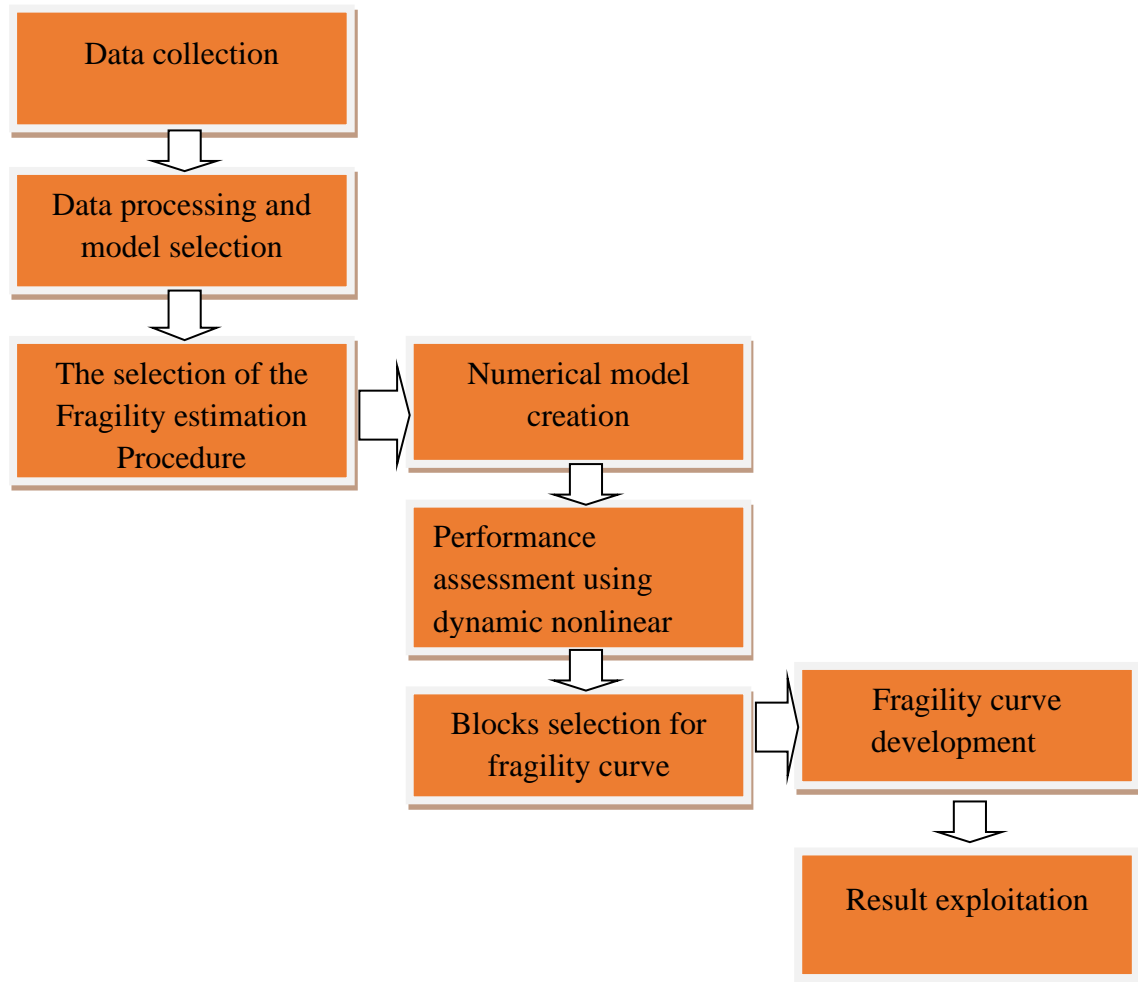


Figure 1. 1: graphical illustration of the research methodology.

Obstacles

Many obstacles were met during the study some of which are:

- The lack of certain technological tools to increase the precision of the results, mainly the lack of access to university's computation station, due to Covid-19 lockdown

- The lack of engineering plans of some of the health care facilities intended for the study, this was due to the fact that such buildings either had been constructed in the 1900s or in some rare cases in the French colonial/ottoman empire period.
- The lack of material sources to conduct material tests of actual masonry units, in order to represent the structural properties more accurately.
- The lack of coordination between the university and the contacted facilities.

 **Chapter 01:****Literature review on seismic
performance and healthcare
facilities**

1.1 Literature review

The rising number of earthquake events pushed scientists and engineers, to create methodologies and frameworks to improve the resilience of healthcare facilities, however this task required a multidisciplinary approach but the first proposed frameworks only concentrated on one aspect of healthcare facilities resilience, either from a physical/economical perspective or from a social and an organizational one.

1.1.1 Physical factors

The traditional approach was purely from a structural point of view, this approach consisted on improving the structural load bearing systems of hospitals and reducing the probability of structural failure. This however was not fully representative of the performance of healthcare structures as opposed to other buildings, since hospitals are composed of a multitude of components, each with their own effect on the overall performance of the facility. However, if the structural performance is the main objective of any study, it is seen that the traditional approach is more than appropriate.

In order to estimate the resilience of hospitals from a holistic perspective, all of the factors which played either a major or a small role on the overall performance had to be identified, while most researchers agree on the main factors they tend to differ on their degree of influence.

One of the most influential factors on hospital functionality is the non-structural factor, while structural damage would render the building unusable, non-structural damage could decrease the functionality rate considerably, this was noticed in previous earthquakes where some sections of facilities were inaccessible and therefore unavailable for usage, while the structural system remained unharmed by the earthquake, this was explained by the non-presence of construction practices or the presence of inadequate code requirements, which are mainly concentrated on the structural aspect.

Non-structural components can range from secondary elements such as ceilings to life-line systems, the latter was largely ignored and it wasn't until the last few years that more works highlighted that aspect, this lack of attention was mainly due to the lack of literature and the none presence of reliable methods to quantify the effects of the aforementioned components.

(Hiete et al, 2011) investigated the effects of power outages on the performance of healthcare facilities, since the loss of power was the most probable scenario in an earthquake event, and also due to the fact that among all the lifeline systems, power supply was the most detrimental on the functionality of the facility. Other authors such as (Hassan and Mahmoud, 2019) investigated the effects of lifelines disruption on each other. According to (Achour et al, 2014) the impact of utilities

failure is relatively comparable in terms of continuity of healthcare services whether its internal or external utilities system damage.

Another factor, which was ignored despite its direct impact on human losses and economical losses, is damage on medical equipment, while all the previously mentioned factors are mainly related to physical resilience; some of them have a significant impact on the economical resilience of health care facilities. As opposed to non-structural factors this aspect was not entirely ignored, since the financial component played a major role in decision making, yet with the rise of new factors which are either largely or slightly related to financial losses, it is only normal that this factor needs to be addressed differently. (Masi et al, 2012) suggested a methodology based on funds availability. This enabled the creation of tools that can be used by decision makers to assign resources and funds in more effective ways, by selecting the most adequate retrofitting and reconstruction strategies in order to regain full functionality while keeping in mind the economical aspect. (Hassan and Mahmoud, 2019) also suggested a similar method based on funds redistribution while fully taking account of the interdependencies of lifelines and structural and non-structural damage.

1.1.2 Organizational and societal factors

As opposed to physical and economical components, which had different degrees of impact but all could be easily quantified, other components emerged which were less defined in terms of standard units. One of the most influential components is the organizational one. (Cimellaro et al, 2010) was the first to investigate this component, and proposed the unit of waiting time as a means to estimate and quantify the functionality of health care facilities, and based on that, the aim of the organizational measures and policies is to decrease the waiting time that patients have to go through in order to receive service. This notion gave rise to adjusting certain policies to increase effectiveness, and thus hospital management was conceived as essential for attaining a more resilient facility, especially in the case of large sized hospitals and that of medium sized ones, which are most likely to receive large numbers of patients in the event of an earthquake. Another factor that proved to be critical is the presence of an emergency plan, since most first world countries were more or less well prepared, developed countries were not. This was investigated by (Munasinghe and Matsui, 2019) where it showed how fragile the Sri lanka healthcare system was when faced with an earthquake scenario, it also highlighted the necessity for emergency training programs designed for employees to handle the rising surge of injured patients.

This however could not always be easily implemented, and sometimes other measures were needed, one of these measures is the distribution of patients between hospitals which was investigated by (Jacques et al, 2013).

1.1.3 Hospitals, bridges & roads network

This idea consisted that all healthcare systems while being complex systems within themselves, would form a network of hospitals, this network cannot reach its full capacity if each system reacted independently, this interaction between each facility would increase the performance on the regional scale and subsequently on the institutional one.

This required hospitals to exchange information with one another, and create plans prior to any event, in some cases an exchange of resources could be implemented such as the temporary exchange of ambulances and staff members with neighbouring facilities to alleviate the pressure and consequently reduce the waiting time and increase the quality of treatment received by the patients.

The introduction of staff and resources exchange helped in the creation of more solutions, but also meant that there were other external factors that could play a role in the resilience of HealthCare facilities, such as regional lifeline systems, and the roads/bridges network which proved to have a big influence on the number of human losses. This is explained by the fact that residential areas and hospitals are connected by roads and bridges, and in the case of damaged bridges for example many would not receive appropriate medical aid, this highlighted that for a more efficient healthcare system, the infrastructure needs to be physically resilient.

The interconnectedness of the two systems led to the creation of the travel time unit. Based on the statistics which suggest that the mortality rate is substantially reduced if patients receive medical care in a short period of time (Lupoi et al., 2013). This notion was then adopted by other works such as Cimellaro et al. (2019). Lupoi et al. (2013) and Cimellaro et al. (2009) making it alongside the waiting time the two units of measuring the performance of healthcare networks and facilities.

1.1.4. Framework models

While identifying the factors necessary for the creation of a framework was relatively easy, the creation of a reliable framework model proved to be a difficult task. One of the first issues encountered was the presence of too many factors, many of which could not have been neglected. This required capable technological tools that were not present at the time, this however was solved by the rapid technological advancements. Eguchi et al. (2003) was one of the first to propose a conceptual framework basing the performance healthcare facilities on 4 dimensions of resilience.

Soon after other works emerged, some of which used the same dimensions and others used different methods. However, many of these frameworks failed to represent the complexity of interacting systems, or failed to present a model that could be implemented.

Aside from the chosen dimensions, the main difference between these works was the analysis method. Jacques et al. (2013) for example proposed a fault tree analysis which proved to be deterministic, yet added that it could be used in conjunction with other methods. This is what was attempted by (Hiete et al, 2011) by applying the fault tree analysis in conjunction with a markov chain process. Other approaches were investigated, such as the one used by (Lupoi et al, 2013) who proposed the implementation of a probabilistic approach and a simulation to solve reliability issues. Another approach which is highly popular due to its simplicity and reliability is factor analysis.

1.2. Hospitals and disasters

“A disaster may be defined as an event or occurrence—usually sudden and unexpected—that intensely alters the beings, objects and localities under its influence. It results in loss of life and health in the local population, causes severe environmental damage and the destruction or loss of material goods resulting in a dramatic disruption of normal patterns of life” (Paho ,2000).

Since the main task of a hospital is to provide aid to the sick and injured, the two notions became intertwined. That is why the structural integrity of the hospital is highly important to prevent further human losses, and assure the continuity of the healthcare facility’s functionality which in turn would increase the resilience of the facility specifically and the whole community/country in general.

But despite the fact that hospitals are useful institutions that can be used to mitigate the effects of natural disasters, it’s not possible to fully dissipate the effects, and therefore all sectors of the community, ranging from the social, economic, and political must work together to improve earthquake loss mitigation.

1.2.1. Damage to healthcare facilities

Earthquakes are a force of nature, which lead many structures to total collapse, hospitals are no different, and while many efforts were made to diminish these losses, many hospitals still collapse both on an international level and in Algeria.

On an international level:

Although seismic codes have been present for quite a while now, it is seen that many healthcare facilities that were built using these standards still undertake huge losses. This highlights that these facilities require more attention than the average building, since the loss of functionality can be attributed to any one of the diverse systems present in a hospital, this means that all the factors contributing to the overall performance must remain undamaged, or at the very least have alternative solutions prepared in advance.



Figure 1. 2: Collapse of the fifth floor of the Municipal Hospital, Kobe, 1995. (Paho, 2000).

Table 1: general effects of earthquakes on selected hospitals (Paho, 2000)

Earthquake	Magnitude (Richter Scale)	General Effets
San Fernando, California, U.S.A.,1971	6.4	Three hospitals suffered severe damage and were unable to operate normally when they were needed most. Furthermore, most of the earthquake victims went to two of the collapsed hospitals. Olive View Hospital, One of the most severely affected hospitals was retrofitted.
Managua, Nicaragua, 1972	5.6	The General Hospital suffered severe damage. It was evacuated and later demolished.
Mexico City, Mexico, 1985	8.1	Five hospitals collapsed and 22 more suffered serious damage. At least 11 facilities were evacuated. Direct losses were estimated at US\$ 640 million. The most seriously damaged hospitals were the National Medical Centre of the Mexican Social Security Institute (IMSS), the General Hospital and the Benito Juarez Hospital. Between destroyed and evacuated hospitals, the earthquake produced a sudden deficit of 5,829 beds. 295 lives were lost at the General Hospital and 561 at Juarez Hospital, including patients, doctors, nurses, administrative personnel, visitors and new-borns.
Guatemala City, Guatemala,1976	7.5	Several hospitals were evacuated.
Tena, Ecuador, 1995	6.2	Velasco Ibarra Hospital (120 beds) suffered. Moderate non-structural damage: cracked walls, broken windows, fallen ceilings, damage to the elevator system and some oxygen and water conduits. Service was suspended and the facilities evacuated.

On a national level:

The state of Blida has experienced a multitude of earthquakes throughout its history, measuring higher than M5.0. Among which is the 1825 earthquake which led to the loss of about 7000 people. Although in recent years there weren't any earthquake reports of hospitals in the Blida area due to the lack of surveys, its neighbour state Boumerdes which possess similar seismic properties has been struck with a recent earthquake in 2003. This latter provided many examples of healthcare facilities that were either structurally damaged to a degree of none functionality to that of limited functionality. In the State of Boumerdes at least 242 healthcare facilities of varying importance were affected, more than 30 of them suffered very severe damage or total collapse (Achour, 2007).

Among the damaged healthcare facilities in the 2003 earthquake are the CHU central Algiers hospital, and the Thenia hospital (Figure 1.2 and Figure 1.3)



Figure 1. 3: Damage to the emergency wing of Thenia hospital (Achour, 2007).



Figure 1. 4: collapse roof of another wing of Thenia hospital (achour,2007).

1.3. Healthcare typologies in Algeria

When performing an earthquake loss estimation study, it is a major task to categorize the building stock into distinct typologies; these typologies can be defined on a large number of criteria such as their vulnerability, damageability during earthquake events.

1.3.1. The advantages of categorization

The need for classification stems from the fact that it is virtually impossible to study all of the structural models individually, and then estimate their vulnerability, therefore it is only normal to choose a limited number of structures with general characteristics such as the material type, the structures height and the load bearing systems as well as other factors depending on the purposes of the study.

Aside from saving valuable time and resources when using classifications, another one of its positive aspects is to allow for a more manageable and efficient study without losing the integrity of the study's results, and last but not least the classification scheme can be used to define a common terminology or taxonomy in order to identify the building variations on a national or an international level.

1.4. Fragility functions

1.4.1 Definition

According to FEMA P58-1, fragility functions are statistical distributions used to indicate the probability that a component, element, or system will be damaged as a function of a single predictive demand parameter, such as story drift or floor acceleration. Fragility functions take the form of lognormal cumulative distribution functions, having a median value, θ , and logarithmic standard deviation, or dispersion, β . The mathematical form for such a fragility function is:

$$F_i(D) = \Phi\left(\frac{\ln(D/\theta_i)}{\beta_i}\right) \quad (\text{Eq 1})$$

Where:

$F_i(D)$ is the conditional probability that the component will be damaged to damage state “i” (or more severe damage state) as a function of a demand parameter, D

Φ : is the standard normal (Gaussian) cumulative distribution function

θ_i : is the median value of the probability distribution;

β_i is the logarithmic standard deviation

1.4.2. Development

fragility functions can be developed for any structure, given that defined limit states are present, and a unit of fragility measurement is also defined, one common measurement is displacement, since inter-story drift or roof drift are indicators of structural behavior. Fragility functions can also be developed using laboratory tests from previous earthquake events or/and from expert opinions although the precision of the results is different in both cases and the reliability of the results are also a matter of discussion.

For the case of this study and due to the lack testing data, a derivation approach was selected where the fragility is developed using analytical tools to estimate the level of demand at which the damage state of interest will occur.

1.4.3. Objectives

Using fragility functions has always been a tool for both researchers and decision makers to:

- Estimate the performance of structures in the case of earthquake events, both on a structural system level and on a nonstructural one.
- Estimate human and financial losses in case of an event.
- Estimate the facilities function both during and after the event.
- Improve structural systems to prevent the aforementioned losses.
- Create policies, and disaster protocols based on the results of fragility function in order to handle the events more effectively and prevent any further losses, and retrieve complete functionality as fast as possible.

1.4.4 Results

A most common way of exploiting the results of fragility estimation, is through developing fragility curves as shows in figure 1.5. This provides a more visual presentation and renders the results more comprehensible.

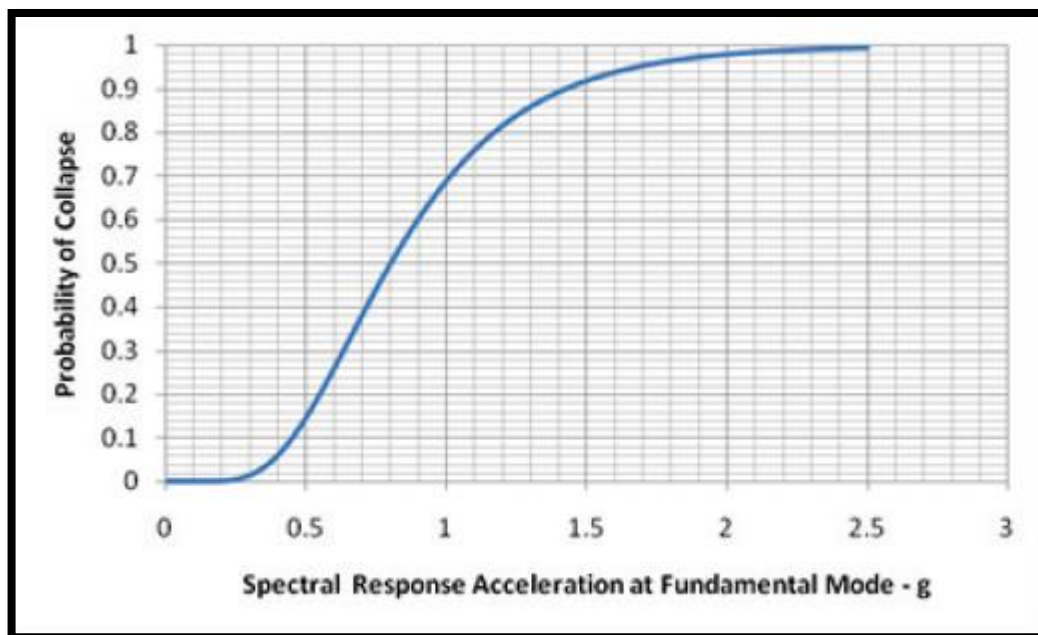


Figure 1. 5: collapse fragility function for a hypothetical building. (FEMA P 58-1).

1.5 Introduction to Seismic Hazard Analysis

1.5.1 Introduction

in this section the necessary tools needed to initiate dynamic nonlinear analysis are discussed, ranging from the principles of probabilistic seismic hazard analysis which is an indisputable methodology on the international level, to its sub sections where the uniform hazard analysis and the conditional mean spectrum are presented, which are the two mostly used target spectrums, when it comes to ground motion selection and scaling, therefore both are discussed and the most appropriate for this studies objectives is selected, for the initiation of nonlinear dynamic analysis.

1.5.2. PROBABILISTIC SEISMIC HAZARD ANALYSIS

Probabilistic seismic hazard analysis/assessment or PSHA for short first emerged in the 1960s in the works of Cornell(1968),and then was developed in the 70s,and has been used widely on an international level for approximately 50years,and while other methods for seismic hazard assessment existed prior to the PSHA, many of them had certain flaws and assumptions that were either inadequate representation of earthquake hazards or had results which were conservative, one of these methods is the deterministic seismic hazard analysis(DSHA) which was based on the notion of the largest credible earthquake, a notion which was both conservative and an inaccurate assumption, this was largely criticized by Cornell and pushed him to create the PSHA.

The main difference that PSHA had from the previous seismic hazard assessment(sha) methods, and the reason it was highly criticized when it came out, was that it accounted for a large set of uncertainties, and that the use of probabilities was not common in seismic design. The uncertainties that the PSHA had ranged from the location, size, intensity and the time of occurrence of future earthquakes, and through the theorem of total probability the PSHA aims to quantify these uncertainties and create seismic hazard curves which could then later be used as a tool for engineers to design and construct structures with lower probabilities of collapse.

1.5.2.1 PSHA uncertainties

While earthquake hazards present too many uncertainties, many of which cannot be predicted, the main concerns for predicting future events are the location of the hazard, and how strong will its magnitude be, and what intensity could be expected from this magnitude and last but not least when will this event take place.

1.5.2.1.1 Spatial uncertainty

While the exact location of earthquakes cannot be determined, an approximation can be used through identifying the locations of earthquake sources closer to the site, these sources have different forms and geometries, these geometries include point sources(volcanoes),linear sources(where the fault is located between 2 tectonic plates),2 dimensional and 3 dimensional sources depending on the geological properties of the region.in the case of having no identified sources in the region a common approach is to use a circular source with a predefined radius and having the site at the center of the source.

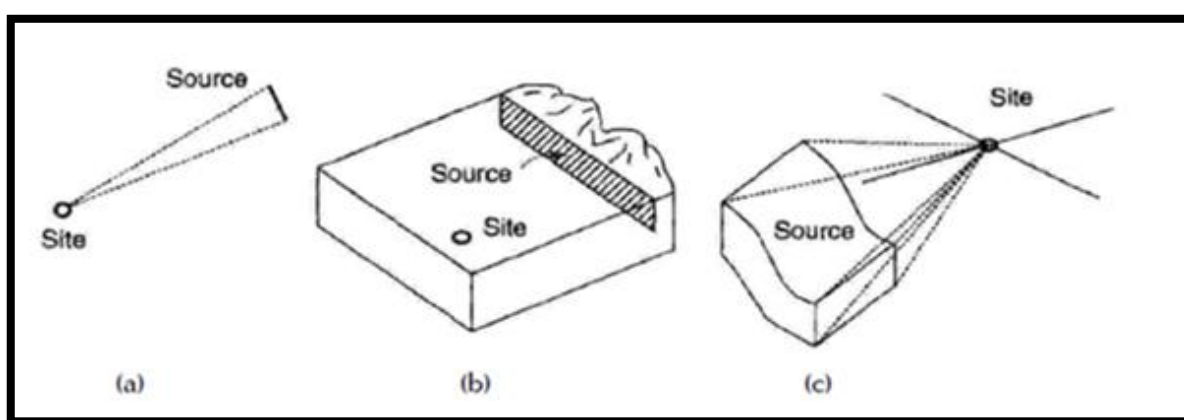


Figure 1. 6: Source zone geometries: (a) point source; (b) two-dimensional areal sources; (c): three dimensional volumetric sources (kramer, 1996)

1.5.2.1.2 Magnitude or size uncertainty

An exact prediction of the magnitude of future earthquakes is not possible, and therefore certain assumptions have to be made in order to account for the size uncertainty. “one basic assumption that was used in which past recurrence rates for a source are appropriate for the prediction of future seismicity”(FEMA P58-1)these recurrence rates represent the distribution of magnitudes over time, these rates are then used alongside probabilistic tools to create recurrence laws to account for size uncertainty, there exists many recurrence laws but the most commonly used ones are :

- the Gutenberg-Richter recurrence law
- the bounded Gutenberg-Richter recurrence law
- the slip dependent recurrence law

-the characteristic earthquake recurrence law

1.5.2.1.2.1 The Gutenberg-Richter recurrence law

In 1944 Gutenberg and Richter observed historical data of earthquake magnitudes in south California, and they noticed that the distribution of magnitudes in this region followed a certain pattern, they later described this distribution using the following equation:

$$\text{Log}\lambda_m = a - bm \quad (\text{Eq 2})$$

This equation can then be used to compute cumulative distribution function (CDF) of a limited set of magnitudes if there is a lower limit and/or an upper limit magnitude of interest depending on the interests of the user, this equation becomes:

$$f_M(m) = \frac{(1-10)^{-b(m-m_{min})}}{(1-10)^{-b(m_{max}-m_{min})}} \quad m_{min} < m < m_{max} \quad (\text{Eq 3})$$

Using The derivative of the CDF the cumulative distribution function is then obtained:

$$f_M(m) = \frac{b \cdot \ln(10) \times 10^{-b(m-m_{min})}}{(1-10)^{-b(m_{max}-m_{min})}} \quad m_{min} < m < m_{max} \quad (\text{Eq 4})$$

With the development of technological tools and a better understanding of earthquakes, the Gutenberg-Richter recurrence law was modified, this new recurrence law unlike the one established in the 1940s which assumed that the distribution of ground motions versus annual rates of exceedance was linear, this recurrence law had an upper limit magnitude and nonlinear distribution close to that limit, this is explained by the fact the all faults have a maximum magnitude, a magnitude which the faults cannot physically exceed due to geological properties, and thus it was named the bounded Gutenberg-Richter recurrence law.

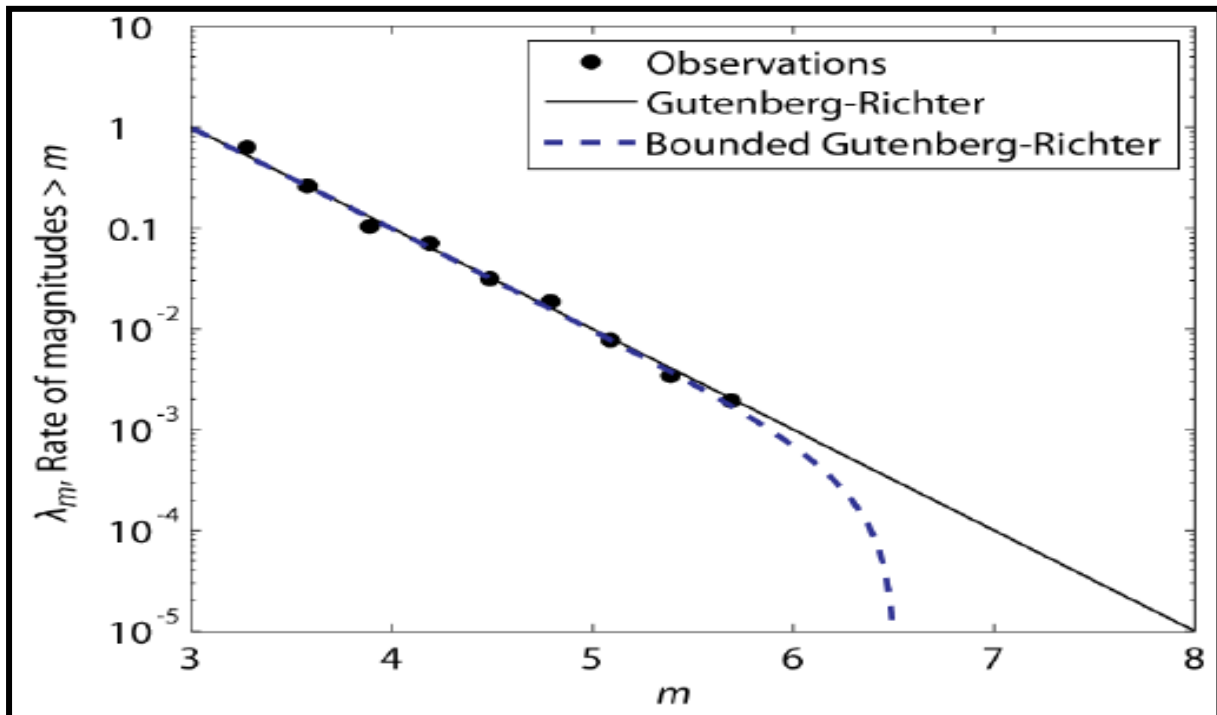


Figure 1. 7: Typical distribution of observed earthquake magnitudes, along with Gutenberg-Richter and bounded Gutenberg-Richter recurrence laws fit to the observations. [Baker 2008]

1.5.2.1.2.2 Fault properties related recurrence laws:

Since the Gutenberg-Richter recurrence law was created based on the data of south California in the 1940s it was only normal that certain factors would have been missing even with the bounded version, and it was in 1985 that paleo seismologists discovered that certain faults had characteristic earthquakes, this meant that these faults generate similar sized earthquakes in the order of 0.5 magnitude closer to their maximum possible magnitude more frequently than other magnitudes, and based on this new discovery the characteristic earthquake recurrence law emerged.

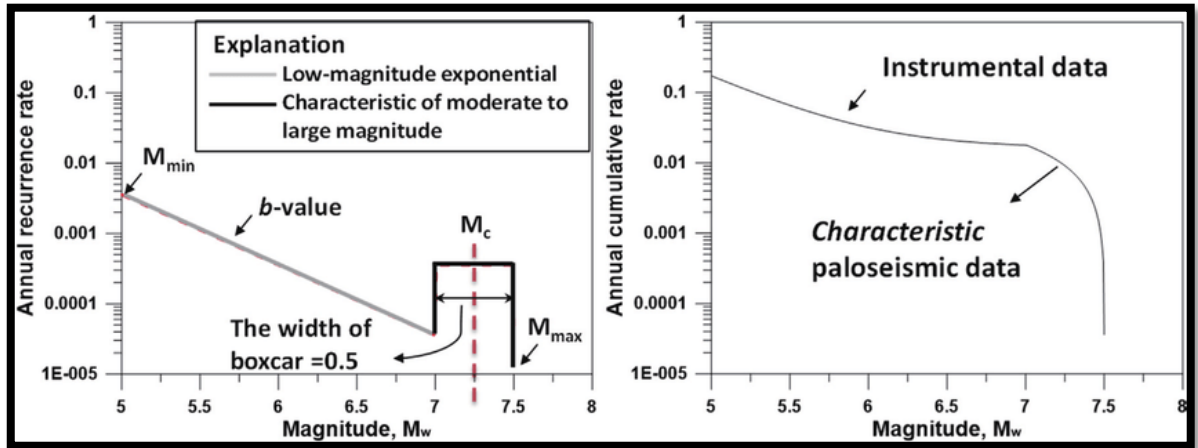


Figure 1. 8: The-Characteristic-Earthquake-Model-from-Youngs-and-Coppersmith-1985-On-the-a-is-theAnother recurrence law is the slip dependent recurrence law, this concerns the faults which have an important amount of annual slip, and it was noted that this slip had

In order to predict the intensity of future ground motions, it is necessary to use a ground motion prediction model, or what was previously known as attenuation relationships this model “predicts the probability distribution of ground motion intensity, as a function of many predictor variables such as the magnitude, distance , faulting mechanism, the near surface site conditions and the potential presence of directivity effects”(baker 2008).which means that the spatial and size uncertainties must be solved first to be used as input to solve the intensity uncertainty. And since this model is constructed using historical data which produces scattered and random results due to different soil conditions of the samples, uncertain results are inevitable and thus the use of probability distribution is unavoidable.

The probability that a ground motion parameter Y exceeds a certain value of y for an earthquake of magnitude M , occurring at a distance r is given by FEMA P58-1 as:

$$P(y) > y \{ m,r \} = 1-f_y(y) = 1-\theta \times \left[\frac{\ln y - \ln \theta}{\beta} \right] \quad (\text{Eq 5})$$

Where:

$FY(y)$: is the value of the cumulative distribution function of Y at m and r .

θ : is the median value of Y .

β : is the dispersion.

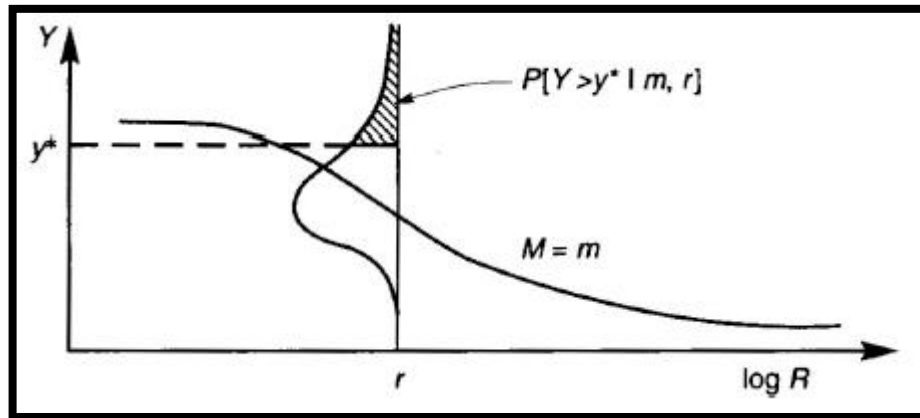


Figure 1. 9: Illustration of the conditional probability of exceeding a ground motion parameter (Kramer, 1996) [FEMA P58-1]

1.5.2.1.4 Temporal uncertainty

In order to compute the probability of occurrence of an earthquake given a certain location and magnitude in a predefined time period, a time distribution process must be assumed or computed, the most commonly used process in the Poisson process, which assumes that each earthquake event in random and independent from any previous events, this permits the description of the number of occurrences in an interval using a simple probability model.

This model is expressed in FEMA P58-1 for a PSHA as follows:

$$P[N=n] = \frac{(\lambda t)^n \times e^{-\lambda t}}{n!} \quad (\text{Eq 6})$$

Where:

λ : is the average rate of recurrence of the event.

t : is the time period.

Although the assumption of independence of events is not entirely correct, it produces negligible errors in most cases, there are however certain cases where different time probability models must be implemented. For example, in the case of time dependent earthquake events, where certain faults have time related characteristics, another case is that of faults which have surpassed their time of rupture.

1.5.2.2 PSHA steps

Since PSHA is a well-established method which has been improved on multiple occasions, its methodology is clear and well agreed upon by many standards, the FEMA P58-1 presents the PSHA in 4 major steps as follows:

1. Identify and characterize geometry and potential MW for all earthquake sources capable of generating significant shaking (i.e., $MW = 4.5$) at the site. Develop the probability distribution of rupture locations within each source. Combine this distribution with the source geometry to obtain the probability distribution of source-to-site distance for each source.
2. Develop a distribution of earthquake occurrence for each source using a recurrence relationship. This distribution can be random or time-dependent.
3. Using predictive models, determine the ground motion produced at the site (including uncertainty) for earthquakes of any possible magnitude, occurring at any possible point, in each source zone.
4. Combine the uncertainties in earthquake location, size, and ground motion prediction to obtain the probability that the ground motion parameter of interest (e.g., peak horizontal ground acceleration, spectral acceleration) will be exceeded in a particular time frame (i.e., 10% chance of exceedance in 50 years).

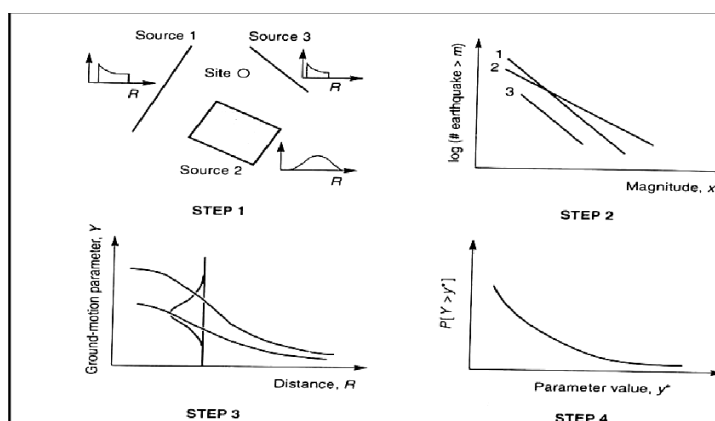


Figure 1. 10: Steps in probabilistic seismic hazard assessment (Kramer, 1996).

1.5.2.3 PSHA implementation

In order to initiate a PSHA a set of input data is necessary, this data is the site of the structure, and the rate of exceedance of interest, which is then combined with the previously mentioned uncertainties using the total probability theorem.

The first step is to compute the probability of exceeding a particular value of x in one source for a specific value of an intensity measure (IM) (this IM could be the spectral acceleration SA or the peak ground acceleration PGA).

$$P(IM > x) = \int_{m_{min}}^{m_{max}} \int_0^{r_{max}} P(IM > X|m, r) \times f_M(m) \times f_r(r) dr \times dm \quad (\text{Eq 7})$$

f_m : is the probability distribution function for the magnitude.

f_r : is the probability distribution function for the distance.

This is later multiplied by the annual rate of exceedance of having that particular earthquake emanating from the chosen source:

$$\lambda(IM > x) = \lambda(M > m_{min}) \int_{m_{min}}^{m_{max}} \int_0^{r_{max}} P(IM > X|m, r) \times f_M(m) \times f_r(r) dr \times dm \quad (\text{Eq 8})$$

And finally, this is done for every possible source, distance and magnitude combination using one the following equations which produce the same results:

$$\lambda(IM > x) = \sum / \lambda(M_I > m_{min}) \int_{m_{min}}^{m_{max}} \int_0^{r_{max}} P(IM > X|m, r) \times f_M(m) \times f_r(r) dr \times dm \quad (\text{Eq 9})$$

Or

$$\lambda(IM > x) = \sum / \lambda(M_I > m_{min}) \sum \sum P(IM > X|m_j, r_k) \times P(M_i, m_j) \times P(R_i, r_k) \quad (\text{Eq 10})$$

Where:

$n_{sources}$: the number of sources considered.

n_R : the number of distances considered.

n_M : the number of magnitudes considered.

1.5.2.4 DISAGGREGATION

Through using the PSHA all possible earthquakes are taken into consideration, this makes the choice of the most likely ground motion to occur hard, this can be solved using deaggregation(also known as disaggregation) this can be done for a given building site and hazard curve, by “establishing the combinations of magnitude, distance, and source that contribute most to particular values of an intensity. This process is termed deaggregation” (FEMA P59). this process helps us see that even in the same site, different ground motions can be used for design purposes with different situations (different sets of distances and magnitudes), an example of deaggregation results is shown in figure 4.5.

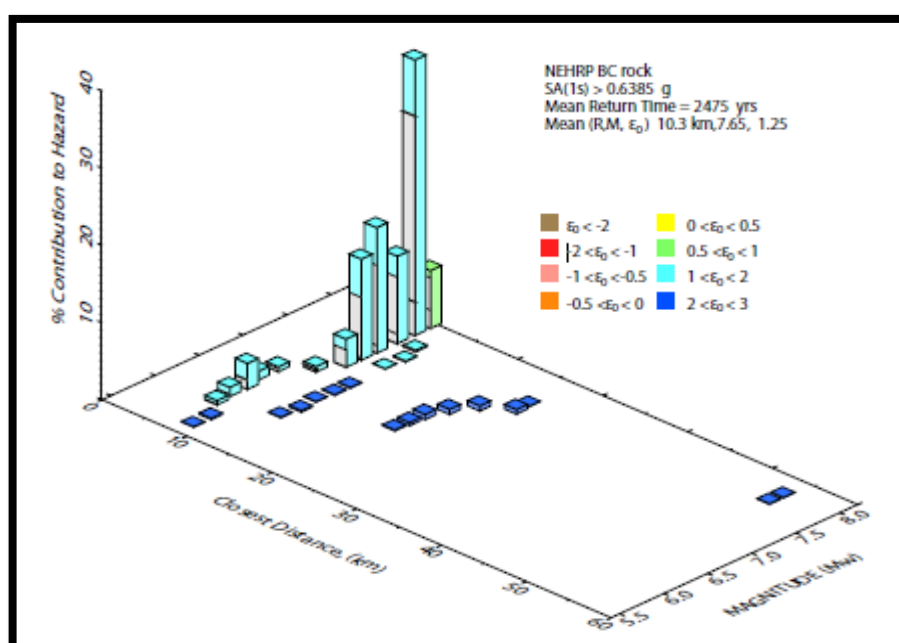


Figure 1. 11: Example disaggregation for Sa (1.0s) at a site in Palo Alto, California (USGS, 2008). [Baker 2015]

1.5.3 UNIFORM HAZARD ANALYSIS

Uniform hazard analysis (UHS) is one of the most commonly used outputs of the PSHA, this is largely due to its simplistic approach and application procedure, and its conservative nature which is also the main reason why it's largely criticized.

“This spectrum is called a uniform hazard spectrum because every ordinate has an equal rate of being exceeded. But it should be clear that this spectrum is an envelope of separate spectral acceleration values at different periods, each of which may have come from a different earthquake

Event” (baker 2008), which is the reason this spectrum does not represent any specific ground motion, but rather a culmination of many, and thus the probability of an earthquake having the properties of a UHS is null.

Steps to creating a uniform hazard spectrum:

Although the PSHA computations don't require a specific method, the most commonly used way of utilizing these results is through developing a UHS, this latter is created following 2 simple steps as follows:

1-defining the desired rate of exceedance for the construction at hand.

2-Combining hazard curves from individual periods to generate a uniform hazard spectrum.

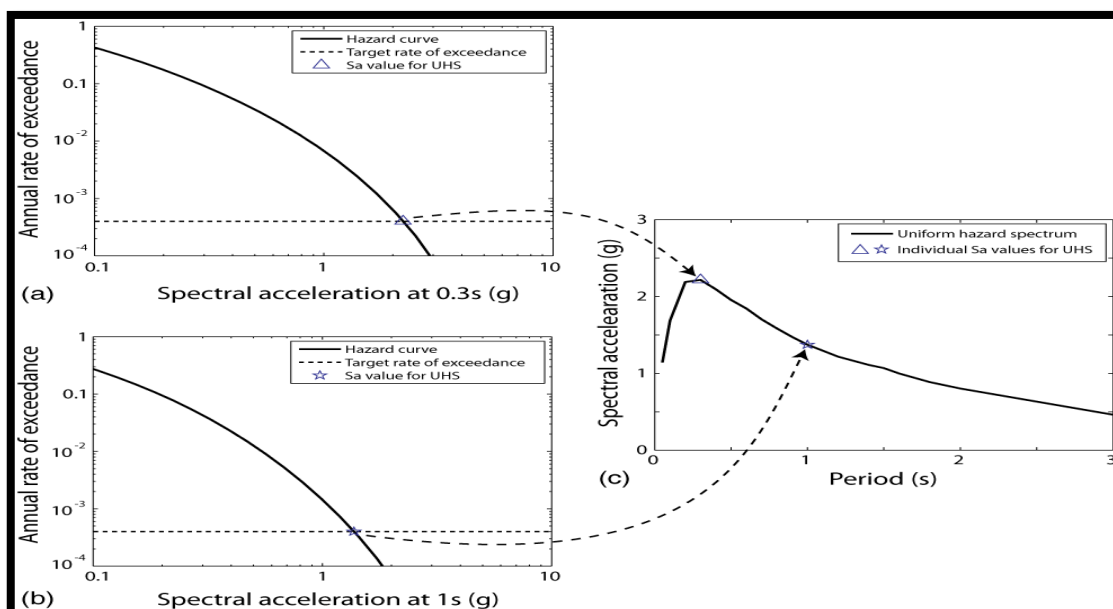


Figure 1.12: Combining hazard curves from individual periods to generate a uniform hazard spectrum with a $4 \cdot 10^{-4}$ rate of exceedance for a site in Los Angeles. (a) Hazard curve for SA(0.3s), with UHS point identified. (b) Hazard curve for SA(1s), with UHS point identified. (c) Uniform hazard spectrum, based on a series of calculations like those in (a) and (b). [baker 2008]

1.5.3.1 the advantages and the limitations of using UHS

this spectrum is still most commonly used due to its many advantages, among these are:

- this spectrum is much easier to develop, and it produces highly satisfactory results.
- in the case of structural behavior which is mainly controlled by the first mode of vibration, it is seen that using UHS or CMS is equivalent since both methods produce the same results.
- the UHS can be used as an additional safety measure, since it uses the envelop of all the considered ground motions.

But nonetheless new methods are emerging to account for the limitations that the UHS presents, these Limitations are as follows:

- no quantitative statements can be obtained from dynamic analysis that use UHS results.
- the UHS is considered too conservative, and thus economically inadequate.

1.5.4 CONDITIONAL MEAN SPECTRUM

In order to assess the performance of a structure it is necessary to scale ground motion records to match a typical target spectrum, in PSHA exists 2 commonly used target spectrums, one of which is the previously mentioned UHS and its recent counterpart the conditional mean spectrum(CMS),this spectrum “provides the expected mean response spectrum conditioned on the occurrence of a target spectral acceleration value at the period of interest”(baker, 2011),it also uses the site related data from the PSHA such as the magnitude, distance and epsilon as input.

Prior to the CMS there existed no other method that represented ground motions while maintaining their properties, another characteristic that the CMS has over its predecessor is its more accurate representation of collapse probabilities as opposed to the UHS which overestimates the demands of earthquake hazards and consequently increase the collapse probability.

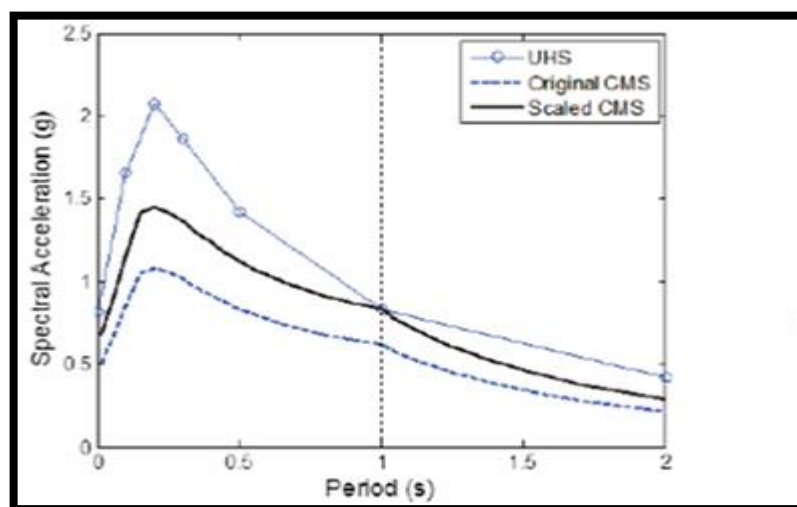


Figure 1. 13: uniform hazard spectrum with 2%probability of exceedance in 50 years, Conditional mean spectrum, and scaled conditional mean spectrum for a rock site in San Francisco.

(FEMA p58-1).

1.5.4.1 Creating a Conditional mean spectrum

Although this method is relatively new and unknown to many engineers, baker (2011) argues that this method is simple and can be computed in 4 easy steps:

1- Determine the target S_a at a given period, and the associated M , R and ε :

The first and foremost step is the definition of a target spectral acceleration S_a value, and the annual rate of exceedance of interest or its counterpart the return period T^* , this return period value can be selected from any period depending on the interest of the study but in most cases its chosen as the first mode period of the structure at hand, the next step consists of using the PSHA to obtain the site related data, mainly the magnitude M , the distance R and the epsilon ε Data, the mean values of these factors can be obtained from the deaggregation curves.

2-Compute the mean and standard deviation of the response spectrum, given M and R :

This step consists of computing the mean and standard deviation of acceleration values, under the assumption that these values have lognormal distribution. Since this is done for each period, the most commonly used approach is to use ground motion models to compute these values

$$\mu_{\ln.s_a}(M, R, T) \quad (\text{Eq 11})$$

$$\delta_{\ln.s_a}(T) \quad (\text{Eq 12})$$

3-Compute ε at other periods, given $\varepsilon(T^*)$:

In this step the assumption that the conditional mean ε values at different T_i periods are related to the ε value at T^* is set by analyzing a large set of ground motions and their respective ε values at different periods (see figure 4.8) this means that there exists a different correlation factor for each $\varepsilon(T_i)$ given $\varepsilon(T^*)$.

$$\mu_{\varepsilon(T_i) | \varepsilon(T^*)} = \rho(T_i, T^*) \varepsilon(T^*) \quad (\text{Eq 13})$$

Where:

$\mu_{\varepsilon(T_i) | \varepsilon(T^*)}$:the mean of $\varepsilon(T_i)$ given $\varepsilon(T^*)$.

$\rho(T_i, T^*)$: is the correlation factor.

This correlation factor can be computed using the following relation developed by (baker and Jayaram 2008):

$$\text{If } T_{\min} < 0.109 \quad \rho_{\tau}(T_1), \tau(T_2) = C_2$$

$$\text{Else if } T_{\min} > 0.109 \quad \rho_{\tau}(T_1), \tau(T_2) = C_1$$

$$\text{Else if } T_{\max} < 0.109 \quad \rho_{\tau}(T_1), \tau(T_2) = \min(C_2, C_1)$$

$$\text{Else} \quad \rho_{\tau}(T_1), \tau(T_2) = C_4$$

Where :

$$T_{\min} = \min(T_1, T_2), \quad T_{\max} = \max(T_1, T_2), \text{ and}$$

$$C_1 = 1 - \cos \left[\frac{\pi}{2} - 0.366 \ln \left(\frac{T_{\max}}{\max(T_{\min}, 0.11)} \right) \right]$$

$$C_2 = 1 - 0.105 \cdot 1 \left[\frac{1}{1 + e^{100T_{\max} - 5}} \right] \left[\frac{T_{\max} - T_{\min}}{T_{\max} - 0.01} \right], \text{ if } T_{\max} < 0.2 \text{ sec}$$

0, Otherwise

$$C_3 = C_2 \text{ if } T_{\max} < 0.11 \text{ sec}$$

$$C_1 \text{ if } T_{\max} > 0.11 \text{ sec}$$

$$C_4 = C_1 + 0.5(\sqrt{C_3} - C_3) \cdot 1 + \cos \left[\frac{\pi T_{\min}}{0.11} \right]$$

These equations are valid for a period range of 0.01 to 10 seconds, another simpler equation which produces nearly equivalent results but for a smaller range of periods (0.01 to 5sec) is available in (baker, 2011):

$$P(T_{\min}, T_{\max}) = 1 - \cos \frac{\pi}{2} - (0.359 - 0.163I(T_{\min})) \ln \frac{T_{\min}}{0.189} \ln \frac{T_{\max}}{T_{\min}} \quad (\text{Eq 14})$$

Where:

$I(T_{\min} 0.189)$: is indicator function equal to 1 if $T_{\min} < 0.189$ s and equal to 0 otherwise.

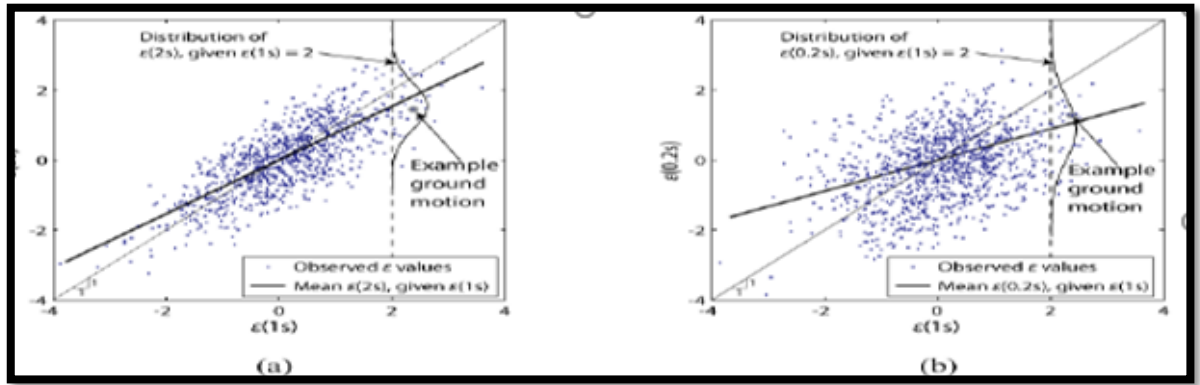


Figure 1. 14: scatter plots of values from a large suite of ground motions. The points associated with the ground motion in figure 5 are highlighted. (a) (1s) versus (2s): (b) (1s) versus (0.2s) (baker, 2008).

1.5.4.2 compute Conditional Mean Spectrum

the CMS can now be constructed Using the previous steps and the following formula, the exponential of $\mu_{lnsa}(T1) lnsa(T^*)$ gives us the Conditional Mean spectrum as shown in figure ():

$$\mu_{lnsa}(T1) lnsa(T^*) = \mu_{lnsa}(M, R, Ti) + \rho(Ti, T^*)\epsilon(T^*)\delta_{lnsa}(Ti) \quad (Eq 15)$$

Where:

$\mu_{lnsa}(M, R, Ti)$: the predicted mean deviation from equation 11.

$\delta_{lnsa}(Ti)$: the predicted standard deviation from equation 12.

$\rho(Ti, T^*)$: the correlation factor either from equation 14 or 15.

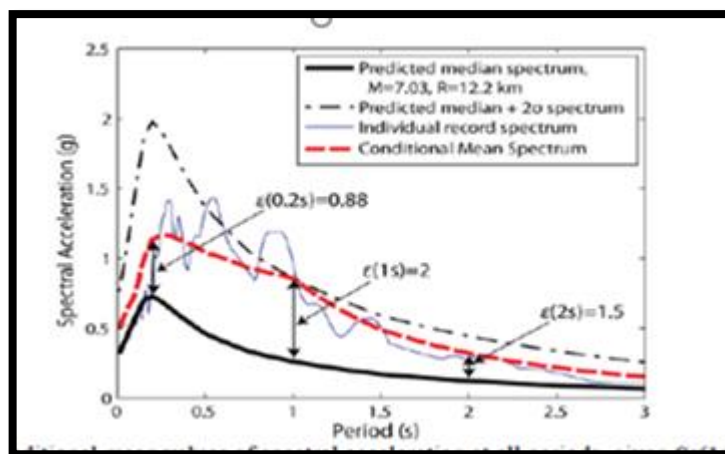


Figure 1. 15: conditional mean values of spectral acceleration at all periods, given sa (1s), and the example castaie old ridge route ground motion. (Baker 2008)

1.5.4.3. The advantages and disadvantages of CMS

The CMS is an emerging methodology which came as a result of previous works, and has capitalized on that specific aspect, some of its many advantages are mentioned as follows:

- the CMS is a more realistic spectrum, compared to other spectrums, this is largely due to the fact that the CMS uses deagration and epsilon data which have not been previously used in other target spectrums.
- conserves the spectral shape of ground motions, this is also done using the epsilon factor.
- “maintains the probabilistic rigor of PSHA, so that consistency is achieved between the PSHA and the ground motion selection This enables one to make quantitative statements about the probability of observing the structural response levels obtained from dynamic analyses that utilize this spectrum” [baker ,2011]
- “it has been noticed that even though scaling ground motions changes their features for no obvious physical reasons, the CMs scaled earthquakes maintain the same results (displacements) as those accelerograms that were not scaled”. [baker ,2011]
- another huge advantage the CMS has over the previously used spectrums, is its economical approach, since many spectrums used the largest credible ground motions or other safety measures, many of the measures proved to be inadequate in certain situation.

But although this method has many advantages, it still struggles to be as widely used as the UHS for example, some of the reasons for that are:

- The economical aspect which is one of its main selling points, is also one of the reasons it's not as widely used as it should have been, this is due to the fact that certain engineers and practitioners prefer to use more safety measures.
- The CMS is harder to scale than its predecessor, which makes it harder to use, although its creator debates that the CMS is easier to use than the UHS, many tend to disagree.
- This method is site specific, meaning that many CMS need to be developed for each region depending on its properties.

1.6. Conclusion

In this chapter a set of notions used during this work are presented in the form of vulnerability and seismic fragility, also the effects of earthquakes on healthcare facilities are shown, and thus explaining the importance of this study, later on the objectives are discussed thoroughly. this helped in the execution of this work and improved its precision considerably.

The selection of tools used throughout this study largely depended on their availability, quality and the time necessary to execute them, this is critical for the study's result, since in the case of ground motion selection it was seen that using a UHS was possible, due to the fact that there existed previous works which developed this curve for the Algerian states, including Blida, unlike the CMS, which no previous curve was developed and therefore it's impossible to use in this study unfortunately.

Chapter 02:

Nonlinear analysis of structural systems

2. Introduction

Nonlinear analysis is a powerful tool for fragility curve development, however if used with the inappropriate material models, it loses most of its potential, these material models, or stress strain model must present the behavior of that material beyond the elastic range and take into account all and any effects of high stress. In this chapter these models are defined in detail, highlighting their important contribution to the fragility curve development process.

2.1 Materials

2.1.1 Steel

Steel is an iron alloy with a small percentage of carbon, its main advantages are in terms of tension, compression and shear. In this study FeE400 was used in accordance with the existing plans. (see Figure 2.2)

2.1.1.1 Stress-strain model

For the aims of this work, the use of a more sophisticated model was necessary, therefore the Menegeto-Pinto steel model with Monti-Nuti (figure 2.1) post elastic buckling was chosen, since the objectives were to assess the performance of the structures at hand beyond their elastic range.

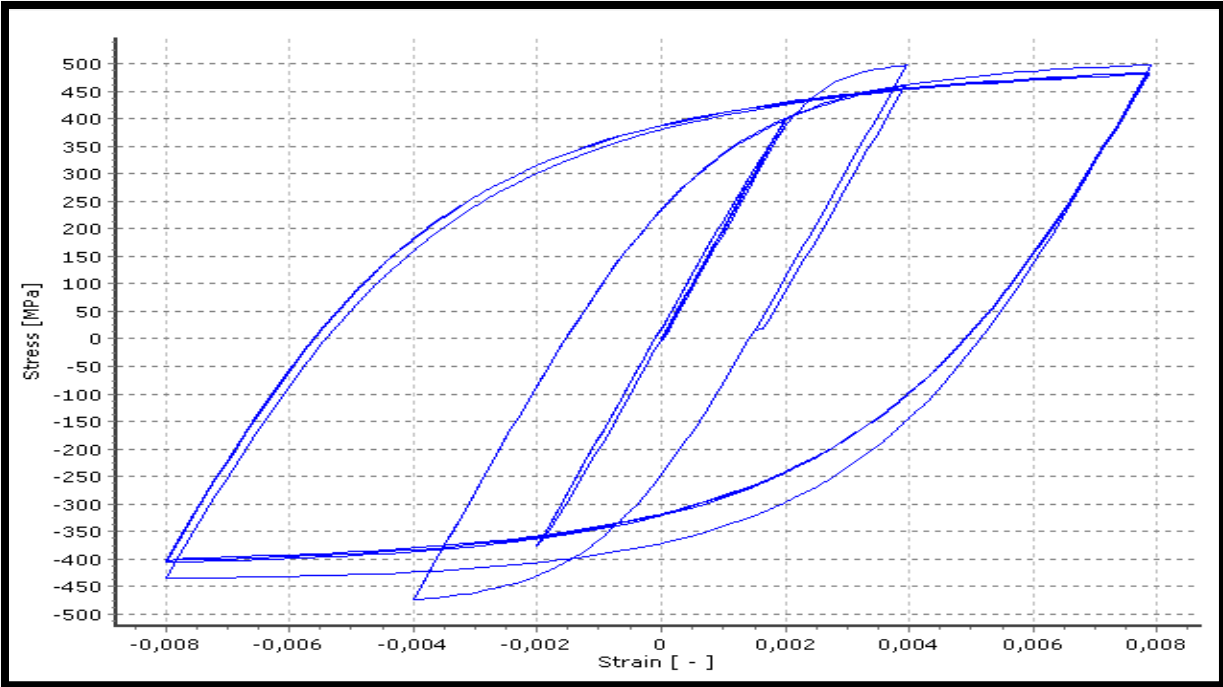


Figure 2. 1: Menegeto-Pinto steel model with Monti-Nuti post elastic buckling (SeismoStruct 2020).

Modulus of elasticity (kPa)	2,0000E+008
Yield strength (kPa)	500000,00
Strain hardening parameter (-)	0,005
Transition curve initial shape parameter (-)	20,00
Transition curve shape calibrating coeff. A1 (-)	18,50
Transition curve shape calibrating coeff. A2 (-)	0,15
Kinematic/isotropic weighting coefficient (-)	0,90
Spurious unloading corrective parameter (%)	2,50
Fracture strain (-)	0,10
Specific Weight (kN/m ³)	78,00

Figure 2. 2: steel parameters extracted from SeismoStruct 2020.

2.1.2 Concrete

As the most used material for construction, concrete is mainly used due to its compressive strength, low cost and easy maintenance.

2.1.2.2 Stress-strain model

-compressive strength

The compressive strength of concrete f_{cj} in j days is determined by standardized test tubes, with a 16cm diameter and a 32cm height.

For these structures, the compressive strength is estimated at 25mpa(28days).

concrete properties are presented in the next 2 figures (Figure 2.3 and Figure 2.4):

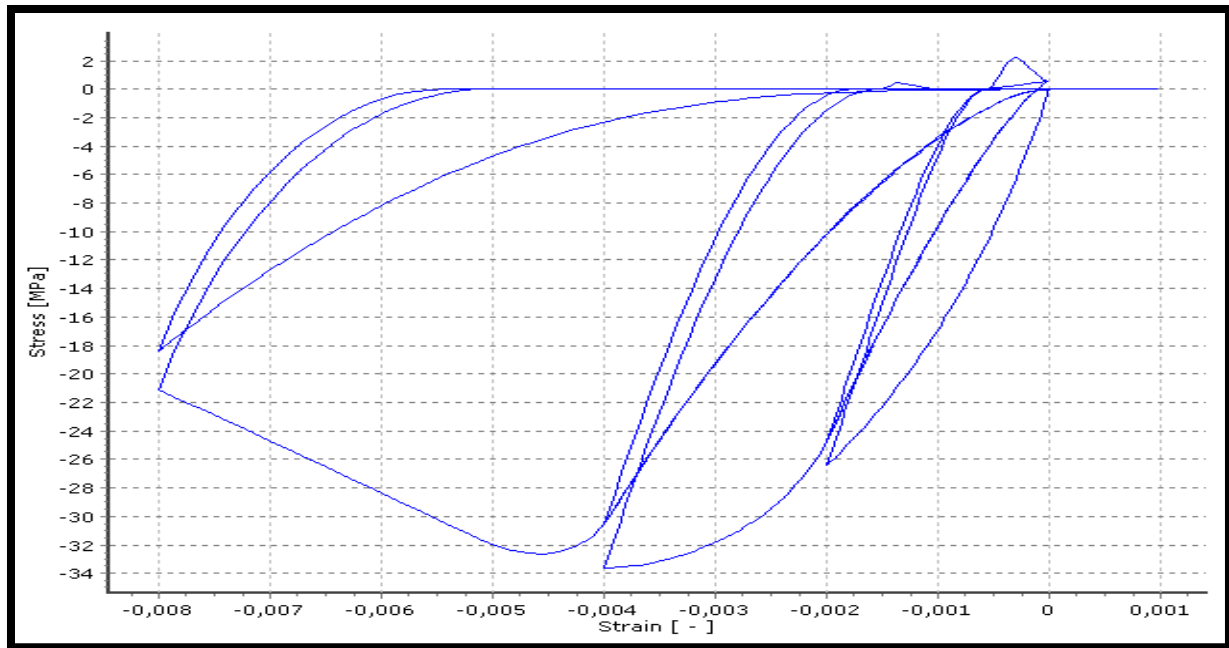


Figure 2. 3: the Chang and Mander nonlinear concrete stress strain model (SeismoStruct 2020).

Mean Compressive strength (kPa)	28000,00
Mean Tensile strength (kPa)	2200,00
Modulus of elasticity (kPa)	2,2960E+007
Strain at peak compressive stress (m/m)	0,002
Strain at peak tensile stress (m/m)	0,0002
Nondimensional critical compressive strain	1,30
Nondimensional critical tensile strain	3,00
Specific Weight (kN/m ³)	24,00

Figure 2. 4: the characteristics of concrete extracted from SeismoStruct 2020.

2.2. Inelastic infill panels

In this study inelastic infill panels were used, to achieve a more realistic model by taking into account their effect on the overall structural behavior. The Cristafulli (1997) model was used since it presented the model with highest ratio of effectiveness over complexity. Each panel is represented by six strut members; each diagonal direction features two parallel struts to carry axial loads across two opposite diagonal corners and a third one to carry the shear from the top to the bottom of the panel. This latter strut only acts across the diagonal that is on compression, hence its "activation" depends on the

deformation of the panel. The axial load struts use the masonry strut hysteresis model, while the shear strut uses a dedicated bilinear hysteresis rule. (SeismoStruct, 2020)

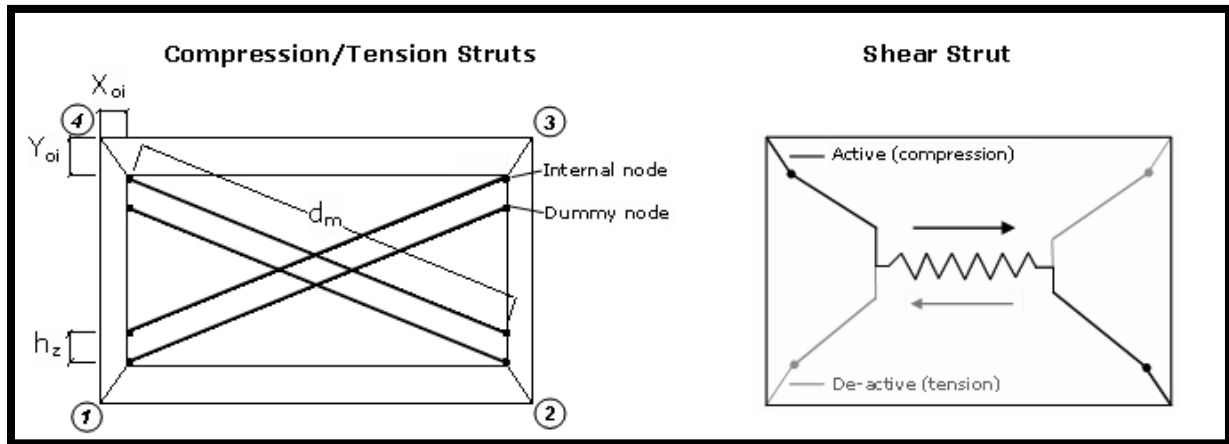


Figure 2. 5: Cristafully 1997 inelastic-infill panel model (SeismoStruct manual)

2.2.1. Infill panels parameters

Since no material test were made for this study the infill strut and shear curve parameters were taken as standard units. And the infill panels geometric characteristics were taken from the existing data. The properties are as follows:

Strut Curve Parameter(s)	300,00 0,70 600,00 1,50
Shear Curve Parameter(s)	1,6000E+006 1000,00 0,00 0,0012 0,024 0,004 0,0006 0,001 1,50 0,20
Panel Thickness t (m)	0,20
Out-of-plane failure drift (% of vert. panel side)	5,00
Strut Area 1 (m2)	0,334
Strut Area 2 (% of Strut Area 1)	60
Equival. contact length hz (% of vert. panel side)	33,33
Horiz. offset xo (% of horiz. panel side)	5,83
Vert. offset yo (% of vert. panel side)	12,53
Proportion of stiffness assigned to shear (%)	20,00
Specific Weight (kN/m3)	20,00

Figure 2. 6: inelastic infill panels characteristics extracted from SeismoStruct 2020.

Where:

strut area A1: the product of the panel thickness and the equivalent width of the strut (bw).

bw: the equivalent strut width of the infill panels.

Strut area A2: is taken a percentage of A1, and represents the effect of cracking on the panels.

2.3. Modelling

in this study SeismoStruct 2020 was used, it's a finite element package capable of predicting structural nonlinear behavior under static or dynamic. The software accounts for both material and geometric nonlinearities.

2.3.1 SeismoStruct

SeismoStruct is an award-winning Finite Element package capable of predicting the large displacement behaviour of space frames under static or dynamic loading, taking into account both geometric

nonlinearities and material inelasticity. Concrete, steel, masonry, Fiber Reinforced Polymer (Frp) and Shape memory alloys(sma) material models are available, together with a large library of 3D elements that may be used with a wide variety of pre-defined steel, concrete and composite section configurations. It is a civil engineering software for structural assessment and structural retrofitting that has been extensively quality-checked and validated.

It provides Nine different types of analysis: nonlinear dynamic and static time-history, conventional and adaptive pushover, incremental dynamic analysis, eigenvalue, non-variable static loading, response spectrum and buckling analysis. And in terms of hysteretic models there are Thirty-one hysteretic models, such as linear/ bilinear/ trilinear kinematic hardening response models, gap-hook models, soil-structure interaction model, Takeda model, Ramberg-Osgood model.

It also provides a huge set of Capacity checks in the form of chord rotation and shear which can be performed, according to Eurocode 8 along with the majority of the available National annexes, ASCE 41-17 (American Code for Seismic Evaluation and Retrofit of Existing Buildings), NTC-18 (Italian National Seismic Code), NTC-08 (Italian National Seismic Code), KANEPE (Greek Seismic Interventions Code) and TBDY (Turkish Seismic Evaluation Building Code) in reinforced concrete structures and for all the limit states of the specified codes.

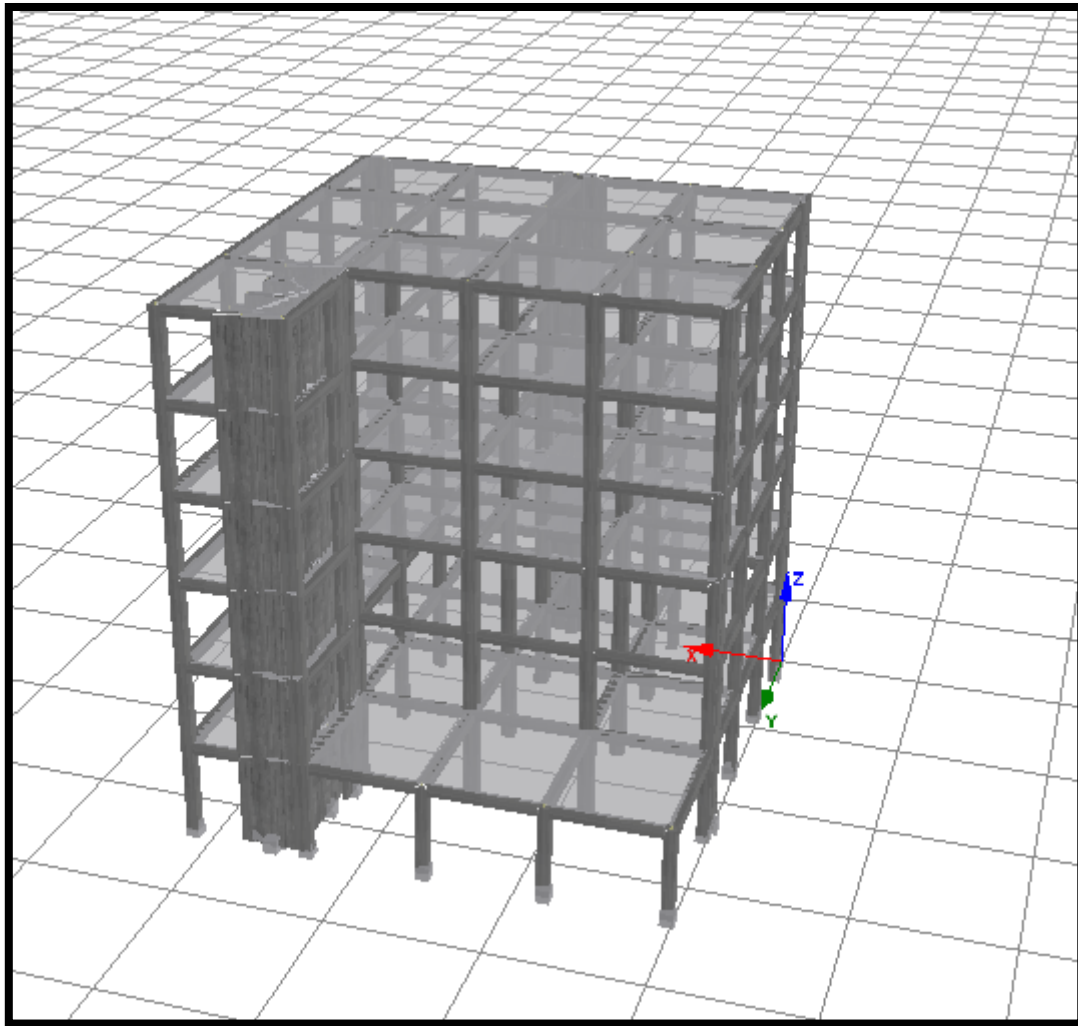


Figure 2. 7: 3D numerical model example of an RC building by SeismoStruct

2.4. Nonlinear analysis

A deeper understanding of structural behaviour has always been the aim of both researchers and civil engineers, and although there existed multiple methods previously, these methods were more or less rudimentary, and with the lack of knowledge of the effects of earthquakes on structures, many important factors were left out, making the design either conservative or inadequate. However, a more appropriate alternative existed in the form of nonlinear analyses, which presented more realistic behaviour of the structure. Since they provided the means for calculating the structural response beyond the elastic range, including strength, stiffness deterioration associated with inelastic material behaviour and large displacements (Reinhorn et al., 2010). Although these methods still have many assumptions, they presented more satisfactory approaches, however these later were not commonly used up until the last few years, since most nonlinear analyses required certain equipment that was not commonly available until such time, and therefore nonlinear analysis is a relatively new tool.

2.4.1. Typical uses of nonlinear analysis

There exists a large variety of applications for nonlinear analysis. The most commonly applications are as follows according to (Reinhorn et al, 2010):

- assess and design seismic retrofit solutions for existing buildings.
- design new buildings that employ structural materials, systems or other features that do not conform to current Building code requirements.
- assess the performance of building for specific owner/stake holder requirements.

2.4.2. Nonlinear Static analysis

One of the two branches of nonlinear analysis, which is the static analysis also known as pushover analysis, consists of subjecting the structural model to an incremental load whose distribution represents the inertial forces expected during ground motion shaking. This load is then increased until the target displacement is reached. The target displacement represents the displacement that the ground motion would inflict on the structure (Reinhorn et al., 2010), and thus the structural behaviour can be analysed.

There exist multiple nonlinear static analyses, but the most widely used methods are the capacity spectrum method, and the coefficient method.

According to Reinhorn et al. (2010) static analysis can be useful to:

- (1) check and debug the nonlinear analysis model.
- (2) augment understanding of the yielding mechanisms and deformation demands.
- (3) investigate alternative design parameters and how variations in the component properties may affect response.

The nonlinear static analysis has other pros such as:

- it is much easier to use, since it requires less developed equipment, and is available in most commercial softwares.
- It produces reliable results equivalent to nonlinear dynamic analysis in the case of low-rise buildings and regular.
- it can be used to assess non-structural elements as well.

2.4.2.1. Disadvantages of static nonlinear analysis

While many of its disadvantages are up for discussion, the main upside to using the pushover analysis is that the procedure should be used in the case of low-rise structures (Usually less than five stories) since the response is dominated by the fundamental mode of vibration. Thus, it doesn't take torsional vibration modes into consideration, and while new modifications emerged to compensate for these two points, it is still seen that the procedure requires other improvements to attain the same level of accuracy as its dynamic counterpart.

2.4.3. Nonlinear Dynamic analysis

When trying to understand the structural behaviour, the dynamic nonlinear analysis is the most Adequate, since it produces more accurate results than its static counterpart. This is because it presents lesser assumptions, and takes into account the hysteretic energy dissipation and other factors as well, and uses recordings of earthquakes instead of using increasing lateral forces, which produces better results.

There exist multiple nonlinear dynamic analyses, some of the most widely used methods are the time history analysis (THA), the multiple stripes analysis, and the incremental dynamic analysis (IDA) which is also known as the dynamic pushover analysis.

2.4.3.1. The advantages of nonlinear dynamic analysis

In a time where multiple methods and approaches are available of structural design/performance assessment, dynamic time history analysis is one of the most powerful tools, this is due to its many advantages, some of which are:

- more accurate than static Nonlinear analysis.
- it has lesser assumptions than static Nonlinear analysis.
- it accounts for the dynamic structural behaviour.
- it accounts for hysteretic energy dissipation and torsional vibration modes.

2.4.3.2 The disadvantages of nonlinear dynamic analysis

Although it has many advantages, the dynamic time history analysis is still not as popular as it should have been, since it provides more advantages than most other analyses. this is due to the fact that some of its defects still hinder its wide use, these defects are:

- most engineers are not familiar with its procedures.

- single dynamic analysis results are deterministic and thus multiple analyses are required, due to the fact that earthquakes with equivalent intensities tend to produce different results and a statistical approach is needed.

-analysing the results requires individuals with a deep understanding of structural seismic behaviour.

-requires expensive equipment, and not all commercial softwares provide it.

2.5. Limit states

When using nonlinear analysis certain limit states are needed to assess the structural behaviour more effectively, namely there are multiple limit states depending the standards but the four main limit states are:

Immediate Occupancy: Achieve essentially elastic behaviour by limiting structural damage (e.g., yielding of steel, significant cracking of concrete, and non-structural damage.)

Life Safety: Limit damage of structural and non-structural components so as to minimize the risk of injury or casualties and to keep essential circulation routes accessible.

Collapse Prevention: Ensure a small risk of partial or complete building collapse by limiting structural deformations and forces to the onset of significant strength and stiffness degradation.

Sideways collapse: it is the complete collapse of the building and the total loss of strength and stiffness degradation; it represents the coordinate E in the backbone curve (see figure2.8)

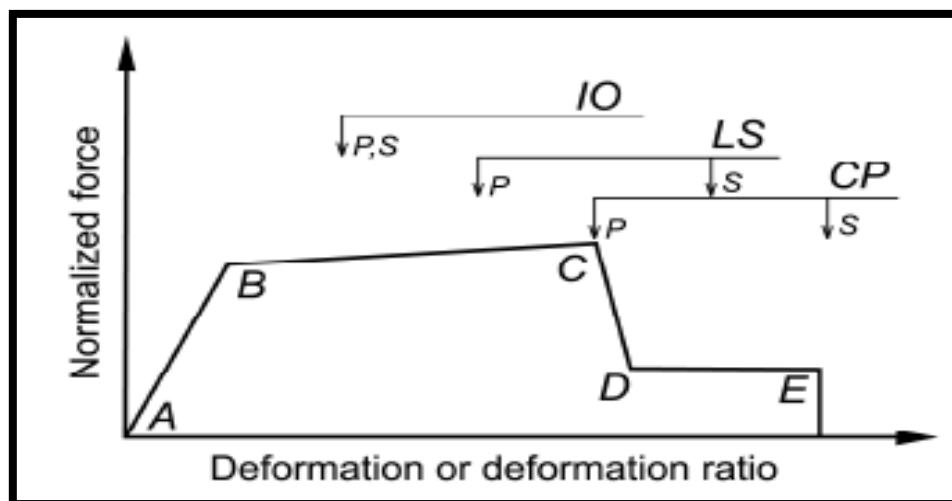


Figure 2. 8: Component or element deformation acceptance criteria (FEMA 356, 2000)

2.6. Hinges

Basically, a hinge represents localized force-displacement relation of a member through its elastic and inelastic phases under seismic loads. For example, a flexural hinge represents the moment-rotation relation of a beam of which a typical one is as represented (Grierson et al., 2008) as seen in the previous figure there are 4 segments in the Force-Deformation curve, where:

Segment AB represents the linear elastic range from unloaded state A to its effective yield B, followed by an inelastic but linear response of reduced (ductile) stiffness from B to C. CD shows a sudden reduction in load resistance, followed by a reduced resistance from D to E, and finally a total loss of resistance from E to F. Hinges are inserted in the structural members of a framed structure typically as shown in Fig.2.8 These hinges have non-linear states defined as ‘Immediate Occupancy’ (IO), ‘Life Safety’ (LS) and ‘Collapse Prevention’ (CP) within its ductile range. This is usually done by dividing B-C into four parts and denoting IO, LS and CP, which are states of each individual hinge (in spite of the fact that the structure as a whole too have these states defined by drift limits)” (Grierson et al., 2008).

However, there is a dispute on the segment BC, which criteria should be used to divide it. For instance, one such specification is at 10%, 60%, and 90% of the segment BC for IO, LS and CP respectively (Inel & Ozmen, 2006).

2.7. Selected nonlinear analyses

2.7.1. Introduction

Seeing that the aim of this study, and the tools present in the authors disposal, two nonlinear analyses were selected based on their merits, the first one is the Static nonlinear analysis, due to its many positive aspects which are mentioned next, and the Incremental dynamic analysis which is the same as the SPO, widely used for fragility curves development and thus these two analyses are adequate for the study’s objectives.

2.7.2 The pushover analysis

In terms of nonlinear analyses, one of the most widely used methods is the Static Pushover Analysis (SPO). This is largely due to its simplistic approach and easy to understand results, since the model is pushed horizontally with an increasing force until collapse, this procedure leads to exposing the weak points of the model, which can then be rectified, or in the case of an existing structure fortified.

2.7.2.2 The objectives

When the SPO analysis was recognized, it was mainly used for structural assessment of existing structures, but later many standards chose to include it as a design tool. The SPO has a large variety of applications, among these applications we mention:

- Understanding the consequences of elements deterioration on the overall structure.
- Pinpoint the structures weak points (elements or joints).
- Estimation of the demands and the displacements during a nonlinear analysis.

2.7.2.3. The methodology

The main assumption in the SPO method is that the response of a MDOF system can be assimilated using a SDOF system with equivalent characteristics. This suggests that the first vibrational mode is the dominant mode and that the spectral shape of the first mode is constant throughout the whole analysis.

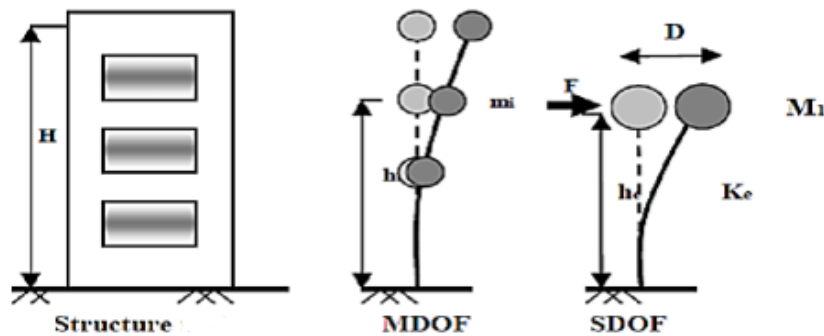


Figure 2. 9: a SDOF system equivalent to a MDOF model (Eurocode 8-1)

According to Eurocode 8-1, the following relation between normalized lateral forces F_i and normalized displacements θ_i is assumed:

$$F_i = m_i \times \theta_i \quad (\text{Eq 16})$$

where m_i is the mass in the i -th storey.

Transformation to an equivalent SDOF system:

The mass of an equivalent SDOF system m_i is determined as:

$$m^* = \sum m_i \times \theta_i = \sum F_i \quad (\text{Eq 17})$$

And the transformation factor is given by:

$$\Gamma = \frac{m^*}{\sum m_i \times \theta_i} = \frac{\sum F_i}{\sum \left(\frac{F_i^2}{m_i}\right)} \quad (\text{Eq 18})$$

The force F^* and displacement d^* of the equivalent SDOF system are computed as:

$$F^* = \frac{f_h}{\Gamma} \quad (\text{Eq 19})$$

$$d^* = \frac{d_n}{\Gamma} \quad (\text{Eq 20})$$

where f_h and d_n are, respectively, the base shear force and the control node displacement of the multi-degree of freedom (MDOF) system.

2.7.2.4. Determination of the target displacement

There are multiple approaches on computing the target displacement, for example in the case of ASCE 41-17, the next formula is used as tool:

$$\delta_I = C_0 \times C_1 \times C_2 \times S_A \frac{T_e^2}{4\pi^2} g \quad (\text{Eq 21})$$

Where:

S_A : the response spectrum acceleration at the effective fundamental period of vibration.

g : the acceleration of gravity.

C_0 : Modification factor to relate spectral displacement of an equivalent single-degree-of-freedom (SDOF) system to the roof displacement of the building multiple degree of Freedom (MDOF)

C_1 : Modification factor to relate expected maximum inelastic displacements to displacements calculated for linear elastic response calculated.

C_2 : Modification factor to represent the effect of pinched hysteresis shape, cyclic stiffness degradation, and strength deterioration.

T_e : the fundamental period.

According to FEMA 356 the following values are suggested:

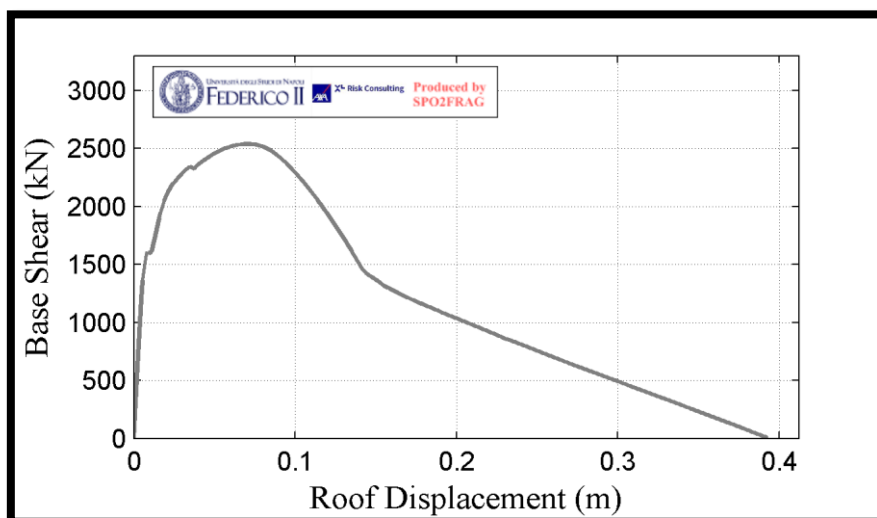
Table 2 1: performance limit states (FEMA 356, 2000)

Structural Performance levels	Permissible Top Story Drift in %
Immediate Occupancy (IO)	1%
Life Safety (LS)	2%
Collapse Prevention (CP)	4%

Note that the latter was used since the structure was not constructed using the ASCE requirements and given the purposes of this work (which is to determine the fragility functions of multiple constructions) it was deemed that using the FEMA 356 approach is more adequate and straight forward.

2.7.2.5. The pushover curves

After performing the SPO analysis, the results are usually displayed in the form of a force-displacement curve. This curve represents the base shear versus the control node displacement (which is most of the times selected as the node located in the last level at the centre of the mass).

**Figure 2. 10:** a typical pushover curve.

According to FEMA 356, the nonlinear force-displacement relationship between base shear and displacement of the control node shall be replaced with an idealized relationship to calculate the effective lateral stiffness, K_e , and effective yield strength, V_y , of the building as shown in Figure 2.10. This relationship shall be bilinear, with initial slope, K_e and post-yield slope α . Line segments on the idealized force-displacement curve shall be located using an iterative graphical procedure that approximately balances the area above and below the curve. The effective lateral stiffness K_e , shall be taken as the secant stiffness calculated at a base shear force equal to 60% of the effective yield strength of the structure. The post-yield slope, α , shall be determined by a line segment that passes through the actual curve at the calculated target displacement. The effective yield strength shall not be taken as greater than the maximum base shear force at any point along the actual curve.

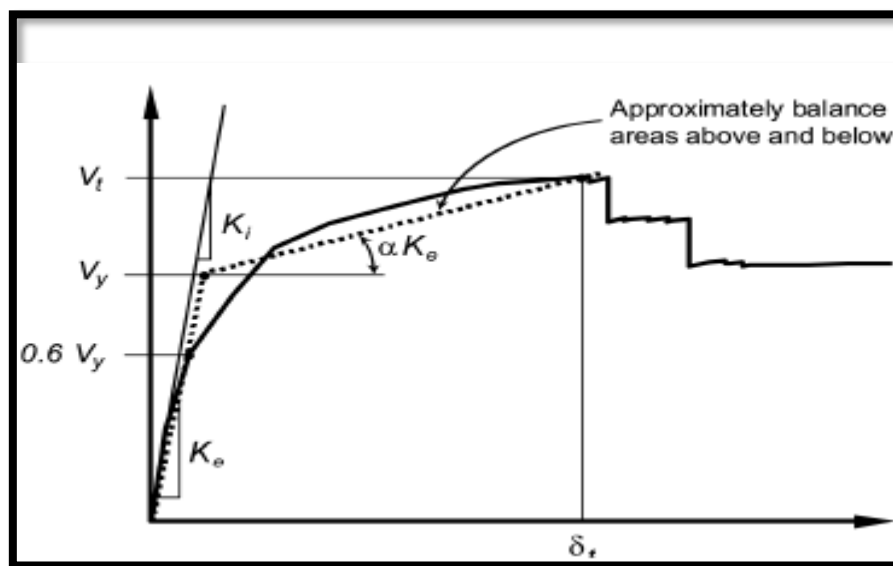


Figure 2. 11: Idealized Force-Displacement Curves FEMA 356

2.7.3 Incremental dynamic analysis (IDA)

Since the start of structural engineering, the main aim was to attain a better understanding of structural behaviour and the implementation of certain methods using this understanding to better safeguard structures from collapse. This quest has seen some increase in momentum in the last few years when technological advancement intensified. Incremental Dynamic Analysis (IDA) is one of those methods/tools that emerged in the last few years, which required strong technical equipment, but in return produced results, which were helpful in assessing collapse fragility more thoroughly, among other features. It involves subjecting a structural model to one (or more) ground motion record(s), each scaled to multiple levels of intensity, thus producing one (or more) curve(s) of response parameterized versus intensity level Vamvatsikos and Cornell (2002). This idea was inspired by the static pushover (SPO) analysis, and thus the IDA is also known as the dynamic pushover analysis.

In accordance with FEMA P58-1 a large number of ground motions (20 pairs or more) is suggested in order to develop collapse fragility more accurately, however there exists other simplified procedures where a smaller set of ground motions can be used, or a smaller number of scales can be used and then using lognormal distribution, collapse fragility is estimated.

2.7.3.1 The objectives of the IDA

According to Vamvatsikos and Cornell (2002), IDA is mainly used for:

- 1- Thorough understanding of the range of response or “demands” versus the range of potential levels of a ground motion record,
- 2- Better understanding of the structural implications of rarer / more severe ground motion levels,
- 3- Better understanding of the changes in the nature of the structural response as the intensities of ground motion increases (e.g., changes in peak deformation patterns with height, onset of stiffness and strength degradation and their patterns and magnitudes),
- 4- Producing estimates of the dynamic capacity of the global structural system and
- 5- Finally, given a multi-record IDA study, how stable (or variable) all these items are from one
- 6- Ground motion record to another.

2.7.3.2 IDA procedure

This methodology is described in FEMA P58-1 and FEMA P695, and it is conducted as the following steps:

- 1- Construct a mathematical model representing the structure;
- 2- 2. Select an appropriate suite of ground motion pairs that represent scenario events likely to result in collapse of the structure, considering the site seismic hazard;
- 3- Scale the ground motion suite such that the mean spectral acceleration at the first mode period of the structure, $SA(T)$ for each pair is at a value low enough for inelastic response to be negligible;
- 4- Analyze the mathematical model for each scaled ground motion pair and determine the maximum value of story drift;
- 5- Increment the intensity of the effective first mode spectral response acceleration $SA(T)$ to which each ground motion pair is scaled;
- 6- Analyze the structure for each incrementally scaled ground motion pair and record the maximum value of story drift;
- 7- Repeat Steps 5 and 6 above for each ground motion pair until the analysis: a. produces a very large increase in drift for a small increment in the value of intensity, indicating the onset of dynamic instability;
 - a. results in numerical instability suggesting collapse;

- b. results in predicted demands on gravity-load carrying components that exceed their reliable capacities; or
 - c. predicts drift levels that exceed the range of model validity
- 8- Determine the value of spectral acceleration $SA(T)$ at which 50% of the ground motion pairs produce predictions of collapse. This value of $SA(T)$ is taken as the median collapse capacity;
- 9-Determine a dispersion for the collapse fragility.

2.8. Conclusion

In this chapter two stress strain models were selected, the Menegeto Pinto with Monti-nuti post elastic buckling was selected for the steel since it takes into account the buckling of the construction steel beyond the elastic limit, and for the concrete the Chang and Mander nonlinear concrete stress strain model was selected to represent the nonlinear behaviour of concrete more accurately, another material related factor taken into consideration is the infill panel behaviour, and it was seen that the Cristafully inelastic panels model was an adequate model of the inelastic behaviour of panels without further delving into more complicated models which resulted into similar results at the expense of more time consumption and more computation capacities which were not available during the works of this study.

Finally, the IDA and SPO were chosen for the fragility curve development since the two methods are closely related in terms of the concept used in both of them, where they consist of increasing the seismic load gradually (either through lateral forces or ground motions) until collapse which befits the study's objectives.



Chapter 03:

Presentation of healthcare building case studies

3.1 Introduction

Since this study is aimed at testing the performance and the vulnerability of healthcare facilities in the state of Blida, this chapter aims to present said facilities that were once considered for the final step, each with its relevant data, this is done to highlight the process with which the final models were selected, and shows the non-used models, and explains the reasons for their non-inclusion.

3.2 The considered models

In this section all of this considered models, are shown and some of their properties, and data are presented, and then the process of selection is determined based on the objectives of this study.

3.2.1 The collected data

As the first step of this work was to collect all of the necessary data of healthcare facilities of the state Blida, 8 facilities were visited and a survey was filled about the working staff and the number of patients, and last not but not least the architectural plans, steel detailing and the materials of construction were obtained as seen in (Table 3.1)

Table 3 1: the available data for the targeted healthcare facilities.

Healthcare facility	Architectural plans	Steel Detailing	Staff data
Anti-cancer center(CAC)	Yes	Yes	Yes
Ben Boulaid Hospital	No	No	Yes
Boufarik hospital	No	No	Yes
Emergency joinville	No	No	Yes
Faubourg hospital	Yes	No	Yes
ORL center	Yes	Yes	Yes
The lung center TOT	Yes	Yes	Yes
Sarah clinic	No	No	Yes

3.2.2 Geographical locations of the healthcare facilities

The distribution of healthcare facilities in Blida posed some issues in the collection of the data, since some of the facilities were not located in the centre of the state (see Figure 3.1) and needed more time to visit, and thus it's proved to be harder to obtain (mainly the Boufarik hospital).

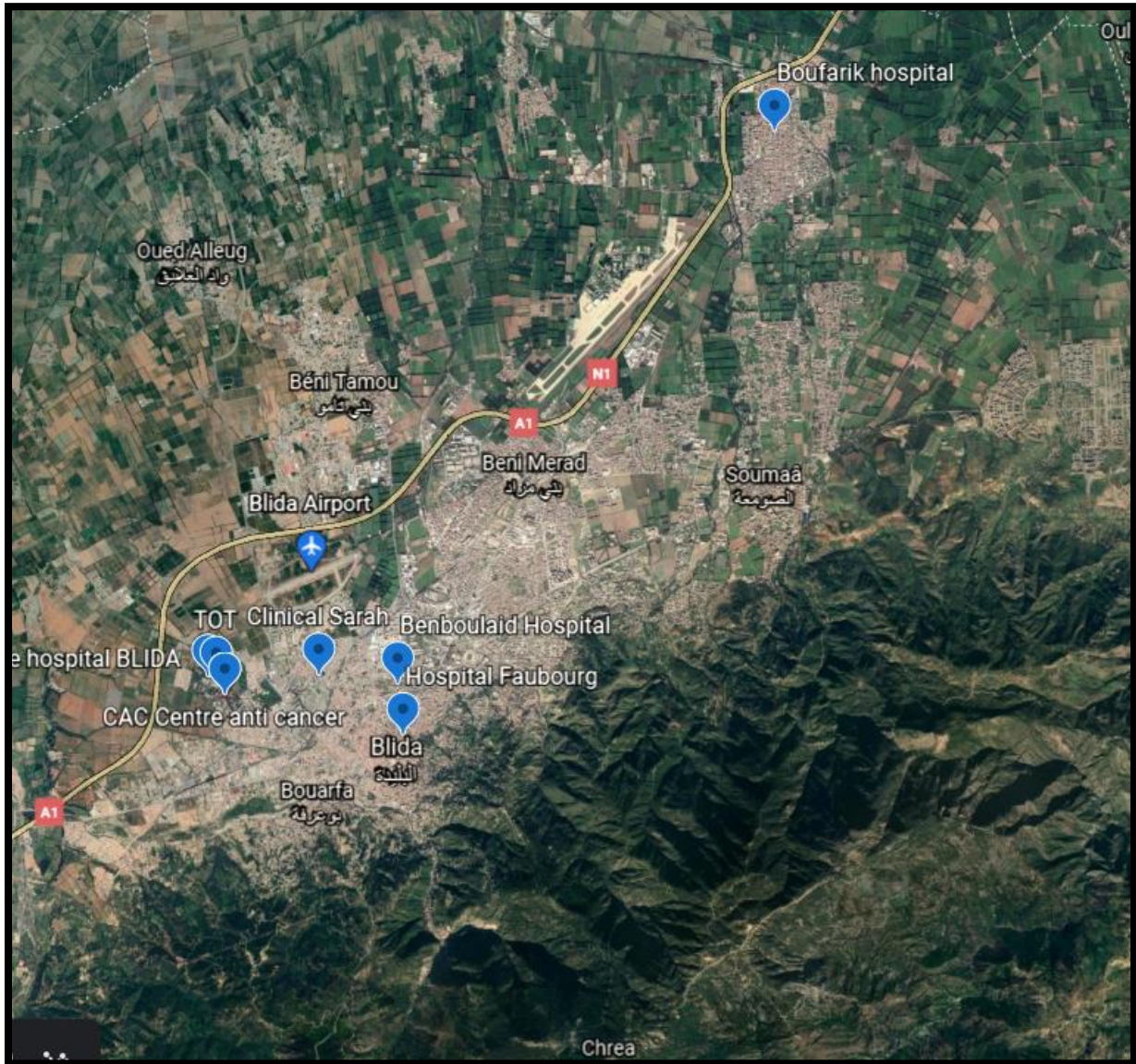


Figure 3. 1: the geographical location of the targeted healthcare facilities.

3.2.3 The geometric configuration

Despite coming across some plans for other models, besides the ones selected for the final step, these plans proved to be either unusable (for the case of Faubourg hospital where the plans were ancient and no digital copy was found besides the ones in their archives), or simply lost within the system. one plan

was found in mint condition(see Figure3.2) but the hospital in itself presented no distinct characteristics that could enrich the study and therefore it was seen that it's inclusion was unnecessary.

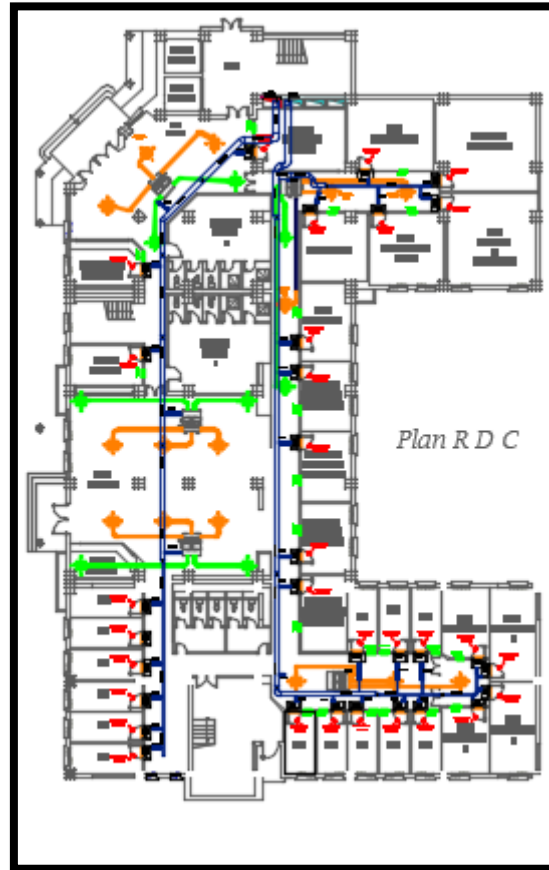


Figure 3. 2: architectural plan of the ORL building

3.2.4 The selection processes

Since most facilities viewed in this work were relatively similar in terms of materials of construction and the geometrical properties, it was deemed that using a limited number of models would serve the work more favourably, as the typology is similar, and for those models with unsimilar data were either selected, if the plans and data were present, or would be rejected due to incomplete data, and the fact that there wasn't any other method to obtain said data.

The approved models are shown in Table 3.2 with some of their data.

Table 3 2: the targeted healthcare facilities for this study

Healthcare facility	Number of levels	Material of construction	Approval For fragility assessment
Anti-cancer center(CAC)	R+3	Concrete/masonry infills	Approved
Ben Boulaid Hospital	R+2	Masonry/concrete	Not Approved
Boufarik hospital	R+2	Masonry/concrete	Not Approved
Emergency joinville	R+2	concrete	Not Approved
Faubourg hospital	R+2	Concrete/masonry	Not Approved
ORL center	R	concrete	Not Approved
The lung center TOT	R+5	Concrete/steel	Approved
Sarah clinic	R+3	concrete	Not Approved

3.3 The chosen typology

On this study, a more simplistic approach to categorization was used, because the number of samples was limited and thus it was seen that classifying buildings on the base of the load bearing system and the materials used in their construction was adequate.

Table 3 3: healthcare typologies in the great Blida

BLOCK	LOAD BEARING SYSTEM	MATERIAL of construction	Typical block Height (m)
TOT	shear walls+ columns	RC	22.78
CAC	RC columns	RC	13.35
CAC+INFILLS	RC columns	RC	13.35

3.3.1 Structural characteristics

In this chapter the structural models of the studied buildings are presented. There are multiple structures, each with a different set of blocs, but only a limited number of blocs can be chosen for the fragility curve development, this is largely due to the similarities between the blocks, either from a structural load bearing system, material of construction perspective or/and the geometrical configuration of the aforementioned blocks.

The first hospital building is the TOT centre (the lungs diseases centre) located in Franz Fanon hospital in the wilaya of Blida. It is composed of 4 main blocs (A, B, C, D) as seen in Table 3.4 and Table 3.5, of which three blocks were used (A, B, and C). Within these blocs there are five structures comprised of six stories and one with three stories. These blocs were constructed after 2003 and therefore have shear walls, they are located in seismic zone III according to RPA 99 ver. 2003.

Table 3 4: basic characteristics of TOT blocks A1, D1 and D2.

Building	A1	D1	D2
No. of stories	3	6	6
Total height (m)	11.56	22.78	22.78
Typical story height (m)	3.74	3.74	3.74
Rc wall section area/floor area at the base	0.005	0.0074	0.0101
Rc column section area/ floor area at the base	0.0102	0.016	0.015
Maximum wall thickness (m)	0.2	0.2	0.2
Maximum column size (m*m)	0.8*0.8	0.5*0.5	0.5*0.5
Maximum longitudinal reinforcement ratio in wall %	0.72	2.21	3.73

Table 3 5: basic characteristics of TOT blocks C1, C2 and C3.

Building	C1	C3	C4
No.of stories	6	6	6
Total height (m)	22.78	22.78	22.78
Typical story height (m)	3.74	3.74	3.74
Rc wall section area/floor area at the base	0.005	0.0085	0.0112
Rc column section area/ floor area at the base	0.013	0.012	0.012
Maximum wall thickness (m)	0.2	0.2	0.2
Maximum column size (m*m)	0.5*0.5	0.5*0.5	0.5*0.5
Maximum longitudinal reinforcement ratio in wall %	0.82	2.08	2.09

The second hospital is the anti-cancer center(CAC in French),located as well in the Franz fanon hospital in the state of Blida, comprised of 3 blocks of almost identical properties as seen in Table 3.6, it was constructed before the 2003 earthquake and therefore it does not have any shear walls, it only has infill panels which are taken into consideration.

Table 3 6: basic characteristics of CAC blocks A, B and C.

Building	A	B	C
No.of stories	4	4	4
Toyal height (m)	13.35	13.35	13.35
Typical story height (m)	3.05	3.05	3.05
Rc column section area/ floor area at the base	0.0062	0.0064	0.0086
Maximum column size (m*m)	0.35*0.35	0.35*0.35	0.35*0.35
Maximum longitudinal reinforcement ratio in column %	1.16	1.16	1.16

3.3.2 Geometric configuration

The geometrical properties of the TOT bloc C3 is represented in Figure 3.3 and on figure 3.4, it was selected based on its importance for the overall study.

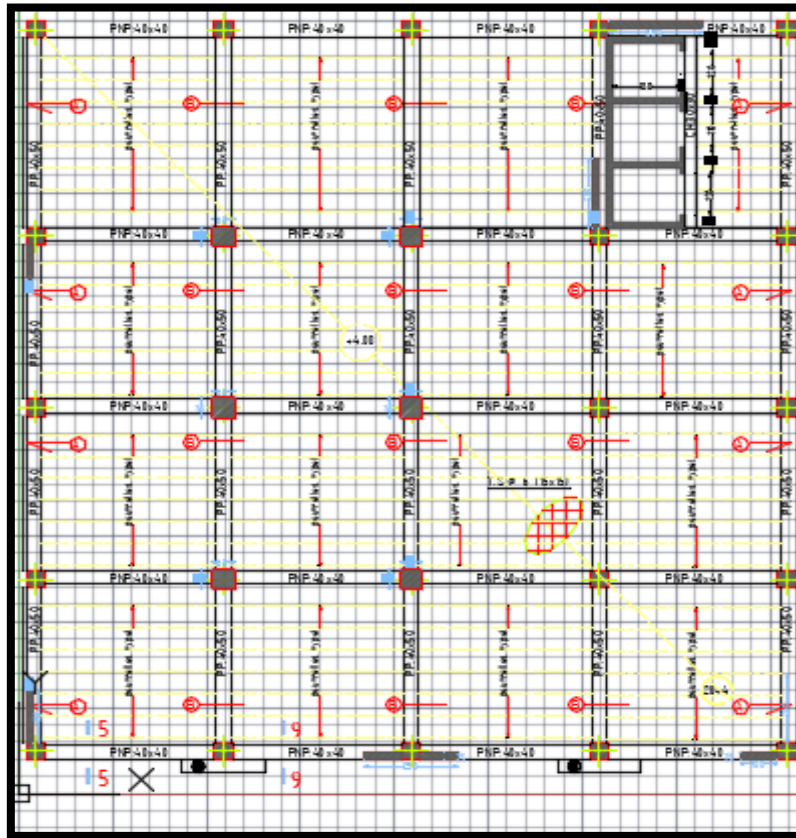


Figure 3. 3: plan view of the first floor of the C3 bloc.

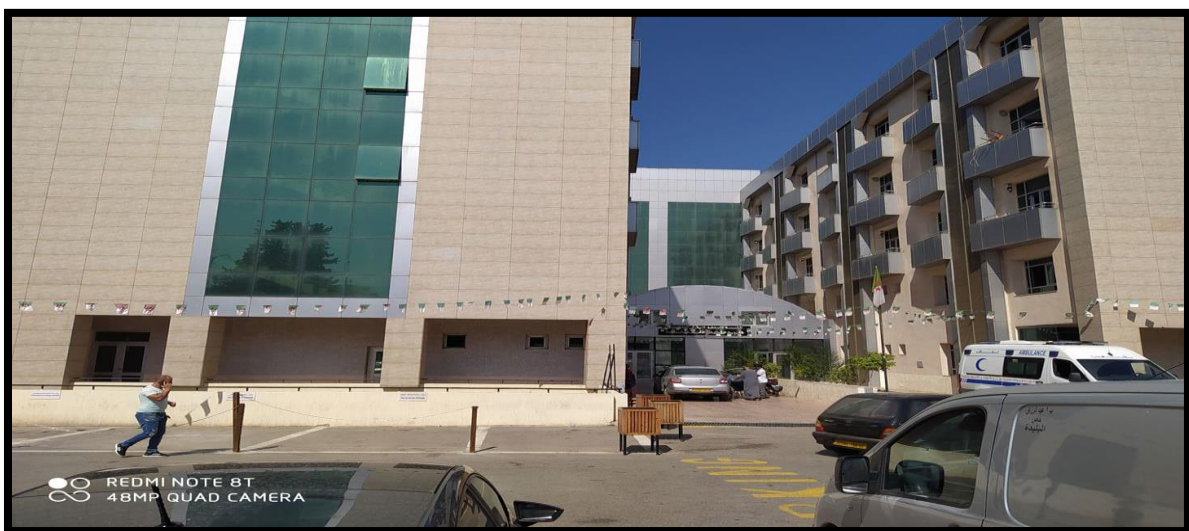


Figure 3. 4: photo of the TOT building.

The geometrical properties of the TOT bloc A1 is represented in Figure 3.5, it was selected based on its importance for the overall study.

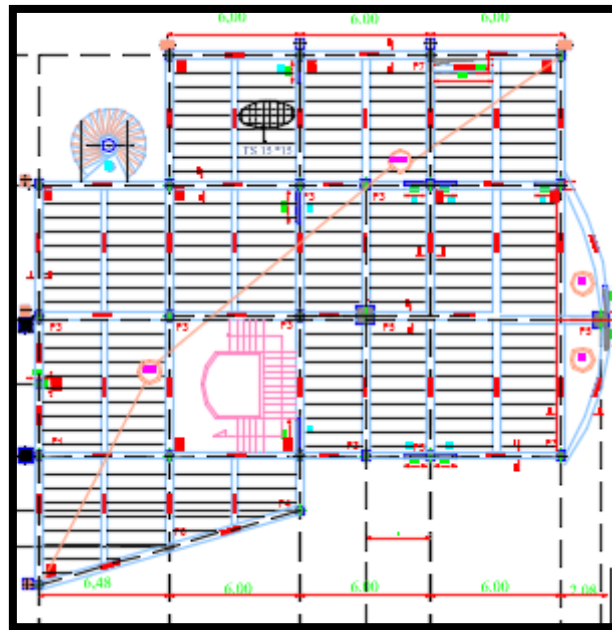


Figure 3. 5: plan view of the first floor of the A1 bloc.

And the anti-cancer centre is presented in figure 3.6 with a recent photograph.

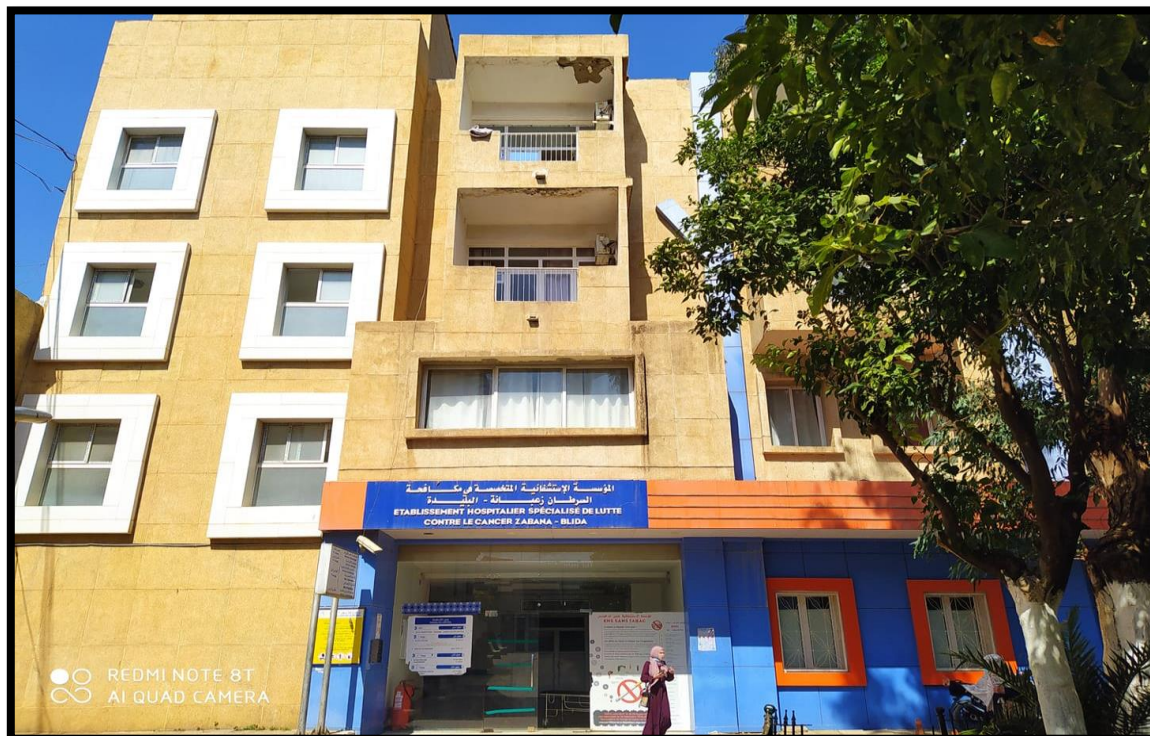


Figure 3. 6: photo of the Anti-Cancer Centre (CAC) building.

The geographical location of the last two models is shown in Figure 3.7.

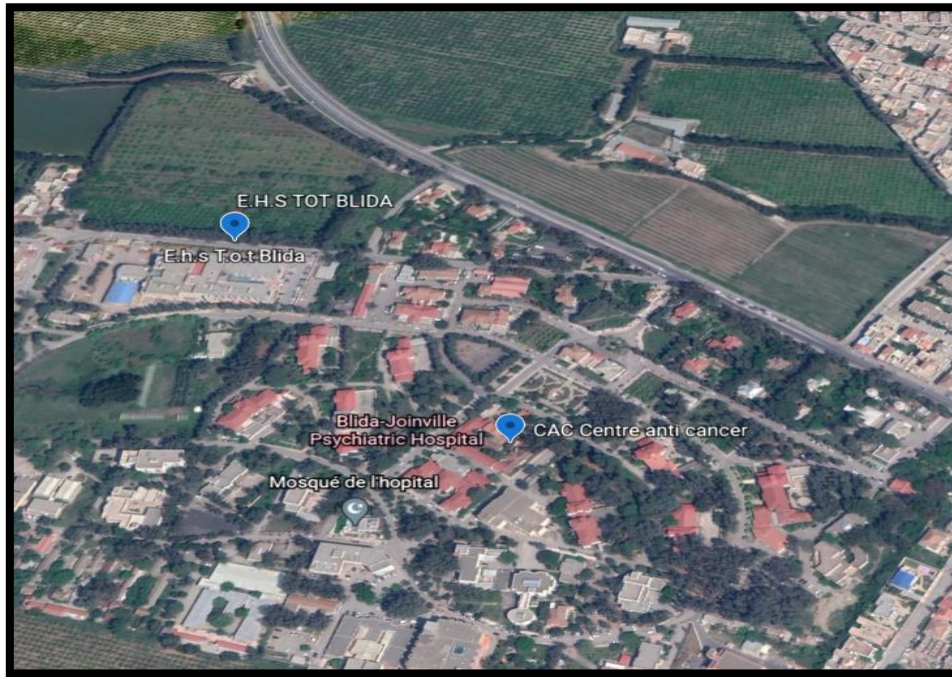


Figure 3. 7: a close up on the geographical location of the CAC and the TOT healthcare facilities.

3.4 Conclusion

In this chapter it was seen, that in order to start a loss estimation study, it is important to first collect the necessary data either through a survey, or in the case of none presence of data, a recreation of said data can be used as an alternative, in this case the first option was deemed to be more adequate since the complete data was found for three hospitals, but only two were selected(CAC and TOT),as the third(ORL),had similar geometric properties, and in terms of elevation it presented no irregularities, and last but not least the material of construction was reinforced concrete the same as the TOT hospital.

Other facilities with different material properties were aimed to be added (masonry for example the Boufarik hospital), but unfortunately during the last steps of the data collection, and due to the public safety, this facility was closed to the public which prevented its inclusion in the final work.



Chapter 04:

Dynamic Nonlinear Analysis

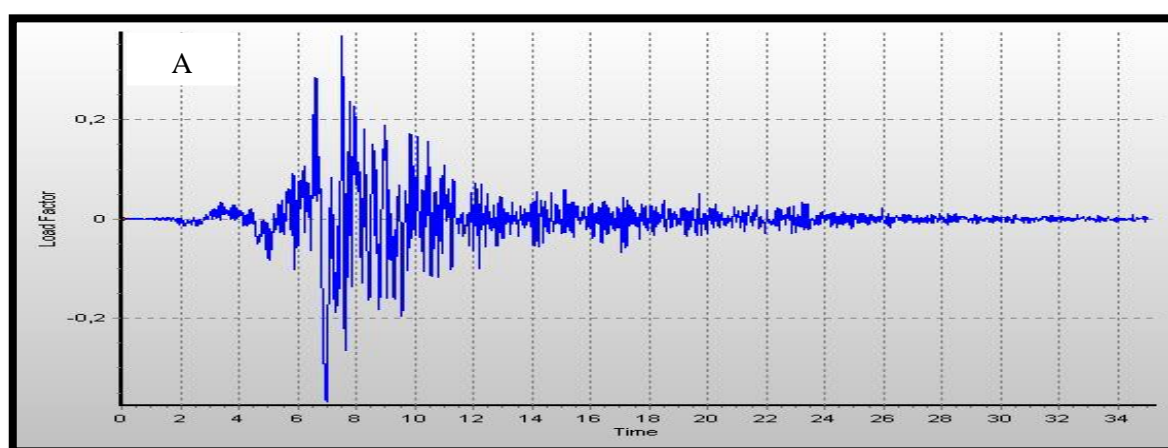
4.1 Introduction

In this chapter the performance of structural models is assessed using nonlinear time history analysis, and the results are then compared to the recommendations of multiple standards (such as RPA, ASCE 7-16 and FEMA 356), this would serve as a tool for the selection of the final models that would be used for the fragility curve development.

Also, the process of performance assessment is discussed in detail to highlight the main themes, and aspects that mustn't be overlooked, and also show the importance of this step in any loss estimation study.

4.2. Ground motion selection

According to the ASCE 7-16, seven ground motions is the adequate amount to assess structural behaviour, and then a statistical approach should be used to implement the results, but the minimum required number of ground motions was chosen for this study (which is three ground motions), since the aim was to develop fragility functions and not structural performance assessment, all three ground motions were taken from the Boumerdes 2003 earthquake (Figure 3.1), these ground motions were then scaled to match a predefined target spectrum, in order to have similar PGA and PGV properties, this will render the results more reliable than using multiple records with different PGA/PGV, the process of the target spectrum selection is described next.



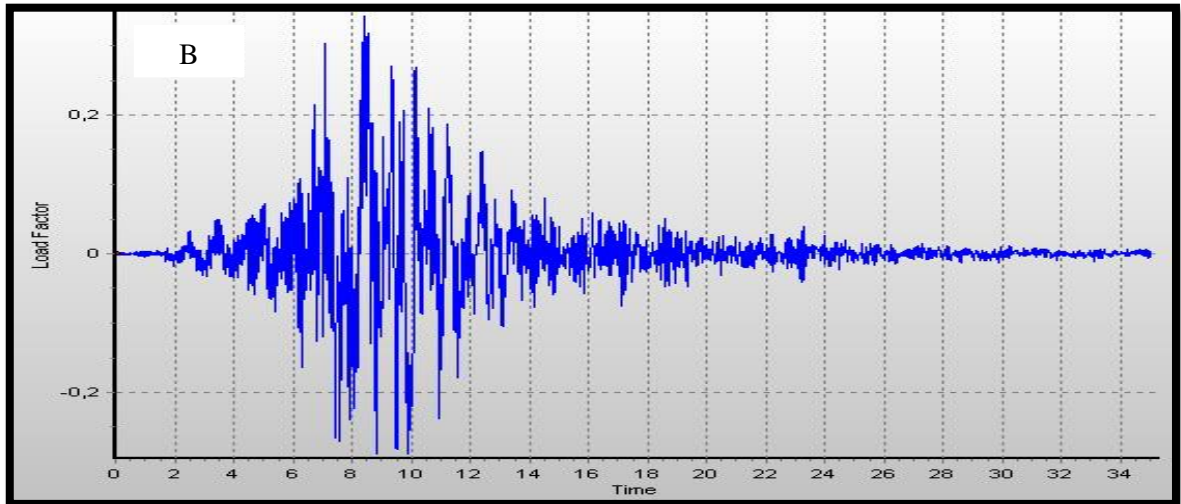


Figure 4. 1: Boumerdes earthquake ground motions recorded from the station of Azazga, a) the E-W component, b) the N-S component.

4.2.1. Target spectrum selection

Both A code-based (RPA) (see Figure 3.2) target spectrum and a UHS were considered for the dynamic analysis, however the results of the code-based target spectrum were too conservative compared to UHS counterpart, which is in itself a conservative target spectrum and thus it was deemed appropriate for this section, the properties of said target spectrum are shown in figure 4.3.

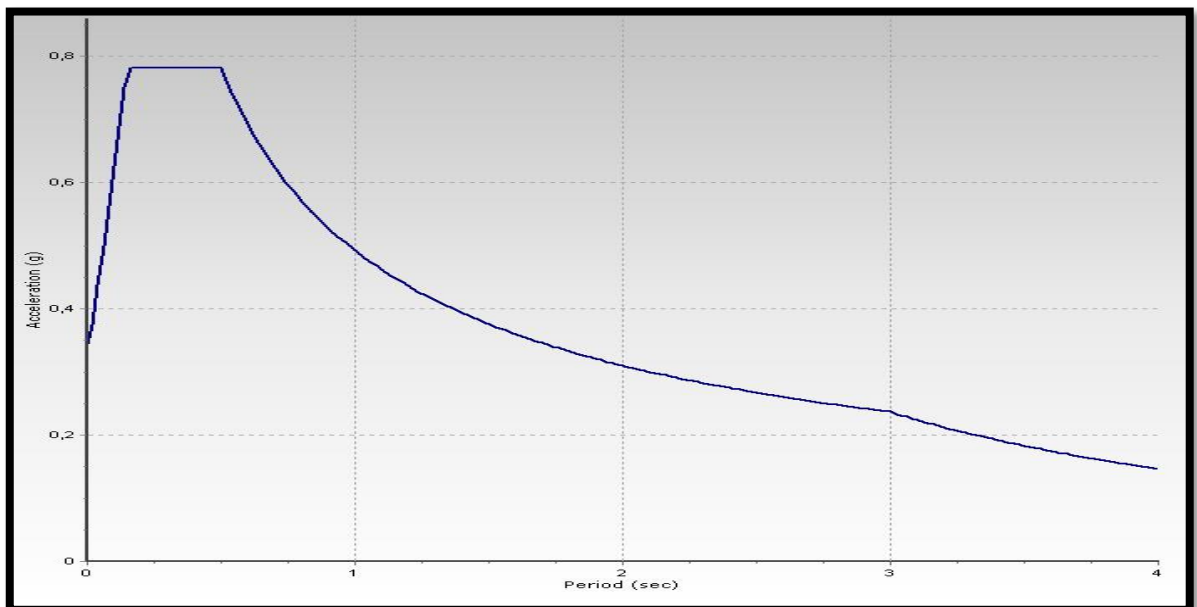


Figure 4. 2: RPA-based target acceleration response spectrum.

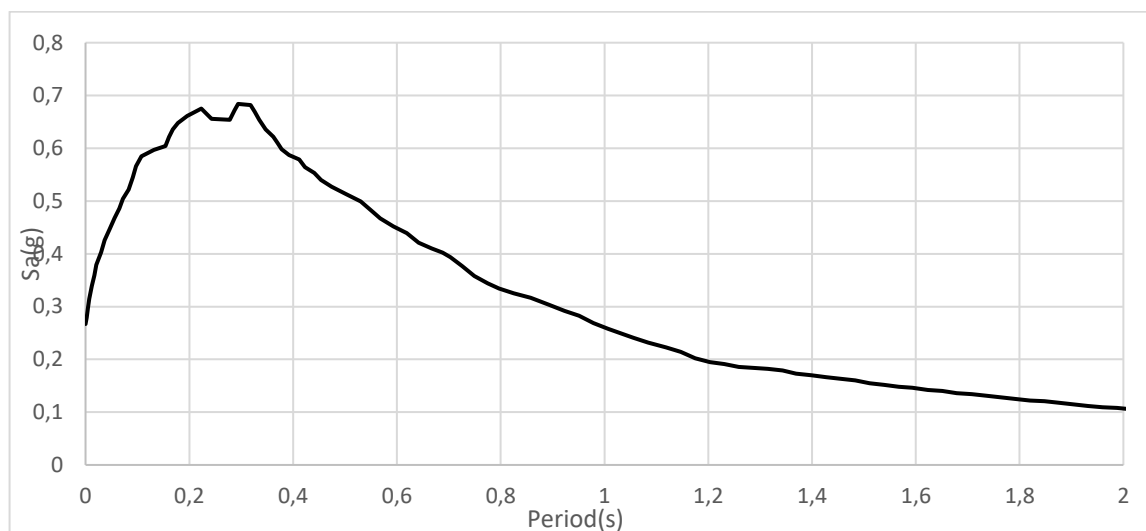


Figure 4. 3: Blida Uniform hazard spectra, damped at 5%, for a return period of 475 years (Hamadache et al,2012)

4.2.2 Ground motion scaling

After choosing an appropriate target spectrum, both a scaling period range and scaling factors were determined in accordance with the ASCE 7-16 recommendations which suggest that the period range shall ‘have an upper bound greater than or equal to twice the largest first-mode period in the principal horizontal directions of response. The lower bound period shall be established such that the period range includes at least the number of elastic modes necessary to achieve 90% mass participation in each principal horizontal direction’ (ASCE 7-16).

This procedure was then implemented using SeismoMatch and SeismoSignal.

4.2.3 Application of ground motions to structural model

in accordance with ASCE 7-16 ground motions shall be applied to the supports of the structural model, and each pair of horizontal ground motion component must be rotated to the fault normal and fault parallel directions and applied to the building in such orientation.

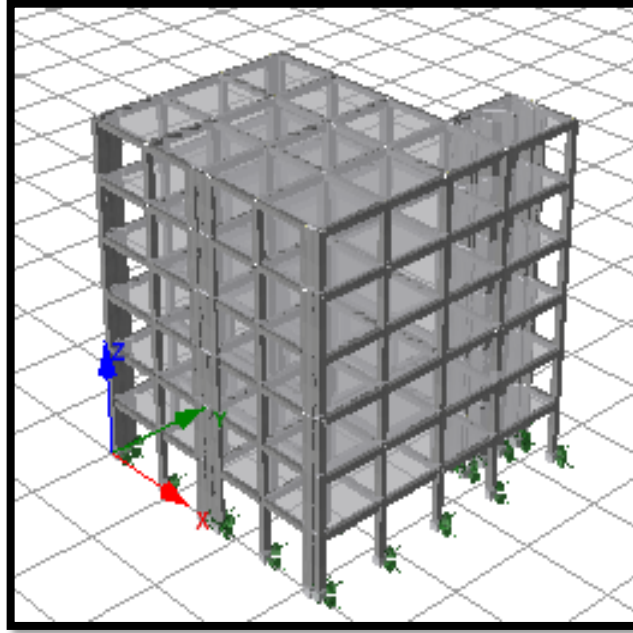


Figure 4. 4: Numerical model of the TOT bloc C3.

4.3-ANALYSIS RESULTS AND ACCEPTANCE CRITERIA

4.3.1. Displacement

When doing a seismic analysis, one of the important tools used to assess structural behaviour is the displacement profile, used to determine the inter-story drift ratio. This tool could highlight any issues with structural design, for example the presence of soft story mechanism, or large displacements in the case of irregular buildings.

There are two required verifications for the both structures studied here in this work, the lung centre and the anti-cancer centre.

4.3.1.1. Inter-story drift (IDR)

IDR is an important demand parameter, especially in the case of nonlinear analysis; it is defined as the relative displacement (drift) of two consecutive stories normalized by story height.

According to the RPA, the horizontal displacement at each level K is computed using the following equation:

$$\delta_k = R \delta_{ek}$$

Where:

R: coefficient de comportement

δ_{ek} : the resulting displacement of seismic forces

In the case of nonlinear analysis, there is no need to multiply the elastic displacement by the R factor and therefore the equation becomes:

$$\delta_k = \delta_{ek}$$

The relative displacement of the level "k" as opposed to the adjacent level "k-1" is equal to:

$$\Delta_k = \delta_k - \delta_{k-1}$$

The relative displacement of two consecutive stories must satisfy (RPA article5.10), which requires that the IDR must be less than 1% of the story height. Thus, the IDR is limited at a value of Hstory/100.

The lung centre (TOT):

Table 4 1: the resulting displacement in the X direction using time history analysis

level	δ_k (cm)	Δ_k (cm)	HEIGHT (m)	Observation
RDC	1,20	1,20	4,20	C. VERIFIED
1 ST	2,80	1,60	3,74	C. VERIFIED
2 ND	4,40	1,60	3,4	C. VERIFIED
3 TH	5,70	1,30	3,74	C. VERIFIED
4 TH	6,70	1	3,74	C. VERIFIED
5 TH	7,60	0,90	3,74	C. VERIFIED

Table 4 2: the resulting displacement in the Y direction using time history analysis

level	δ_k (cm)	Δ_k (cm)	HEIGHT (m)	Observation
RDC	0,90	0,90	4,20	C. VERIFIED
1 ST	1,80	0,90	3,74	C. VERIFIED
2 ND	2,80	1	3,4	C. VERIFIED
3 rd	3,60	0,80	3,74	C. VERIFIED
4 th	4,20	0,60	3,74	C. VERIFIED
5 TH	4,70	0,50	3,74	C. VERIFIED

The anti-cancer centre (CAC):

Table 4 3: the resulting displacement in the X direction using time history analysis

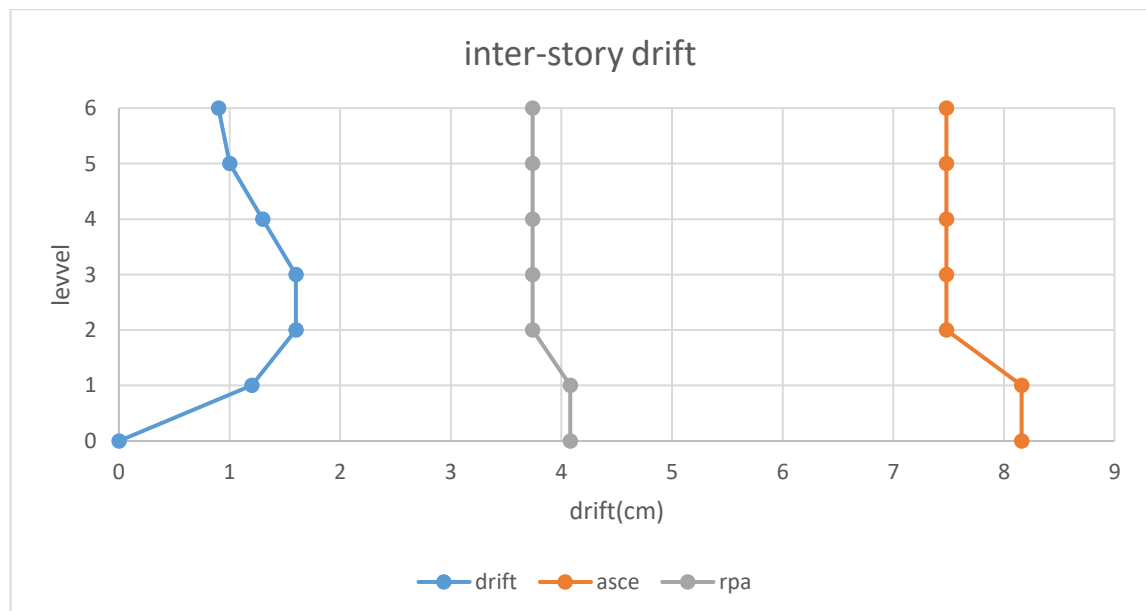
level	δ_k (cm)	Δ_k (cm)	HEIGHT (m)	Observation
RDC	4.8	4.8	4.2	C. NON-VERIFIED
1 ST	6	1.2	3.05	C. VERIFIED
2 ND	6.6	0.6	3.05	C. VERIFIED
3 rd	6.8	0.2	3.05	C. VERIFIED

Table 4 4: the resulting displacement in the Y direction using time history analysis

level	δk (cm)	Δk (cm)	HEIGHT (m)	Observation
RDC	6.5	6.5	4.2	C. NON-VERIFIED
1 ST	1.2	1.2	3.05	C. VERIFIED
2 ND	0.5	0.5	3.05	C. VERIFIED
3 rd	0.3	0.3	3.05	C. VERIFIED

Other IDR criteria were also verified according to the ASCE:

The lung centre (TOT):

**Figure 4. 5:** inter-story drift checks in the X direction.

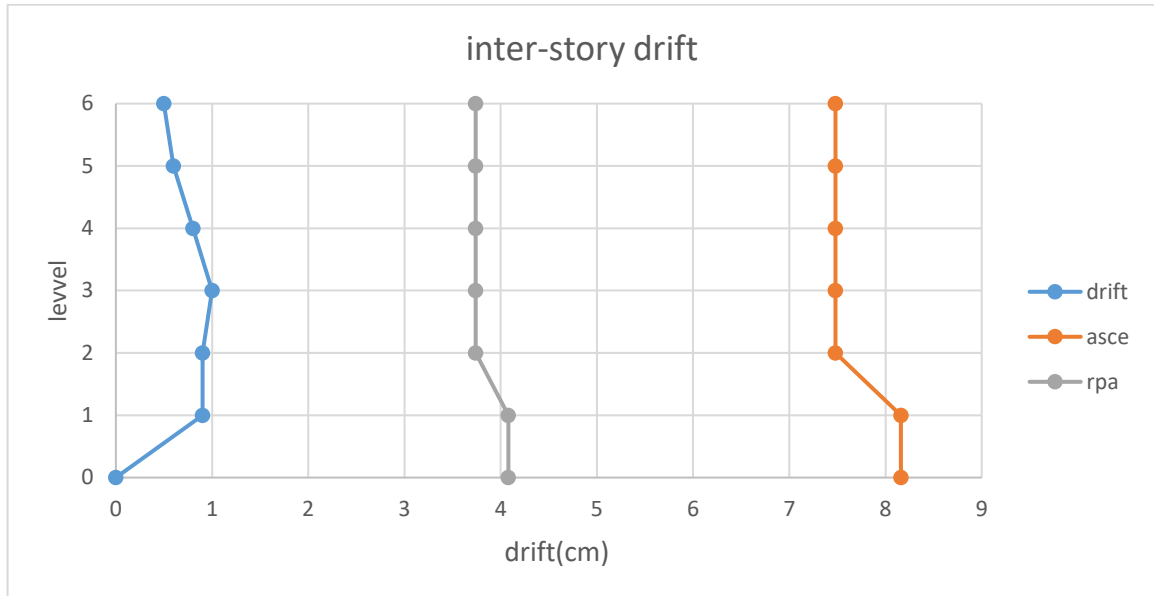


Figure 4. 6: inter-story drift checks in the X direction.

The Anti-cancer centre (CAC):

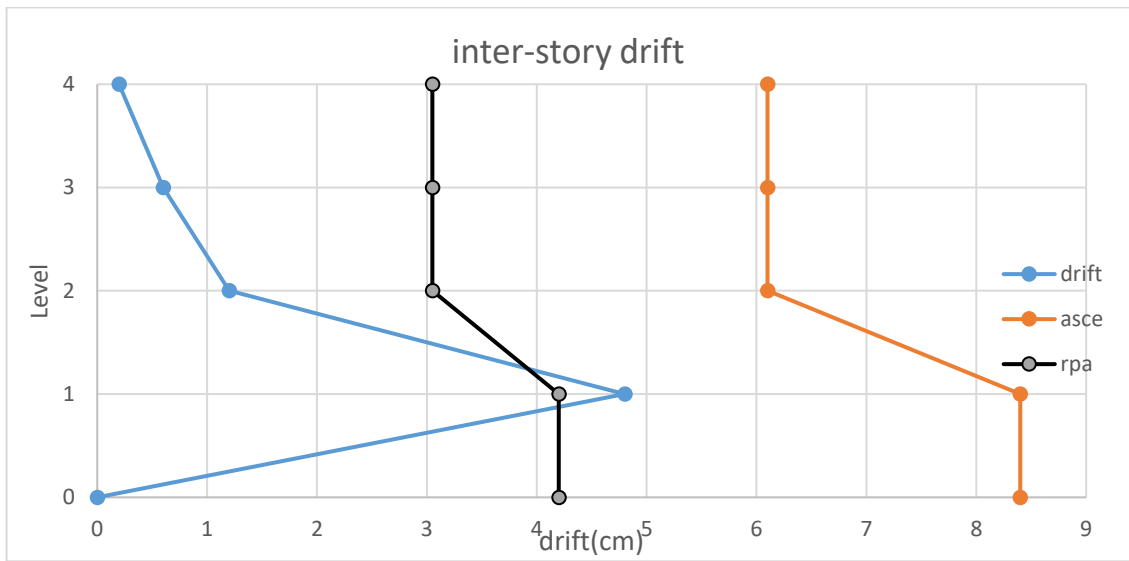


Figure 4. 7: inter-story drift checks in the X direction.

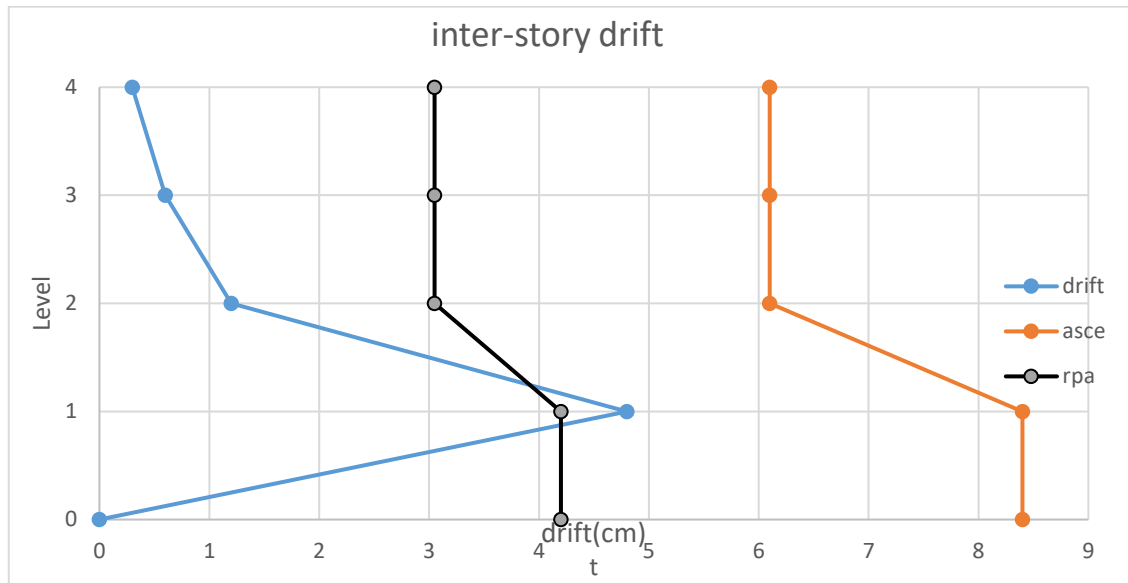


Figure 4. 8: inter-story drift checks in the X direction.

Observation: The IDR is higher than the RPA limits in two instances, for the CAC centre in the first story due to the lack of shear walls, however in the case of the ASCE limits which are less constraining all of the structural displacements were verified.

4.3.2 Second order effect (P-Δ effect)

The second order effect or the P-Δ effect, is a product of large displacements and compressive loads on vertical elements, according to the Algerian seismic standards, it can be ignored if the following condition is satisfied:

$$\Theta = \frac{P_K \times \Delta_K}{V_K \times h_K} < 0.10$$

with:

P_k : the total load of the levels starting the level "k" upwards.

$$P_k = \Sigma(W_{GI} + 0.25W_{QI})$$

V_k : the shear load on the level "k".

Δ_k : the relative displacement of the two consecutive levels "k" and "k-1".

h_k : the height of the level "k".

Table 4 5: P- Δ effect verification for the TOT bloc.

COLUMN C33 TOTC3KE					
Story	HEIGHT (mm)	Pstory (KN)	Displacement (mm)	Vstory (KN)	Ratio
GF	4080	-636.8661	12	13.38476	0.139945
1 st	3740	-251.7792	16	24.90277	0.043253
2 nd	3740	-90.1132	16	47.43101	0.008128
3 rd	3740	-258.419	13	44.75771	0.020069
4 th	3740	-226.325	10	-4.61833	0.131032
5 th	3740	-138.35	9	21.65665	0.015373

Table 4 6: P- Δ effect verification for the CAC bloc.

COLUMN CAC					
Story	HEIGHT (mm)	Pstory (KN)	Displacement (mm)	Vstory (KN)	Ratio
GF	4200	-342.914	65	44.11745	0.1203
1 st	3050	-243.47	12	40.2611	0.0239
2 nd	3050	-155.631	5	30.61157	0.0084
3 rd	3050	-72.9006	3	23.6294	0.003

Observation:

- Although in nonlinear analysis the P- Δ effect is implemented in the analysis parameters, but the aim of this section is to note whether the P- Δ effect is significant according to RPA seismic regulations.

- For both blocs, P- Δ has a significant effect on the structural behavior.

4.3.3. Chord rotation

The chord rotation capacity of beams, columns and walls, θ , that is the angle between the tangent to the axis at the yielding end and the chord connecting that end with the end of the shear span. The chord rotation is also equal to the element drift ratio, which is the deflection at the end of the shear span with respect to the tangent to the axis at the yielding end divided by the

shear span (SeismoStruct manual, 2018). when it comes to nonlinear analysis the chord rotation capacity checks are vital signs on whether the longitudinal detailing is appropriate or not.

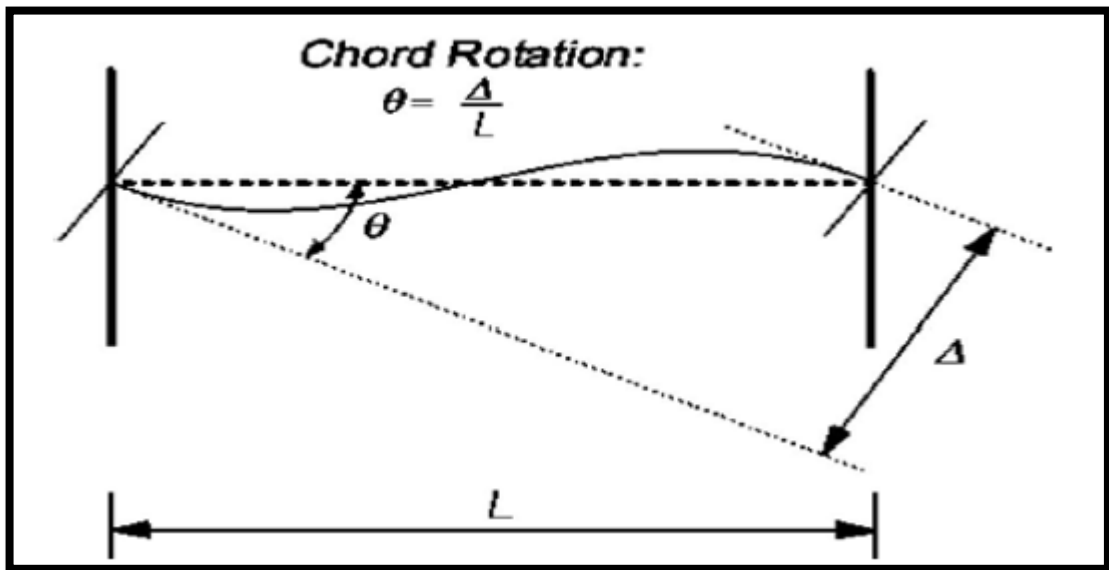


Figure 4. 9: Chord rotation for structural wall coupling beams (ASCE 7-16,2016).

The total chord rotation capacity at ultimate of concrete members under cyclic loading is computed as the sum of the chord rotation at yielding and the plastic part of the chord rotation capacity

$$\theta = \theta_y + \theta_p$$

Each element has its own set of expressions to compute its capacity:

The chord rotation capacity at yield, θ_y , is calculated as described below:

- For beams and columns from the equation (4.29) of D. Biskinis (2007):

$$\theta_y = \frac{M_y L_s}{3EI_{\text{eff}}}$$

where the effective stiffness value, EI_{eff} , is calculated according to Table 10-5 of ASCE 41-17.

- For walls from equation (10-5) of ASCE 41-17:

$$\theta_{yE} = \left(\frac{M_{yE}}{(EI)_{\text{eff}}} \right) l_p$$

Where:

l_p : is the plastic hinge length.

The plastic part of the chord rotation capacity is calculated as indicated below:

- For beams according to Table 10-7 of ASCE 41-17
- For columns according to Table 10-8 of ASCE 41-17
- For walls controlled by flexure according to Table 10-19 of ASCE 41-17

The deformation capacity of walls controlled by shear is defined in terms of the inter-storey drift ratio as indicated in Table 10-20 of ASCE 41-17.

For the TOT centre:

Table 4 7: chord rotation checks in both ends of the vertical and horizontal elements.

element type	element	demand (rda)	capacity (rda)	performance ratio	LIMIT STATUS
shear wall	W60-1 TOTC3DA	0.008	0.037	0.214	NOT REACHED
column	C34-2 TOTC3DA	0.089	0.058	1.548	REACHED
beam	b148-1 TOT1AZ	0.0957	0.026	3.605	REACHED

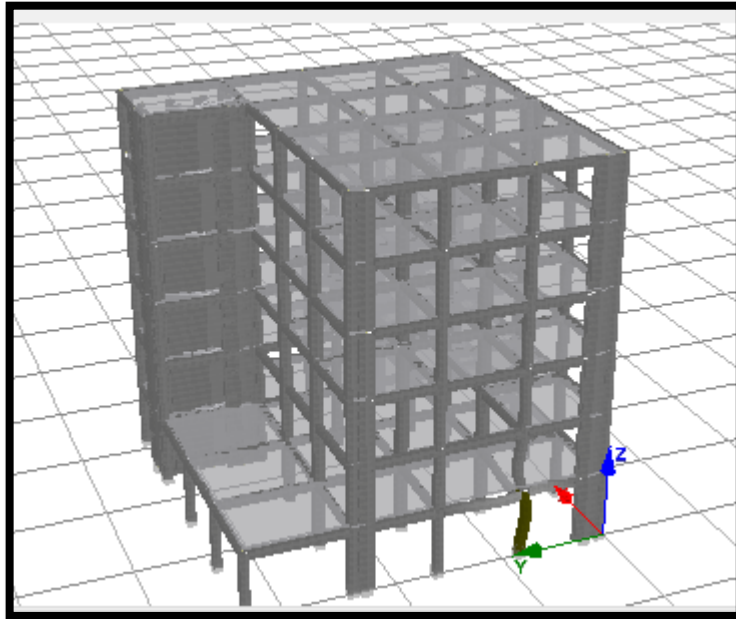


Figure 4. 10: chord rotation capacity surpassed in TOTC3 block column 32-1.

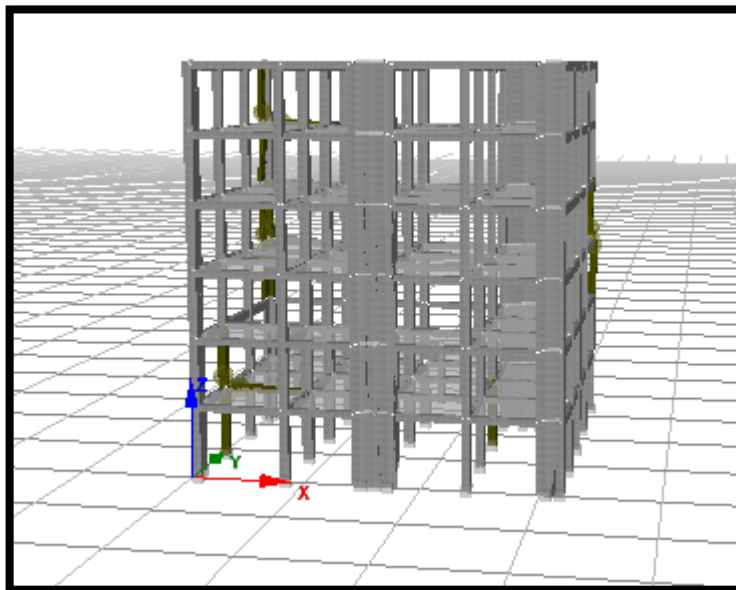


Figure 4. 11: chord rotation capacity surpassed in TOTC3 block beam 148-1.

For the CAC structure:

Table 4 8: chord rotation checks in both ends of the vertical and horizontal elements.

element type	element	demand (rad)	capacity (rad)	performance ratio	STATUS
Column	C36-1 CAC BDA	0.00773	0.06142	0.1258	NOT REACHED
beam	b77-2 CAC BDA	0.0426	0.0928	0.459	NO TREACHED

Observation: the chord rotation limits have been exceeded in the case of the TOT bloc, both in element horizontal and vertical elements, shown in Figure 4.10 and Figure 4.11 which is due to the torsional modes present as opposed to the CAC bloc which is more regular horizontally and vertically.

4.3.4 The axial load ratio

The axial load ratio is defined as:

$$v = \frac{N_d}{B_c \cdot f_{cj}}$$

Where:

N_d : is the vertical load acting on the element.

B_c : is the raw section of the element.

f_{cj} : is the characteristic strength of the concrete.

For the TOT centre:

Table 4 9: The axial load ratio verifications for the TOT blocs.

Story	N(kn)	Area(mm ²)	ratio
GF	-619.543	200000	0.123909
1 st	-514.743	200000	0.102949
2 nd	-411.222	200000	0.082244
3 rd	-307.806	200000	0.061561
4 th	-199.753	200000	0.039951
5 th	-99.4626	200000	0.019893

For the CAC structure:

Table 4 10: The axial load ratio verifications for the CAC blocs.

Story	N(kN)	Section(mm ²)	Ratio
GF	-1383.665	122500	0.45180898
1 st	-1089.291	122500	0.35568686
2 nd	-838.7692	122500	0.27388382
3 rd	-704.3498	122500	0.22999177

Note: the axial load ratio is slightly superior to the limits predefined in RPA in the TOT bloc as opposed to the CAC bloc where the limits have been surpassed by a large amount.

4.4. Conclusion

In This chapter the performance of three blocks was estimated, As seen in the previous verifications and it was seen that the structural behaviour of each block was sufficient although minor issues were detected, for example the rebar detailing of certain columns in the TOT block was insufficient as proven in the chord rotation section, and in terms of displacements, the TOT block did not surpass the limits in both the RPA and the ASCE standards, as opposed to the CAC block which only met the ASCE requirements, but surpassed those of the RPA.



Chapter 05:

Seismic fragility functions

5.1 Introduction

In this chapter, fragility curves of three typologies of hospital building structures in Algeria were developed. These tools used to develop fragility curves are described in detail providing each step and the necessary information needed to attain it. Further on these three fragility curves are compared and conclusions are drawn to emphasize on the need for certain practices to evaluate vulnerable hospital structures and thus a resilient healthcare system and community.

5.2 Collapse fragility development

5.2.1 Collapse fragility development using IDA

For each ground motion, the probability of collapse given a certain intensity measure is estimated using cumulative distribution function. This is then used to obtain all parameters needed for fragility function development, an example of an IDA results is shown in Figure 5.1.

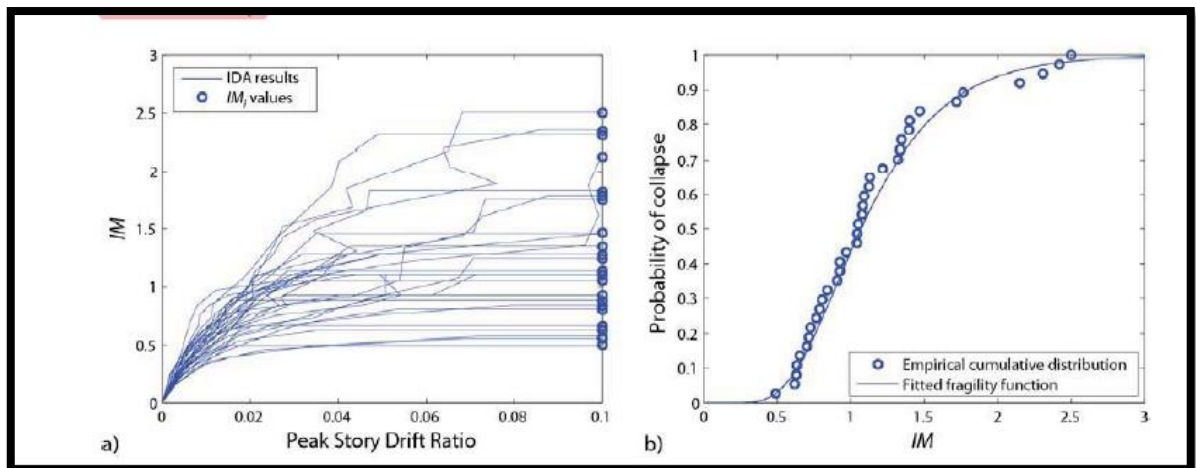


Figure 5. 1:. a) Example incremental dynamic analyse results, used to identify IM values associated with collapse for each ground motion. b) Observed fractions of collapse as a function of IM, and o fragility function. (Baker, 2015).

5.2.2 Collapse fragility development using truncated IDA

In the case of using a limited number of intensity measures, a common method is to define a limit intensity measure and the rest of the probabilities of collapse are estimated using probabilistic tools described in a research work by Baker (2015).

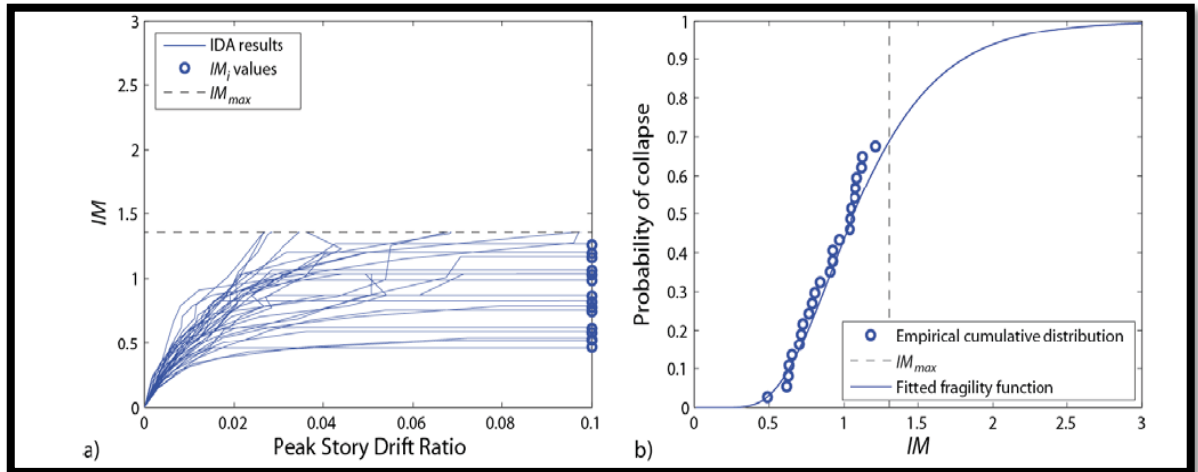


Figure 5. 2: a) Example truncated IDA analysis results. b) Observed fractions of collapse as a function of IM (Baker, 2015).

5.3 Pushover based derivation of fragility curves

5.3.1 SPO2IDA

SPO2IDA is an Excel workbook application that was originally developed by Vamvatsikos and Cornell (2006). This tool uses empirical relationships from a large database of incremental dynamic analysis results to convert static pushover curves into probability distributions for building collapse as function of ground shaking intensity” (FEMA P58-1,).

The SPO2IDA is straightforward procedure which require the user to:

- 1- Perform a static pushover analysis.
- 2- Exploit the result the SPO analysis, and create the pushover curve.
- 3- Transform the SPO curve into an IDA curve using the spo2ida excel sheet, by inserting the base shear vs roof displacement data, and the characteristics of the structure including the weight, height, first vibration mode period, and then finally fit the SPO curve using the elastic/hardening shear values and displacement coordinates.

5.3.2 SPO2FRAG

5.3.2.1 Definition

SPO2FRAG is a MATLAB coded tool which simulates the results of the IDA using only the results of the SPO analysis. This is done using the SPO2IDA excel sheet, and then using a set of fragility curve development tools such as the limit states and the variability model, the total collapse or any other limit state is then estimated.

This tool is a proven viable tool for fragility curve development, since its results were compared to multiple analytical results, and SPO2FRAG produced satisfactory results. This is however conditioned on the respect of the limitations of the SPO analysis.

In order to create a fragility function using the SPO2FRAG tool, one must follow the following steps:

- 1- Insert the SPO curve.
- 2- Define a single degree of freedom backbone curve, using either a bilinear or quadrilinear fit.
- 3- Introduce the model's dynamic characteristics. (Figure 5.3)

The screenshot shows the SPO2FRAG software interface for defining dynamic characteristics. It includes the following fields and controls:

- Number of stories:** 2
- Uniform storey height:** 3.0 (Total height: 6.00)
- Uniform storey mass:** 50.0 (Total mass: 100.00)
- Modal Characteristics:** Γ_1 = 1.30, Participating mass factor = 0.78
- Periods (s):** T_1 = 0.20, T_2 = 0.06
- Equivalent SDOF:** T^* = 0.34, Use Γ_{eff} (checkbox)
- Elastic Limit:** 195.19 kN
- Units:** Height: m, Mass: Ton
- Buttons:** Evaluate, Calculate, Use excel template for input, Read active template, Help, Ok

Figure 5. 3: Dynamic characteristics of a structure.

- 4- Generate IDA curves (fractile IDA curves).(Figure 5.4)

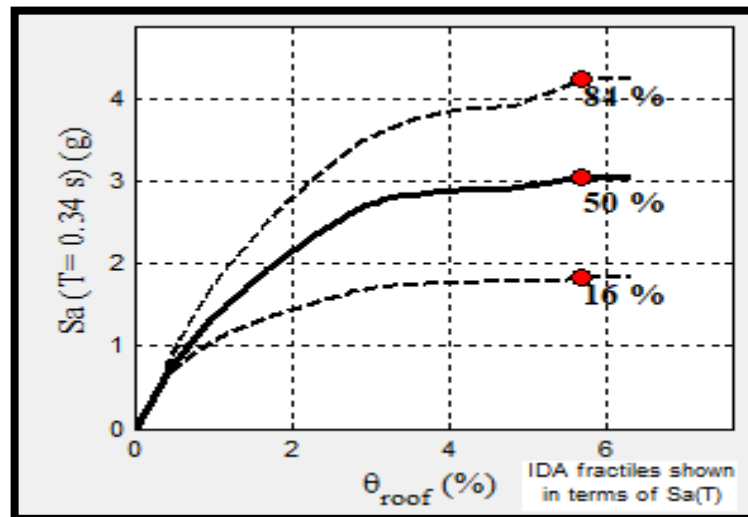


Figure 5. 4: IDA fractile curves.

- 5- Chose the appropriate engineering demand parameter, either the IDR or the roof displacement (which is the one used in our case).
- 6- Define the limit states in accordance with the objectives of the study.

- 7- Include additional variability by defining standard deviation of the median IM causing exceedance of a limit state, or use the Monte Carlo simulation in the case of modelling uncertainty, depending on the level of accuracy required by the user.

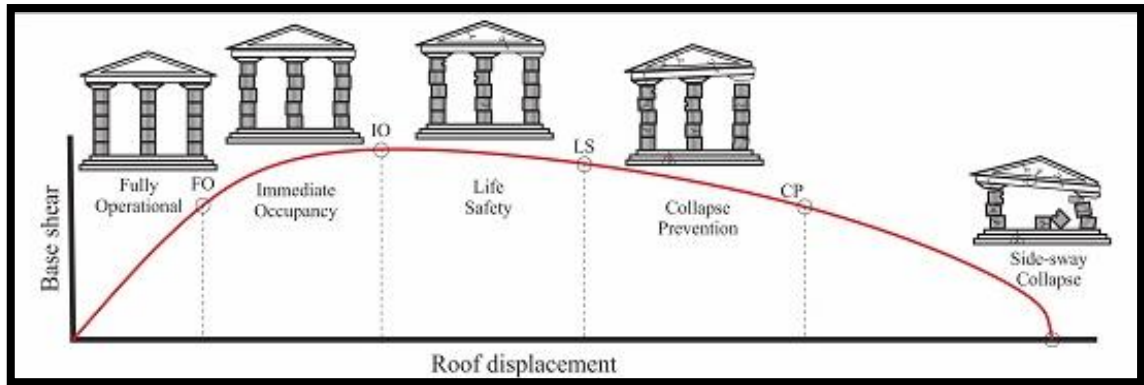


Figure 5. 5: Graphical representation of performance limit states.

Since SPO2FRAG uses both the SPO analysis and the IDA, it is only normal that it uses the same options as these two methods, for the case of the SPO, the structural modal must be dominated by the first vibrational mode, and also it must be regular.

For the case of the IDA, three major assumptions are assumed:

- 1- The first assumption is that such an intensity measure(IM) is sufficient, that is, the engineering demand parameter(EDP) random variable conditioned on the IM is independent of other ground motion features needed to evaluate the seismic hazard for the site, such as magnitude and source-to-site distance (e.g., Luco and Cornell 2007).
- 2- The second assumption is the so-called scaling robustness of the chosen IM, meaning that using records scaled to the desired amplitude of the IM, rather than records where said amplitude occurred naturally, will not introduce bias into the distribution of structural responses obtained (e.g., Iervolino and Cornell, 2005).
- 3- The third one assumes that in the numerical model of the structure employed for IDA, stiffness and strength degradation under dynamic loading are acceptably represented. Consequently, failure of the analysis to provide an EDP value after scaling a record to a certain IM level can be attributed to the onset of dynamic instability, which would physically correspond to the structure's side-sway collapse (see also Adam and Ibarra 2015).

5.4 Fragility curves development

In this section three fragility curves are developed, two for the CAC block with and without infills, to gain a better understanding on the effects of infill panels on the overall fragility of the facility, which can then be used to enable better construction practices.

The other block which is discussed in this section is the TOT block, this latter is considered using RPA recommendations, and has shear walls as opposed to the two previously mentioned blocks, which are constructed using columns/beams only. This will highlight the effects of shear walls on structural vulnerability, and the difference between construction practices prior to and post the RPA standards.

5.4.1 Fragility functions for the CAC building with infills

For the CAC block with infills the steps and results of the fragility curve development are as follows:

1st the pushover curve is obtained (Figure 5.8):

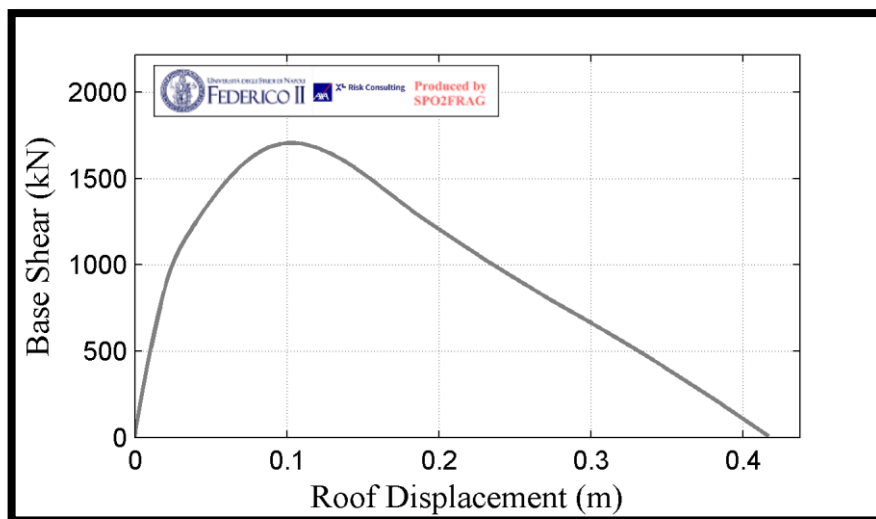


Figure 5. 6: the CAC BLOC with masonry infills pushover curve.

2nd choosing the appropriate fitting scheme:

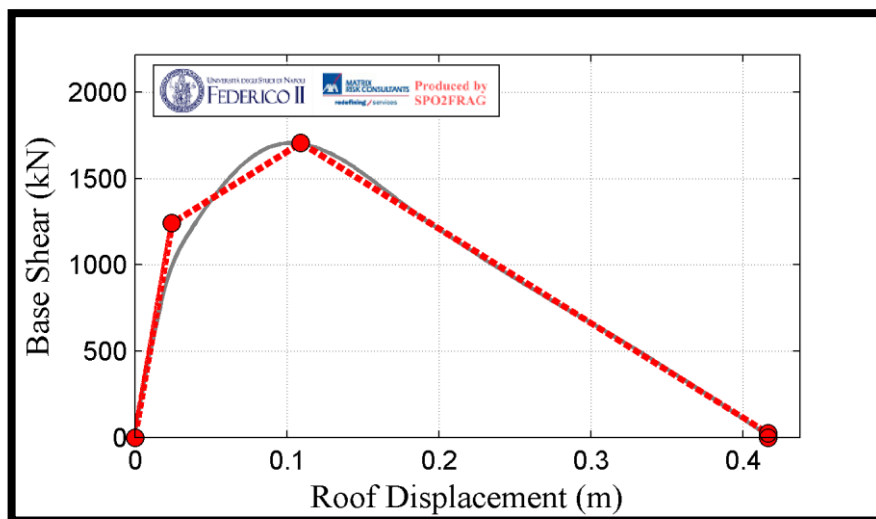


Figure 5. 7: the CAC bloc with infills pushover curve fitted using a quadrilinear-fitting scheme.

3rd the IDA fractile curves are obtained:

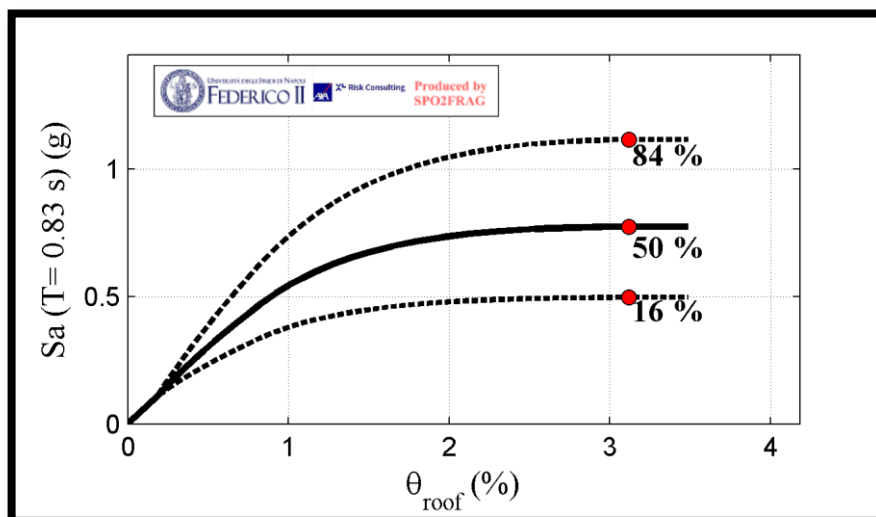


Figure 5. 8: the IDA fractile curves of the CAC bloc with infills.

The last step is to generate the fragility curve:

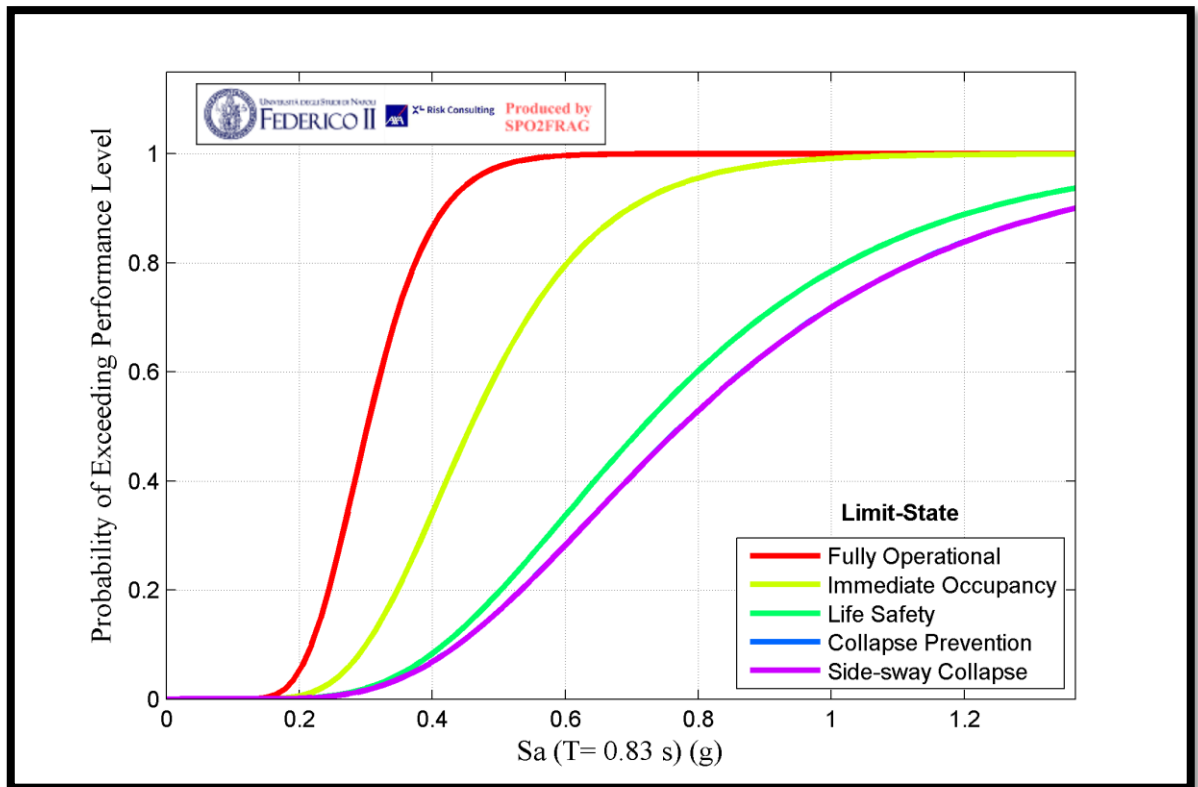


Figure 5. 9: the CAC bloc with infills fragility curve

Observation:

When seeing the results of the CAC block with infills fragility curve, the first observation is that the probability of exceeding the performance level of collapse prevention at $S_a=1g$ is about 70%, which is reasonable despite the construction having been built without any shear walls.

Concerning other performance levels, at $S_a=1g$, the probability of exceedance for each performance state are as follows, its 78% for: life safety, 98% for immediate occupancy and 100% for fully operational.

5.4.2 Fragility functions for the CAC building without infills

For the CAC bloc without masonry infills the steps and results of the fragility curve development are shown as follows:

1st the pushover curve is obtained Figure5.10

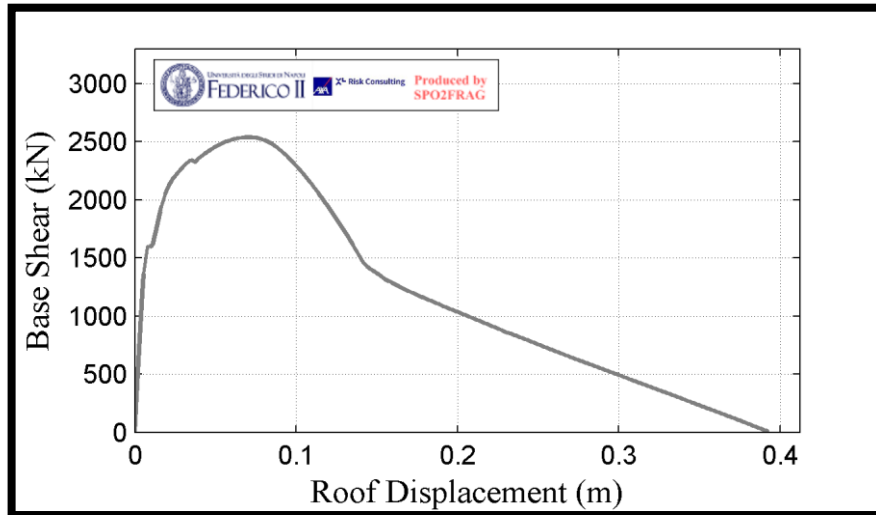


Figure 5.10: the CAC BLOC without masonry infills pushover curve.

2nd choosing the appropriate fitting scheme:

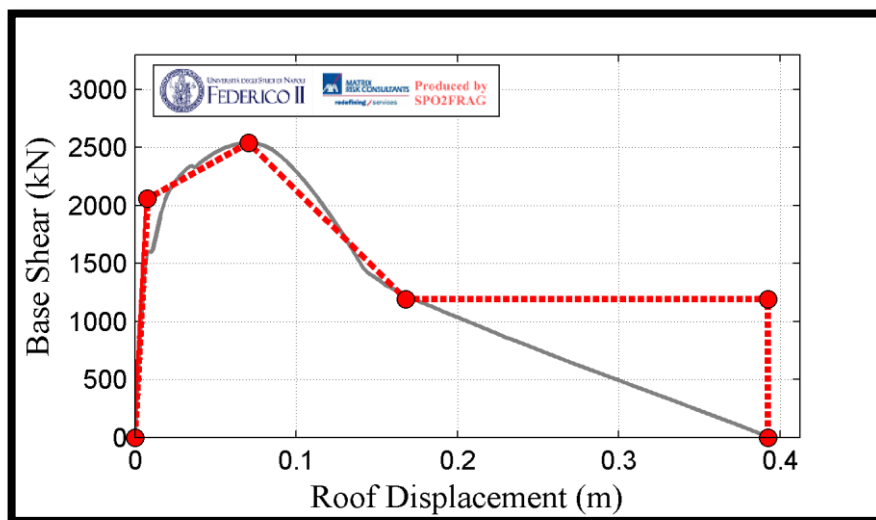


Figure 5.11: the CAC bloc without infills pushover curve fitted using a quadrilinear-fitting scheme.

3rd the IDA fractile curves are obtained:

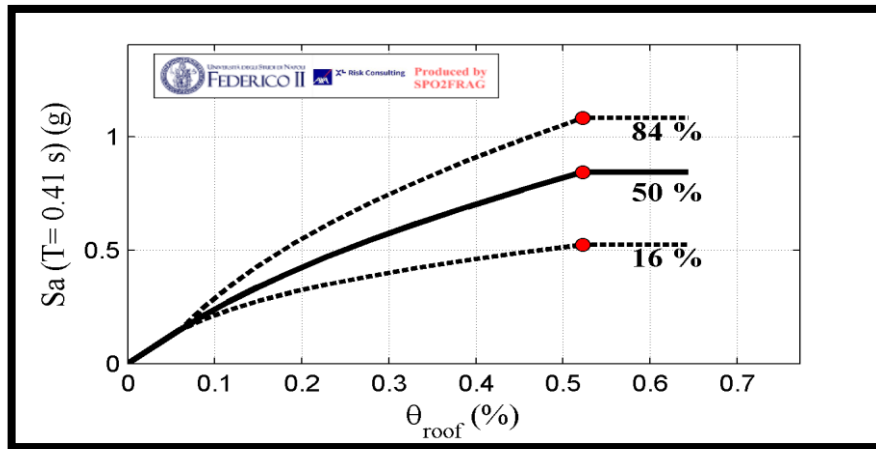


Figure 5. 12: the IDA fractile curves of the CAC bloc without infills.

The last step is to generate the fragility curve:

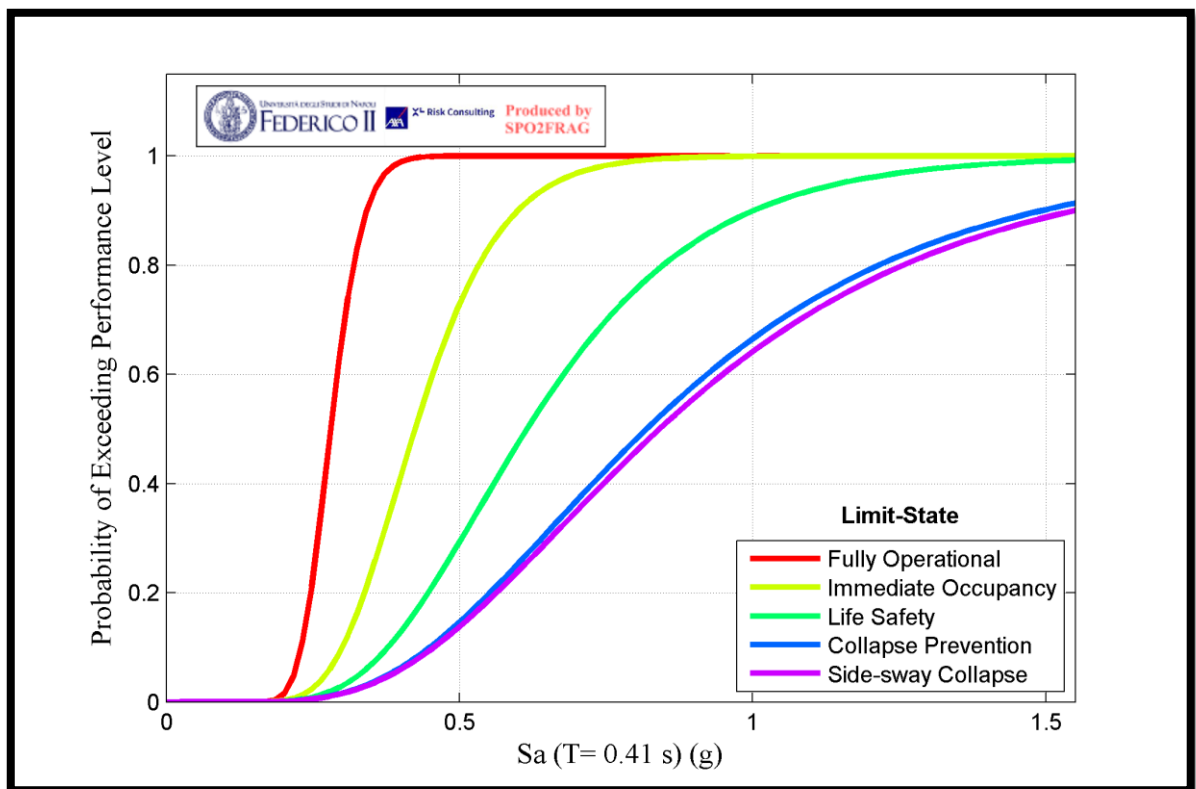


Figure 5. 13: the CAC bloc without infills fragility curve.

Observation:

When seeing the results of the CAC without infills fragility curve, the first observation is that the probability of exceeding the performance level of collapse prevention at $S_a=1g$ is about 67%, which is slightly better than that of the block with masonry infills.

Concerning other performance levels, at $S_a=1g$, the probability of exceedance for each performance state are as follows, its 88% for: life safety, 100% for immediate occupancy and 100% for fully operational.

5.4.3 Fragility functions for the TOT building

For the TOT bloc the steps and results of the fragility curve development are as follows:

1st the pushover curve is obtained Figure5.14

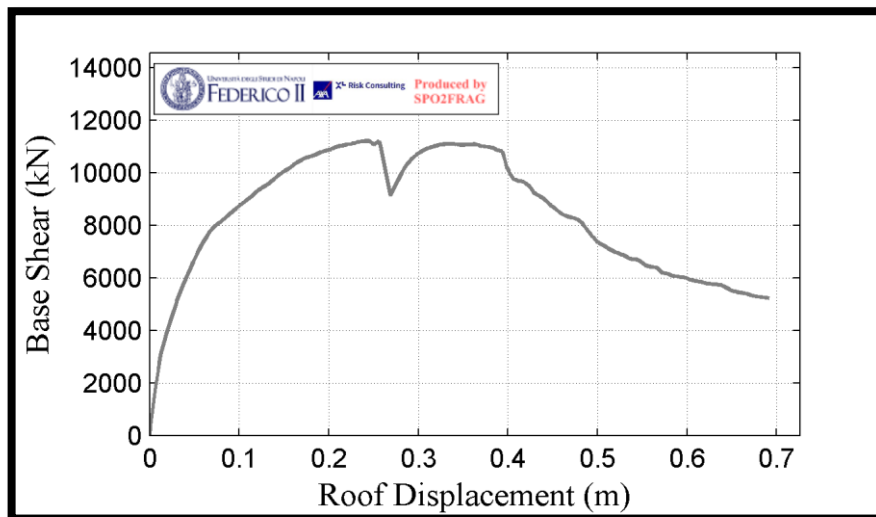


Figure 5. 14: the TOT bloc pushover curve.

2nd choosing the appropriate fitting scheme:

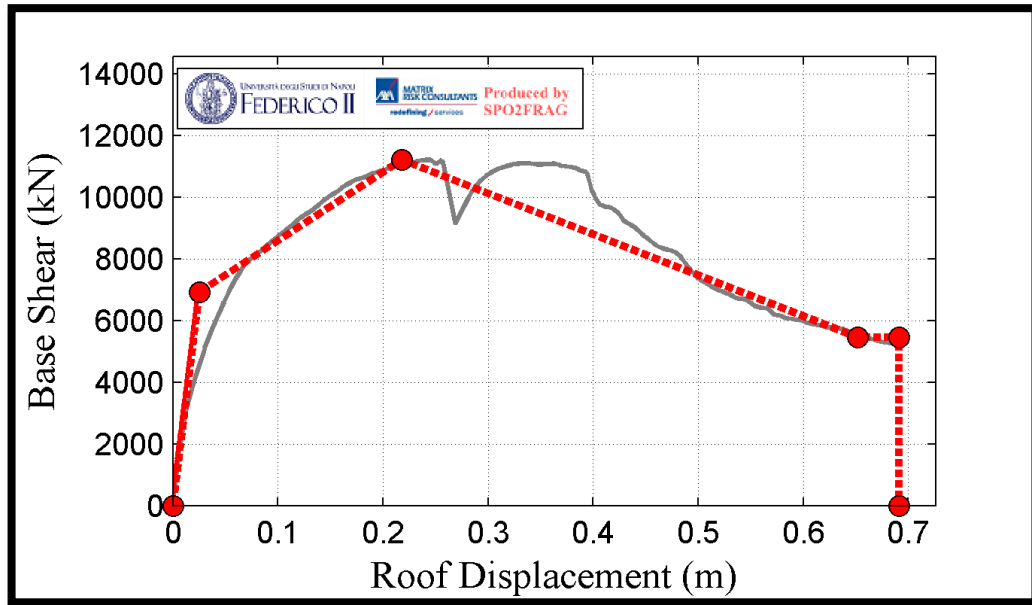


Figure 5.15: TOT bloc pushover curve fitted using a quadrilinear fitting scheme.

3rd the IDA fragility curves are obtained:

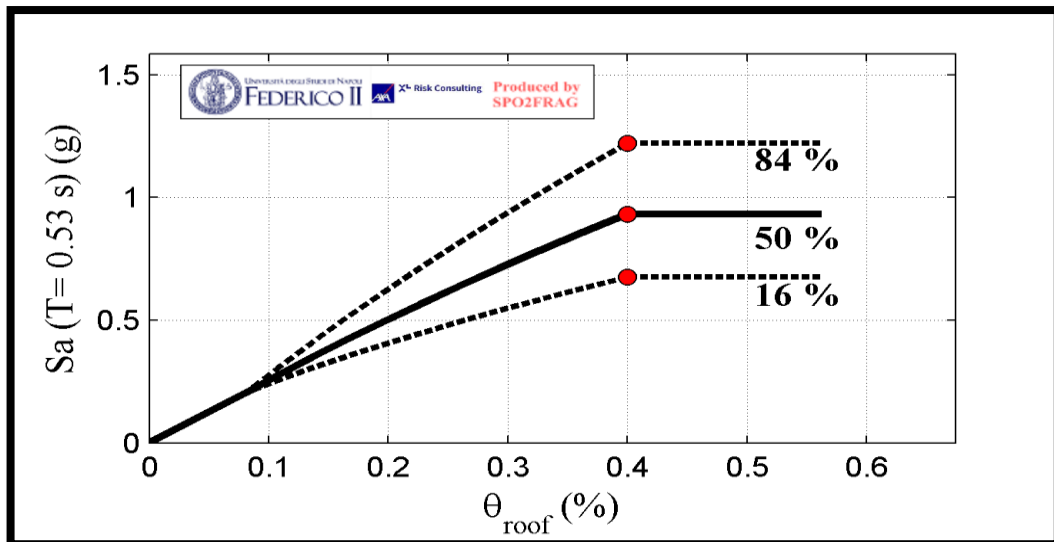


Figure 5.16: the IDA fragility curves of the TOT bloc.

The last step is to generate the fragility curve:

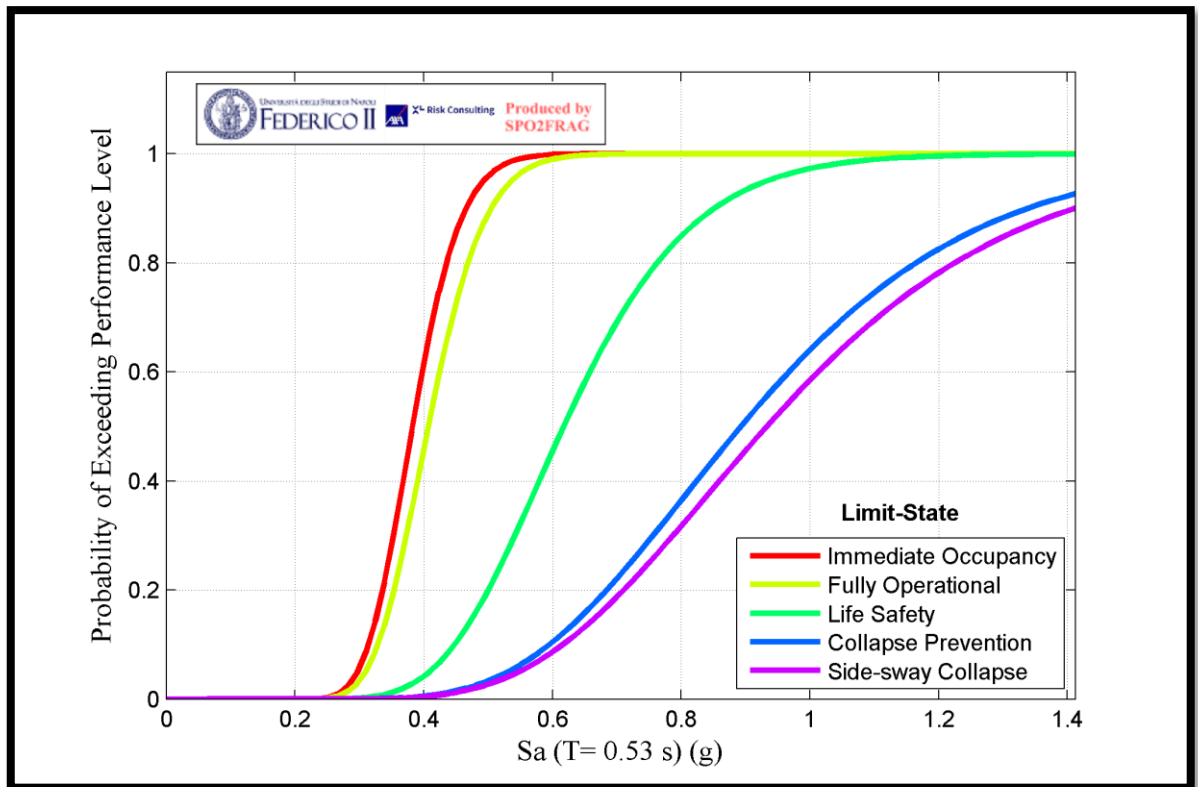


Figure 5. 17: the TOT fragility curve.

Observation:

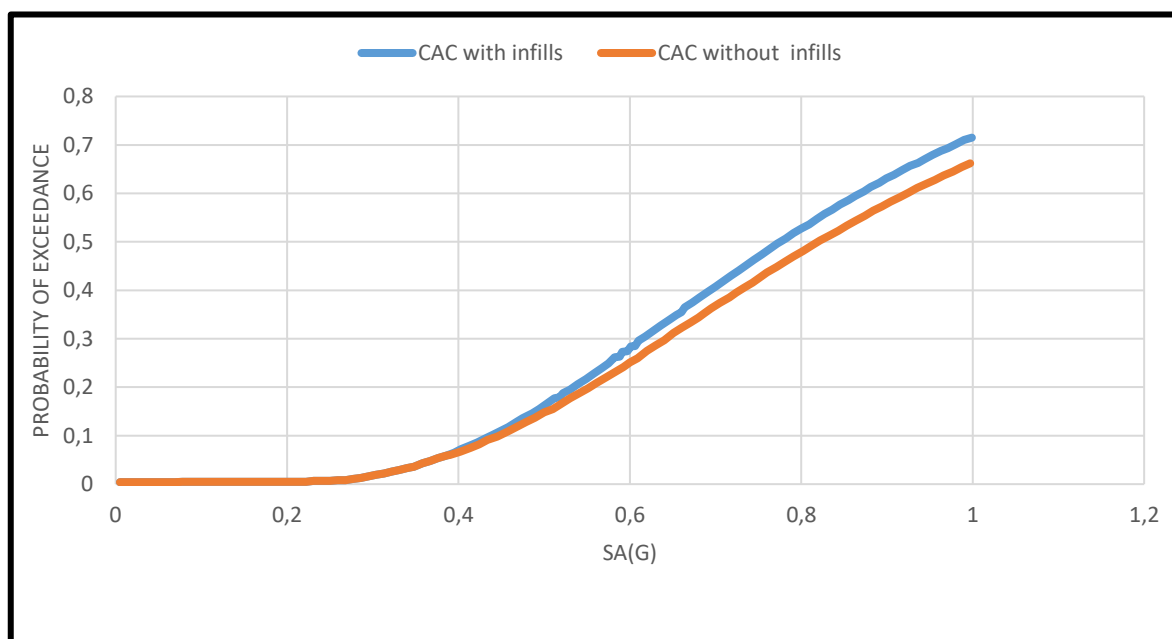
When seeing the results of the TOT blocks fragility curve, the first observation is that the probability of exceeding the performance level of collapse prevention at $S_a=1g$ is about 58%, which is better than both CAC blocks.

Concerning other performance levels, at $S_a=1g$, the probability of exceedance for each performance state are as follows, its 97% for: life safety, 100% for immediate occupancy and 100% for fully operational.

The results of the three fragility curves are resumed in Table 5.1.

Table 5 1: the probability of exceeding performance levels for the three blocks at $S_a=1g$.

Performance level	Fully functional	Immediate occupancy	Life safety	Collapse prevention
CAC without infills	100%	100%	88%	67%
CAC with infills	100%	98%	78%	70%
TOT block	100%	100%	97%	58%

**Figure 5. 18:** Comparison between the CAC Block with and without infills.

5.5 Results discussion

As seen in Figures 5.19 , 5.15 , 5.11 and Table 5.1 in terms of the performance limit of full functionality, all models have a 100% rate of exceedance when $S_a=1g$, this is normal since the intensity is high and even the risk of losing functionality is high it can be easily dealt with, the same can be said for immediate occupancy limit state where all three models except the infills model have a 100% rate of exceedance, and the infills model with a 98% which can be explained by the unit of measurement which is either inter-story drift ratio (IDR) or roof displacement (which is the one used in this case), that is highly affected by the infill panels which reduce the displacement at the expense of overall vulnerability as seen in the collapse prevention state, where the CAC block with infill is the most probable model to fail under the predefined conditions.

The same can be said for the case of the life safety performance, where the infills model seems more durable than the other models, this is due to the fact that although the TOT Block is comprised of shear walls, the displacements are large due its irregularity and thus the initial limit states are easily surpassed compared to the CAC infills Block however, it presents lower probability of exceedance in collapse prevention and therefore it is more durable.

And last but not least the collapse prevention performance limit state is the highest for the CAC infills model, which loses some of its ductility due to the presence of the infills when compared to the CAC without infills block (see Figure 5.18), this suggests that these units could put the facility at a greater risk than improve its durability, another point to notice is that the least vulnerable structure is the TOT block, however it should more resistant, but due to the presence of weak detailing in certain elements as pointed out in chapter 4, and the non-regularity, the block lost some of its capacities. But still the CAC block without infills is more vulnerable than its TOT counterpart despite its lower height and more regular geometry.

5.6 Solutions and recommendations

In order to decrease the fragility of the previously mentioned healthcare facilities and other facilities on both the state and national level, there exists solutions among which are the planning of retrofitting strategies to mitigate the effects of seismic hazard, therefore each facility must be dissected to either reinforce certain elements or modify the load bearing system as a whole (the CAC block). Since this has become a trend in a lot of countries (for example Italy), where structures built using no standard or old standards are modified to meet the current international criteria of seismic design. This is mandatory for essential buildings that respond to the emergencies derived from earthquakes

Another solution is to start a thorough inspection of these facilities, since this work only used analytical data and no complete material data was to be found, therefore the situation could be even worse and thus the fragility of such facilities might increase considerably.

One of the aspect which was not included in this work is the fragility of non-structural elements, which may prove to be equally pivotal to the functionality of healthcare facilities and thus it is recommended that other studies or inspections, of the effects of these elements on the overall vulnerability must be included to further decrease the probability of human, financial and in some cases structural losses.

Concluding remarks

In this work, the seismic fragility of healthcare facilities in the district of great Blida was studied using a variety of numerical tools. Numerous scientific papers were reviewed and analysed to select the proper methodology for fragility assessment of healthcare facilities, and two nonlinear analyses were selected for the final objective: Static pushover analysis and the Incremental dynamic analysis. In order to attain the study objectives two major facilities were selected as representative models of the typologies present in the Algerian hospital building inventory based on the material/geometrical properties.

After the development of seismic fragility curves, it was seen that the hospital facilities that were studied proved to be vulnerable, despite the fact that some of the buildings were constructed after the 2003 revised seismic design regulation. This highlights that healthcare facilities require a different approach when it comes to seismic design.

Some of the suggestions that the authors propose to solve these issues, is to start a series of inspections of the healthcare infrastructure in Algeria, and based on the individual results of each facility, either retrofitting or reconstruction strategies must be initiated. Another suggestion that would solve the issue of the fragility of healthcare facilities in the future is through creating specific standards for the construction of healthcare infrastructures following the more rational international standards.

Since this work only accounted for a portion of the healthcare facilities in Algeria, it concentrated on the structural aspect of healthcare facilities. More studies should be initiated to account for the different aspects of hospitals functionality and decrease their vulnerability, by following the footsteps of other countries that added more standards to account for the complexity of the healthcare infrastructure.

References

American Concrete Institute. ACI 318-19 Building Code Requirements for Structural Concrete (ACI 318-19) ACI Committee 318 (2019).

Achour, Nebil & Miyajima, Masakatsu & Pascale, Federica & Price, A. (2014). Hospital resilience to natural hazards: Classification and performance of utilities. *Disaster Prevention and Management*. 23. 40-52. DOI 10.1108/DPM-03-2013-0057.

Achour, Nebil. (2007). Estimation of malfunction of a healthcare facility in case of earthquake. Doctoral Thesis

Adam, Christoph & Ibarra, Luis. (2015). Seismic Collapse Assessment. 10.1007/978-3-642-36197-5_248-1.

ASCE 7-16. (2017). Minimum Design Loads for Buildings and Other Structures Commentary. American Society of Civil Engineers. DOI 10.1061/9780784412916.

ASCE 41-17 (2017) American Society of Civil Engineers: Seismic Evaluation and Retrofit of Existing Buildings.

Baker, Jack & Cornell, C. (2006). Spectral shape, epsilon and record selection. *Earthquake Engineering & Structural Dynamics*. 35. 1077 - 1095. DOI 10.1002/eqe.571.

Baker, Jack & Jayaram, Nirmal. (2008). Correlation of Spectral Acceleration Values from NGA Ground Motion Models. *Earthquake Spectra* - 24. DOI 10.1193/1.2857544.

Baker, Jack W. (2013). Probabilistic Seismic Hazard Analysis. White Paper Version 2.0.1, 79 pp

Baker, Jack. (2011). Conditional Mean Spectrum: Tool for Ground-Motion Selection. *Journal of Structural Engineering*. 137. 322-331/1943. DOI 10.1061/(ASCE)ST.1943-541X.0000215.

Baker, Jack. (2013). Efficient Analytical Fragility Function Fitting Using Dynamic Structural Analysis. *Earthquake Spectra*. 31. DOI 10.1193/021113EQS025M.

Baltzopoulos, Georgios & Baraschino, Roberto & Iervolino, Iunio & Vamvatsikos, Dimitrios. (2017). SPO2FRAG: software for seismic fragility assessment based on static pushover. *Bulletin of Earthquake Engineering*. DOI 10.1007/s10518-017-0145-3.

Bruneau, Michel & Chang, Stephanie & Eguchi, Ronald & Lee, George & O'Rourke, Thomas & Reinhorn, Andrei & Shinozuka, Masanobu & Tierney, Kathleen & Wallace, William & Winterfeldt, Detlof. (2003). A Framework to Quantitatively Assess and Enhance the Seismic Resilience of Communities. Earthquake Spectra - EARTHQ SPECTRA. 19. DOI 10.1193/1.1623497.

Cimellaro, G. & Reinhorn, Andrei & Bruneau, Michel. (2010). Seismic resilience of a hospital system. Structure and Infrastructure Engineering - Struct infrastruct eng. 6. 127-144. 10.1080/15732470802663847.

Cimellaro, G. & Marasco, Sebastiano & Zamani Noori, Ali & Mahin, Stephen. (2019). A first order evaluation of the capacity of a healthcare network under emergency. Earthquake Engineering and Engineering Vibration. 18. 663-677. DOI 10.1007/s11803-019-0528-3.

Cimellaro, G. & Reinhorn, Andrei & Bruneau, Michel. (2011). Performance-based metamodel for healthcare facilities. Earthquake Engineering & Structural Dynamics. 40. DOI 1197 - 1217. 10.1002/eqe.1084.

Crisafulli F.J. (1997) Seismic Behaviour of Reinforced Concrete Structures with Masonry Infills, PhD Thesis, University of Canterbury, New Zealand.

EN 1998-1 (2004) : Eurocode 8: Design of structures for earthquake resistance – Part 1: General rules, seismic actions and rules for buildings.

EN 1998-3 (2004) : Eurocode 8: Design of structures for earthquake resistance -Part 3: Assessment and retrofitting of buildings.

FEMA (2000), Prestandard and Commentary for the Seismic Rehabilitation of Buildings, Publ. No. 356, prepared by the American Society of Civil Engineers for the Federal Emergency Management Agency, Washington, D.C.

FEMA P695 (2009), Quantification of Building Seismic Performance Factors, Federal Emergency Management Agency, Washington, D.C.

Grierson, Donald & Gong, Yanglin & Xu, Lei. (2006). Optimal performance-based seismic design using modal pushover analysis. Journal of Earthquake Engineering. 10. 73-96. DOI 10.1080/13632460609350588.

Hamburger, Ronald. (2014). FEMA P58 seismic performance assessment of buildings. NCEE 2014 - 10th U.S. National Conference on Earthquake Engineering: Frontiers of Earthquake Engineering. DOI 10.4231/D3ZW18S8N.

- Hassan, Emad & Mahmoud, Hussam.** (2019). Full functionality and recovery assessment framework for a hospital subjected to a scenario earthquake event. *Engineering Structures*. 188. 165-177. DOI 10.1016/j.engstruct.2019.03.008.
- Hiete, Michael & Merz, Mirjam & Trinks, Christian & Schultmann, Frank.** (2011). Scenario-based impact analysis of a power outage on healthcare facilities in Germany. *International Journal of Disaster Resilience in the Built Environment*. 2. 222-244. DOI 10.1108/17595901111167105.
- <http://www.iterate-eu.org/>
- Iervolino, Iunio & Cornell, C.** (2008). Probability of Occurrence of Velocity Pulses in Near-Source Ground Motions. *Bulletin of The Seismological Society of America - BULL SEISMOL SOC AMER*. 98. DOI 10.1785/0120080033.
- Inel, Mehmet & Ozmen, Hayri.** (2006). Effects of plastic hinge properties in nonlinear analysis of reinforced concrete buildings. *Engineering Structures*. 28. 1494-1502. DOI 10.1016/j.engstruct.2006.01.017.
- Jacques, Caitlin & McIntosh, Jason & Giovinazzi, Sonia & Kirsch, Thomas & Wilson, Tom & Mitrani-Reiser, J.** (2014). Resilience of the Canterbury Hospital System to the 2011 Christchurch Earthquake. *Earthquake Spectra*. 30. 533-554. DOI 10.1193/032013EQS074M.
- Kramer, S. L.** (1996). *Geotechnical earthquake engineering*, Prentice Hall, Upper Saddle River, N.J. A geotechnical-engineering focused book.
- Luco, Nicolas & Cornell, C.** (2007). Structure-Specific Scalar Intensity Measures for Near-Source and Ordinary Earthquake Ground Motions. *Earthquake Spectra*. 23. DOI 10.1193/1.2723158.
- Lupoi, Alessio & Cavalieri, Francesco & Franchin, Paolo.** (2013). Seismic Resilience of Regional Health-Care Systems. DOI 10.1201/b16387-611.
- Mander J.B., Priestley M.J.N., Park R.** [1988] "Theoretical stress-strain model for confined concrete," *Journal of Structural Engineering*, Vol. 114, No. 8, pp. 1804-1826.
- Masi, A., Santarsiero, G., and Chiauzzi, L.** (2012). Vulnerability assessment and seismic risk reduction strategies of hospitals in Basilicata region (Italy), in *Proc. of the 15th World Conference on Earthquake Engineering*, Lisbon, Portugal.
- Miniati, Roberto & Iasio, C.** (2012). Methodology for rapid seismic risk assessment of health structures: Case study of the hospital system in Florence, Italy. *International Journal of Disaster Risk Reduction*. 2. 16-24. DOI 10.1016/j.ijdr.2012.07.001.

Ministry of Housing and Town Planning, Algerian Earthquake Rules RPA 99 / Version 2003, CGS Edition, 2003.

Mohamed, Hamdache & Peláez, José & Talbi, A. & Mobarki, Mourad & Casado, C. (2012). Ground-Motion Hazard Values for Northern Algeria. *Pure and Applied Geophysics*. 169. 711-723. DOI 10.1007/s00024-011-0333-z.

Monti G., Nuti C. (1992) Nonlinear cyclic behaviour of reinforcing bars including buckling, *Journal of Structural Engineering*, Vol. 118, No. 12, pp. 3268-3284.

Munasinghe, Nimali & Matsui, Kenichi. (2019). Examining disaster preparedness at Matara District General Hospital in Sri Lanka. *International Journal of Disaster Risk Reduction*. 40. DOI 101154. 10.1016/j.ijdr.2019.101154.

Pan American Health Organization. Principles of disaster mitigation in health facilities. Washington, D.C. : PAHO, 2000. 123 pp.—(Disaster Mitigation Series)

Reinhorn, Andrei & Deierlein, Gregory & Willford, Michael. (2010). *Nonlinear Structural Analysis for Seismic Design- A Guide for Practicing Engineers*.

SeismoStruct (2020), A computer program for static and dynamic nonlinear analysis of framed structures, SeismoSoft, Ltd. Available from: www.seismosoft.com.

Vamvatsikos, Dimitrios & Cornell, C. (2002). Incremental Dynamic Analysis. *Earthquake Engineering & Structural Dynamics*. 31. 491 - 514. DOI 10.1002/eqe.141.

Vamvatsikos, Dimitrios & Cornell, C. (2006). Direct Estimation of the Seismic Demand and Capacity of Oscillators with Multi-Linear Static Pushovers through IDA. *Earthquake Engineering & Structural Dynamics*. 35. 1097 - 1117. DOI 10.1002/eqe.573.

Youngs, R. & Coppersmith, K. (1986). Implications of fault slip rates and earthquake recurrence models to probabilistic seismic hazard estimates *Bull Seismol Soc Am* V75, N4, Aug 1985, P939–964. *International Journal of Rock Mechanics and Mining Sciences & Geomechanics Abstracts*. 23. 125-125. DOI 10.1016/0148-9062(86)90651-0.